

# A

## Forbidden Symmetry, Fibonacci's Rabbits, and a New State of Matter

*The above proposition [1 + 1 = 2] is occasionally useful.*

—A. N. WHITEHEAD and B. RUSSELL,  
in *Principia Mathematica*

*Modern theoretical physics is a luxuriant . . . world of ideas and a mathematician can find in it everything to satiate himself except the order to which he is accustomed.*

—YURI MANIN

In this chapter we shall taste some of the forbidden fruits that self-similarity breeds: a new solid state of matter, namely, a “quasicrystal” with a fivefold axis of rotational symmetry (like that of a five-legged starfish and many flowers). Curiously, the new matter is related to a simple iterated map that was itself bred by multiplying rabbits—rather rare rabbits, that is, of the famous Fibonacci family. Said simple iterated map is in turn intimately entangled with the continued fraction for the golden mean, easily abased to the “silver means,” which predict more forbidden symmetries—some of which have since been seen in actual quasicrystals.

### The Forbidden Fivefold Symmetry

From snowflakes to gemstones, people have forever prized crystals, formations in which the individual atoms are arranged in orderly periodic lattices. But we are also familiar with *disordered* substances, such as most liquids, in which the

atoms are randomly distributed. Likewise, most solid substances encountered in nature are disordered, or *amorphous*, just like a liquid, except that they are solidified. Glasses are transparent examples of amorphous solids. In fact, among physicists the designation *glass* has become the generic term for disordered systems. Thus, a *metallic glass* does not mean a pewter cup, nor does it have much else to do with glass: it is simply a metal in which the individual atoms are arranged in disorderly fashion. And a *spin glass* is not spun glass, nor is there much spinning going on. Rather, a spin glass is a disordered arrangement of magnetic spins or, by extension, the values of any other physical variable that has two<sup>1</sup> preferred states, such as on-off neurons in a neural network.

And then there are some showy states of matter, such as *liquid crystals*, which are now ubiquitous as alphanumeric displays (LCDs) in watches and calculators. In a liquid crystal, the molecules are randomly located but their orientations are well ordered, under the control of an external voltage, which permits the displayed information to be changed.

Until recently, few if any people suspected that there could be another state of matter sharing important aspects with both crystalline *and* amorphous substances. Yet, this is precisely what D. Shechtman and his collaborators discovered when they recorded electron diffraction patterns (see Figure 1) of a rapidly cooled aluminum-manganese alloy ( $\text{Al}_6\text{Mn}$ ), now called a *quasicrystal* [SBGC 84]. The diffraction pattern (essentially a two-dimensional Fourier transform) of their quasicrystals showed *sharp peaks*, implying long-range order, just as for periodic crystal lattices. But the pattern also showed a *fivefold* symmetry that is forbidden for periodic crystals; see Figure 2 for a simple proof. Fivefold symmetry means that the lattice can be brought into coincidence with itself by a rotation through  $360^\circ/5 = 72^\circ$ . But the only allowed symmetry axes are two-, three-, four-, and sixfold; all other rotational symmetries conflict with the translational symmetry of a periodic crystal.

What then is going on in these new substances? Several other quasicrystals with other forbidden symmetries have been identified since the original discovery. Thus, quasicrystals are not an isolated quirk; they represent a new solid state of matter—Linus Pauling’s tenacious doubts notwithstanding [Pau 85]. And as we shall shortly see, the explanation of their existence is rooted in self-similarity.

---

1. There is a strong link between the physicists’ *spin* and the number 2 (also known as the “oddest prime” because it is the only even prime). Because elementary spin is a two-valued variable (“up” or “down”), two electrons are allowed in the same atomic orbit, thereby explaining (together with Pauli’s exclusion principle) the periodic table of elements. Einstein, in the only experiment he ever performed himself (with W. J. de Haas), on the gyromagnetic ratio of the electron, got a result that was off by a factor of 2 (an error of 100 percent!). However, this did not bother the great theorist in the least—*close enough*, he is said to have remarked. Subsequently, it turned out that his result was quite accurate and the factor of 2 had to do with the spin of the electron. Later on, many occasions arose in physics and chemistry where one had to “multiply by 2 because of the spin.” (However, the fact that the *proof* figure on a liquor bottle is the alcohol percentage multiplied by 2 is probably unrelated to the spin induced in some imbibers by the liquid potion.)

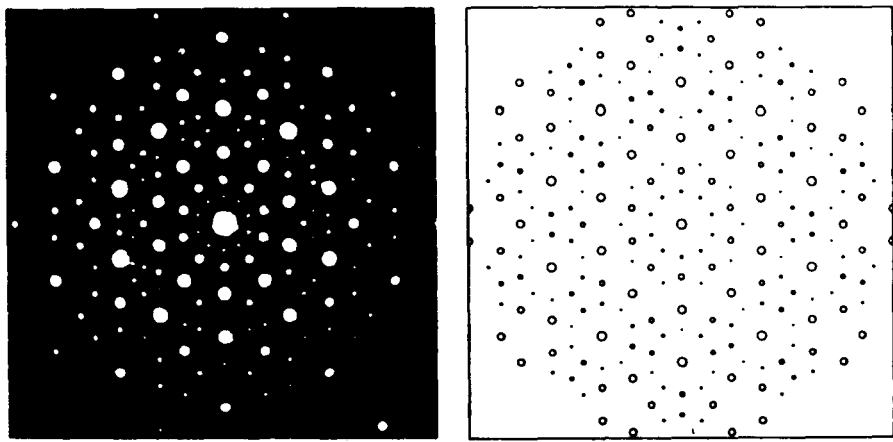


**Figure 1** Electron diffraction pattern of crystal with forbidden fivefold symmetry [SBGC 84].

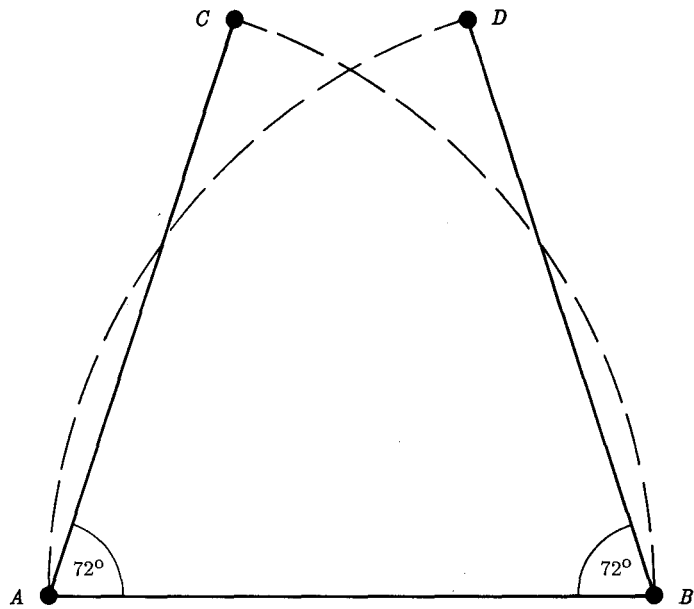


**Figure 2** Simple proof that fivefold symmetry is impossible in a periodic crystal. In a periodic crystal there is a smallest distance between two atoms. Let the segment  $\overline{AB}$  be one of these shortest distances. If the crystal has fivefold symmetry, then, in addition to the points  $A$  and  $B$ , the points  $C$  and  $D$  (obtained by  $360^\circ/5 = 72^\circ$  rotations) should also be occupied by atoms. But the distance between  $C$  and  $D$  is smaller (by a factor of  $0.382\dots$ , equal to the golden mean squared) than  $\overline{AB}$ —contradicting the claim that  $\overline{AB}$  was the smallest distance.

## Long-Range Order from Neighborly Interactions

As we know from the number-theoretic Morse-Thue sequence (see Chapter 12), sharp spectral peaks and aperiodicity are no contradiction, as long as *long-range order* prevails. In fact, the simplest example of aperiodicity and long-range order leading to sharp spectral peaks is furnished by the superposition of two sine waves with incommensurate frequencies, for example,

$$s(t) = \sin(\omega_0 t) + \sin(\alpha\omega_0 t)$$

where the frequency ratio  $\alpha$  is an irrational number. There is no nonzero value  $T$  for which  $s(t) = s(t + T)$  for all  $t$ . Yet Fourier-analyzing  $s(t)$  (properly windowed to make the Fourier transform converge) will, of course, show sharp peaks at the incommensurate radian frequencies  $\omega = \omega_0$  and  $\omega = \alpha\omega_0$ .

Periodicity in crystals is easy to explain. For example, in a crystal of table salt (sodium chloride, chemically speaking), sodium atoms ( $\text{Na}$ ) prefer chlorine atoms ( $\text{Cl}$ ) as neighbors and vice versa: chlorine atoms like to surround themselves with sodium atoms. Thus, going along one of the crystal axes, sodium and chlorine alternate:  $\text{Na}-\text{Cl}-\text{Na}-\text{Cl}-\text{Na}-\text{Cl}$ , and so on. The result is perfect periodicity and long-range order.

But how can we explain long-range order in an aperiodic quasicrystal? That is not so easy. If there is no simple mutual attraction between different kinds of atoms or molecules (or if high temperature overcomes this), the usual result is *no* long-range order: a random structure, as in liquids (or “frozen” liquids, such as window glass).

Perhaps the only way to produce long-range order from the short-range interactions that dominate solid structures *without* resulting in a periodic lattice (as in our table salt example) is to rely on iterated maps. Iterated maps are models of short-range interactions. For example, a 0 attracts a 1, which engenders the mapping  $0 \rightarrow 01$ ; and a 1 attracts a 0, or  $1 \rightarrow 10$ . Yet, as we know from the Morse-Thue sequence, iterated maps can also produce aperiodic long-range order. Since iterated maps often lead to self-similarities, an explanation of quasicrystals by this approach means that the crystals (and their diffraction patterns) must exhibit scaling invariances. This is indeed the case, as a closer inspection of the diffraction pattern in Figure 1 shows. The most prominent scaling factor in Figure 1 turns out to be the golden mean  $\gamma = (\sqrt{5} - 1)/2 = 0.618 \dots$ . (Note: Some authors—including the present one, in another book—call the *reciprocal* of the golden mean,  $1/\gamma = 1.618 \dots$ , the golden section or golden mean.)

Thus, there is an odds-on chance that quasicrystals might be modeled by an iterative map related to the golden mean. To find such a map, we have to turn the clock back a bit.

Around the year 1200, Leonardo da Pisa (ca. 1175–1250)—better known as “Fibonacci,” that is, son of Bonacci—was considering the problem of how

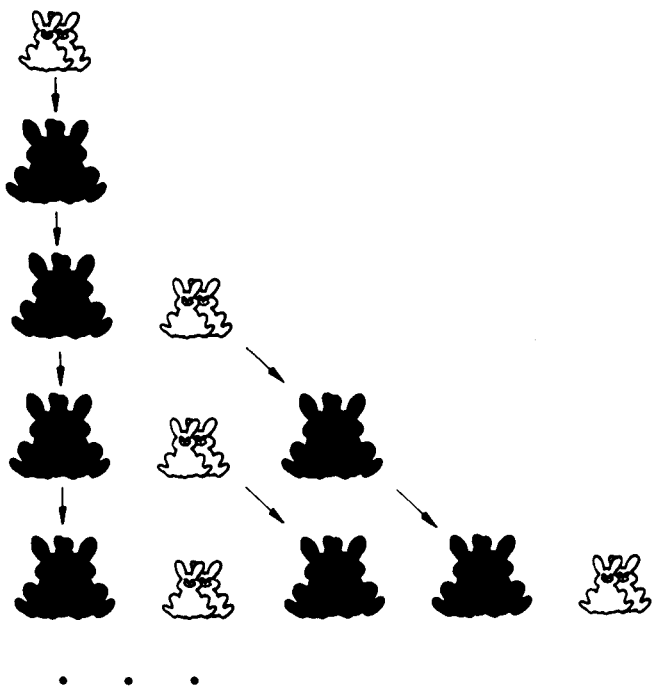


**Figure 3** Multiplying rabbits, as Fibonacci saw them. Small, "white" rabbit symbols: immature pairs; large, "filled" symbols: mature pairs.

*rabbits multiply, something rabbits were obviously very good at even then [Fib 1202]. In best modern style he postulated a highly simplified model of the procreation process: each season every adult pair of rabbits begets a young pair, which will be mature one generation later. Starting with one immature pair of rabbits and assuming that rabbits go on living forever, the rabbit population grows rapidly, as shown in Figure 3.*

More formally, Fibonacci was considering the iterated map  $0 \rightarrow 1$  and  $1 \rightarrow 10$ , where 0 stands for an immature rabbit pair and 1 for a mature pair. Thus, the first six generations are represented by the binary sequences

$$\begin{array}{ll}
 0 & \\
 1 & \\
 10 & \\
 101 & \\
 10110 & \\
 10110101 & \text{(1)}
 \end{array}$$

which, like the Morse-Thue-sequence, is a self-generating sequence. The  $n$ th generation has precisely  $F_n$  pairs of rabbits, where  $F_n$  is the  $n$ th Fibonacci number defined by  $F_1 = F_2 = 1$  and the recursion  $F_{n+2} = F_{n+1} + F_n$ . This yields the well-known Fibonacci sequence 1, 1, 2, 3, 5, 8, 13, . . . A simple formula for generating the  $F_n$  for  $n > 0$  is obtained by rounding the value of  $\gamma^{-n}/\sqrt{5}$  to the nearest integer, where  $\gamma = 0.618 \dots$  is the aforementioned golden mean. Thus, the ratio of two successive Fibonacci numbers asymptotically approaches the golden mean, as does the ratio of 0s to 1s in each line of pattern 1. In fact, the numbers of 0s and 1s in the  $n$ th line are precisely  $F_{n-2}$  and  $F_{n-1}$ , respectively. (Note that, by backward recursion,  $F_0 = 0$  and  $F_{-1} = 1$ .)

Another law for constructing the infinite sequence whose beginning is shown in pattern 1, and which I have called the *rabbit sequence*, is quite apparent: after the first two rows, simply append to each row the previous row to form the next one. This property is a direct consequence of iterating the mapping. The first iteration of the map  $0 \rightarrow 1$ ,  $1 \rightarrow 10$  gives  $0 \rightarrow 10$ ,  $1 \rightarrow 101$ , and iterating the iterated map results in  $0 \rightarrow 101$   $10$ ,  $1 \rightarrow 101$   $10$   $101$ , and so on. Thus, the fifth line ( $101$   $10$ ) in pattern 1 can be considered to have been generated from the third line ( $10$ ) by using the once iterated map  $1 \rightarrow 101$  and appending to it the result of  $0 \rightarrow 10$ . But  $101$  is, of course, the fourth line, and the appended  $10$  is in fact the third line. Thus, each sequence in pattern 1 can be obtained by appending to the predecessor sequence the *predecessor*, an “inflation” rule which mirrors the original map  $0 \rightarrow 1$  and  $1 \rightarrow 10$ . It is this kind of structure that causes *long-range order* to occur in the rabbit sequence although it was defined on the basis of only a *short-range* law ( $0 \rightarrow 1$ ,  $1 \rightarrow 10$ ) involving only next neighbor symbols.

As we saw in Chapter 11, iterated maps often lead to self-similarity, and the rabbit sequence is no exception: it abounds with self-similarities. One self-similarity of the rabbit sequence can be demonstrated by retaining the first two out of every three symbols for every 1 in the sequence and retaining the first one out of every two symbols for every 0. This decimation indeed reproduces the infinite rabbit sequence, as indicated in the following by underlining:

101101101101 . . .

This property reflects the fact that the rabbit sequence reproduces itself upon *reverse mapping* (also called *block renaming* or “deflation” in renormalization theories in physics) according to the law  $10 \rightarrow 1$ ,  $1 \rightarrow 0$ . (Note that the *non-underlined* bits also mimic the 1s and 0s of the rabbit sequence—there is no escaping from those foxy rabbits.)

Let us try to get some useful work out of our rabbits. Consider the following “synchronization” problem (with potential applications to keeping digital transmission channels in step, as in picture transmission from distant space vehicles). How many steps do we have to move to the right in the rabbit sequence

101101011011010110101 . . . ,

to find a given subsequence (e.g., 10) again? We find the answer by inspection. First we have to move 3 places, then 2, then 3 again, and so forth: 3, 2, 3, 3, 2, 3, 2, . . . , a sequence (of Fibonacci numbers, incidentally) that mimics the rabbit sequence, which is in fact reproduced by the substitution  $2 \rightarrow 0$  ( $F_3 \rightarrow F_0$ ) and  $3 \rightarrow 1$  ( $F_4 \rightarrow F_1$ ). To cope with large synchronization errors, one has to focus on long subsequences. In general, a subsequence of length  $F_n - 1$  does not reoccur before  $F_{n-1}$  steps. It will, however, reoccur after at most  $F_{n+1}$  steps.

There is a simple formula (first encountered on pages 53–54) for calculating the indices  $k$  for which the rabbit sequence symbol  $r_k$  equals 1:

$$k = \left\lfloor \frac{n}{\gamma} \right\rfloor \quad n = 1, 2, 3, \dots$$

while the indices for which  $r_k = 0$  are given by

$$k = \left\lfloor \frac{n}{\gamma^2} \right\rfloor \quad n = 1, 2, 3, \dots$$

where the “floor function”  $\lfloor x \rfloor$  means the largest integer not exceeding  $x$ .

These two equations can be interpreted as formulas for generation of 1s and 0s by two incommensurate frequencies:  $\gamma$  and  $\gamma^2$ , respectively. Note that  $\gamma + \gamma^2 = 1$ , which is the frequency of occurrence of either 1 or 0, also called the “sampling” frequency by engineers. If  $\gamma$  is replaced by any positive irrational number  $w < 1$  and  $\gamma^2$  by  $1 - w$ , then the resulting two sequences, which together cover all the positive integers, are called a pair of *Beatty sequences*. Because of this covering property, Beatty sequences are useful as index sequences [Slo 73].

With the rabbit sequence being generated by the frequencies  $\gamma \approx 0.618$  and  $\gamma^2 \approx 0.382$ , it is small wonder that the spectrum (i.e., the magnitude of the Fourier transform) should show pronounced peaks at these two frequencies; see Figure 4, which was obtained by truncating the rabbit sequence after 144 terms and taking the Fourier transform [Schr 90]. The two main peaks are located at the harmonic numbers 55 and 89 corresponding to the frequencies  $\frac{89}{144} \approx \gamma$  and  $\frac{55}{144} \approx \gamma^2$ . The spectrum also reflects the self-similarity of the rabbit sequence. In fact, the peaks occur at frequencies that scale with the golden mean  $\gamma$  (actually, the ratio of successive Fibonacci numbers for the truncated sequence), and the amplitudes scale approximately as  $\gamma^2$ .

## Generation of the Rabbit Sequence from the Fibonacci Number System

For most purposes we do not need the *index* sequences for the 1s or 0s of the rabbit sequence but we need the sequence itself and a *direct* formula to generate it. Here is a first stab:

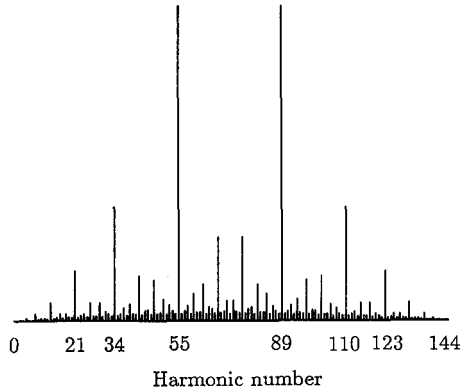


**Figure 4** Fourier amplitude spectrum of binary rabbit sequence (the first 144 terms repeated periodically) [Schr 90].

Consider

$$r_k = m_i + 1 \bmod 2$$

where  $m_i$  is the *index* of the least significant term in the representation of  $k$  in the Fibonacci number system [Schr 90]. In this system,  $n$  is represented as the unique sum of Fibonacci numbers with descending indices, starting with the largest-index Fibonacci number not exceeding  $n$ :

$$n = F_{m_1} + F_{m_2} + \cdots + F_{m_r}$$

where  $m_1 > m_2 > \cdots > m_r$ . For example,  $12 = 8 + 3 + 1 = F_6 + F_4 + F_2$ . Thus, since the index (2) of the last term ( $F_2$ ) is even,  $r_{12} = 1$ . (Note that in this representation no two adjacent indices can appear; i.e.,  $m_{i+1} \geq 2 + m_i$ . Also, by convention,  $1 = F_2$ , so that  $r_1 = 1$ . However, while this approach does address itself to the  $r_k$  themselves, the calculation via the Fibonacci number system can hardly be called direct.)

## The Self-Similar Spectrum of the Rabbit Sequence

A more direct representation of the rabbit sequence  $r_k$  is the following:

$$r_k = \begin{cases} 1 & \text{if } \langle (k+1)\gamma \rangle_1 < \gamma \\ 0 & \text{otherwise} \end{cases} \quad (2)$$

where, as before,  $\langle x \rangle_1$  is the fractional part of  $x$ . This formula for  $r_k$  has an attractive geometric representation; see Figure 5.

Two direct formulas for generating the rabbit sequence, which also put its long-range order *and* aperiodicity into direct evidence, are given by

$$r_k = \lfloor (k+1)\gamma \rfloor - \lfloor k\gamma \rfloor$$

and, rewriting equation 2,

$$r_k = \frac{1}{2} + \frac{1}{2} \operatorname{sgn} [\gamma - \langle (k+1)\gamma \rangle_1] \quad (3)$$

where  $\operatorname{sgn}[x]$  is the algebraic sign of  $x$  (+1 or -1) for  $x \neq 0$  ( $\operatorname{sgn}[0]$  is defined as 0).

Interpreted in engineering terms, equation 3, with  $k$  considered a continuous variable ("time"), says that  $r_k$  is a square wave (jumping between the values 1 and 0) with a fundamental frequency  $\gamma$  (and a "duty cycle" of  $\gamma$ ). However,  $k$  is *not* a continuous variable; it is discrete, increasing in steps of 1. This means that the square wave is *sampled* with a sampling frequency of 1. Since the frequencies  $\gamma$  and 1 are incommensurate, the resulting sequence of samples is aperiodic, while retaining a perfectly rigid long-range order. For example, setting  $k = 144$ , we find that  $r_{144} = 1$ , which is quickly confirmed by noting that  $144 = F_{12}$  and by applying the general rule  $r_{F_n} = (1 + (-1)^n)/2$ . (Note: For  $F_n = 1$ , one has to take  $n = 2$ .)

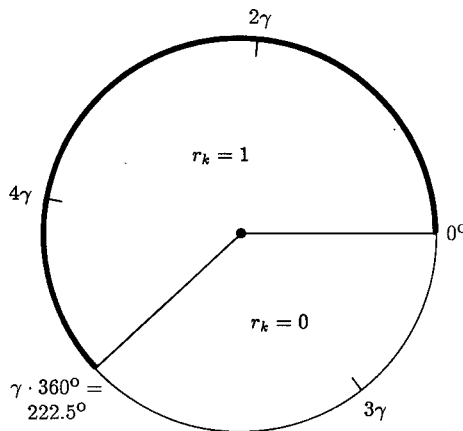


**Figure 5** The rabbit sequence, generated geometrically. The sequence term  $r_k$  equals 1 if the angle  $\langle (k+1)\gamma \rangle_1 \cdot 360^\circ$  falls within the heavy circular arc. Otherwise  $r_k$  equals 0.

Since the period  $\gamma$  is an *irrational* number, the samples  $r_k$  taken at sampling intervals are aperiodic. As a result, the spectrum of  $r_k$  shows strong peaks at certain preferred frequencies, namely, the sampling frequency multiplied by  $\gamma^2$ ,  $\gamma^3$ ,  $\gamma^4$ ,  $\gamma^5$ , and so on, and the corresponding mirror frequencies ( $1 - \gamma^2 = \gamma$ ,  $1 - \gamma^3, \dots$ ).

A mathematical expression of the spectrum of  $r_k$  is obtained by Fourier-transforming  $r_k$  as given by equation 3. This yields

$$R_m = \text{sinc } m\gamma \quad \text{for frequencies } f_{nm} = n + m\gamma$$

where the “sinc function”  $\text{sinc } x$  is defined as  $(\sin \pi x)/\pi x$ .

## Self-Similarity in the Rabbit Sequence

Where do these spectral self-similarities come from? Obviously, they must be hiding already in the sequence itself. Indeed, if we look at the index sequence  $[n/\gamma]$  for the 1s, we see that scaling  $n$  by a factor of  $\gamma$ , that is, by substituting  $n/\gamma$  for  $n$ , will give the index sequence  $[n/\gamma^2]$  for the 0s. Thus, the magnitude of the Fourier transform of  $r_k$  will remain unchanged under this rescaling, except for the constant scaling factor.

We can also observe the self-similarity in  $r_k$  itself. Since the self-similarity factor is  $1/\gamma$ , we have to “hop along” 1.618... places on average to effect the scaling by  $1/\gamma$ . Since the asymptotic ratio of 1s to 0s is precisely  $\gamma$ , we might try to skip two terms in  $r_k$  if we encounter a 1 and skip only one term every time we encounter a 0 in the original sequence. This indeed reproduces the series:

$$1 \ 0 \ \underline{1} \ 1 \ \underline{0} \ 1 \ 0 \ \underline{1} \ 1 \ 0 \ \underline{1} \ 1 \ \underline{0} \dots = 1 \ 0 \ 1 \ 1 \ 0 \dots$$

as the reader may be tempted to show. This decimation process is the complement of the “deflation” or *block renaming* that we mentioned before. Here we have renamed each 101 block 1 and each 10 block 0. The block renaming is the inverse of the generating map  $(0 \rightarrow 1, 1 \rightarrow 10)$  iterated once, that is,  $0 \rightarrow 10, 1 \rightarrow 101$ .

## A One-Dimensional Quasiperiodic Lattice

How do we convert our discoveries about self-similar sequences producing aperiodic long-range order into something more physical, such as a one-dimensional (1D) lattice, say, as a precursor to a full-blown 3D quasicrystal? A simple method is illustrated in Figure 6. We place atoms on a straight line according to the following rule. For each 1 in the rabbit sequence  $r_k$  we take an

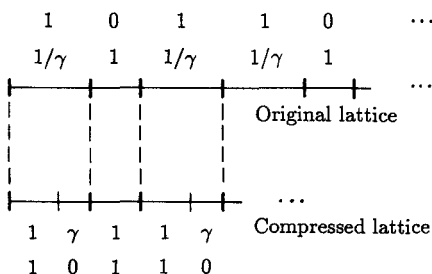


**Figure 6** One-dimensional quasiperiodic “crystal,” obtained from the rabbit sequence. The self-similarity factor is the golden mean  $\gamma$ .

interatomic distance of  $1/\gamma = 1.618 \dots$  units (say, Ångström units), and for each 0 we take a distance of 1 unit. The lower part of Figure 6 shows the same 1D lattice compressed by a factor of  $1.618 \dots$ , which demonstrates that every atom in the original lattice coincides precisely with an atom in the compressed lattice. (The compressed lattice, having a higher atomic density, will of course have some extra atoms with no partners in the original lattice.) Thus, the 1D lattice, so constructed, has self-similarity. (The reader may want to generalize this result to self-similar 1D lattices based on suitable irrational numbers other than the golden section  $\gamma$ .)

If every atom in the “rabbit lattice” is represented by a Dirac delta function, we obtain the Fourier transform [ZD 85]:

$$S_{nm} = \text{sinc}\left(\frac{f}{\sqrt{5}} + m\right) \quad \text{at frequencies } f_{nm} = \frac{n}{\sqrt{5}} - m$$

## Self-Similarity from Projections

An alternative method of constructing the 1D rabbit lattice is illustrated in Figure 7 [de B 81]. It shows the square 2D integer lattice, called  $\mathbb{Z}^2$ , and a straight line with a slope (the tangent of the angle between it and the abscissa) equal to  $1/\gamma$ . For each unit square that this straight line enters, the upper left corner of the square is projected normally onto the line. And lo and behold, the footprints of these projections generate the previously defined 1D rabbit lattice. The rabbit sequence is recovered by designating the larger intervals by 1s and the shorter intervals by 0s. This geometric construction is a direct consequence of the arithmetic description of the rabbit sequence (equation 2), as the reader may want to show.

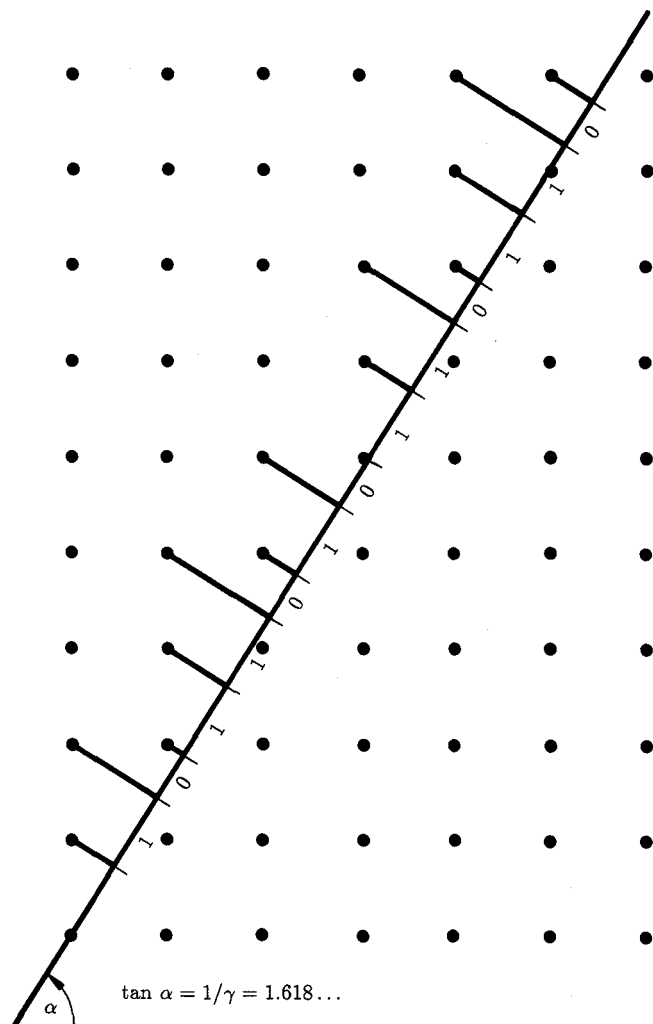


**Figure 7** The one-dimensional crystal of Figure 6, obtained by projections from a square lattice [deB 81].

The projection method, being based on a perfectly periodic square lattice, also demonstrates again both the long-range order in the 1D rabbit lattice and its aperiodicity (because of the irrational slope of the straight line). But most important, the projection method can easily be generalized to generate quasi-periodic lattices in two and three dimensions that mimic real quasicrystals [Mac 82, DK 85, Els 85, Jan 89].

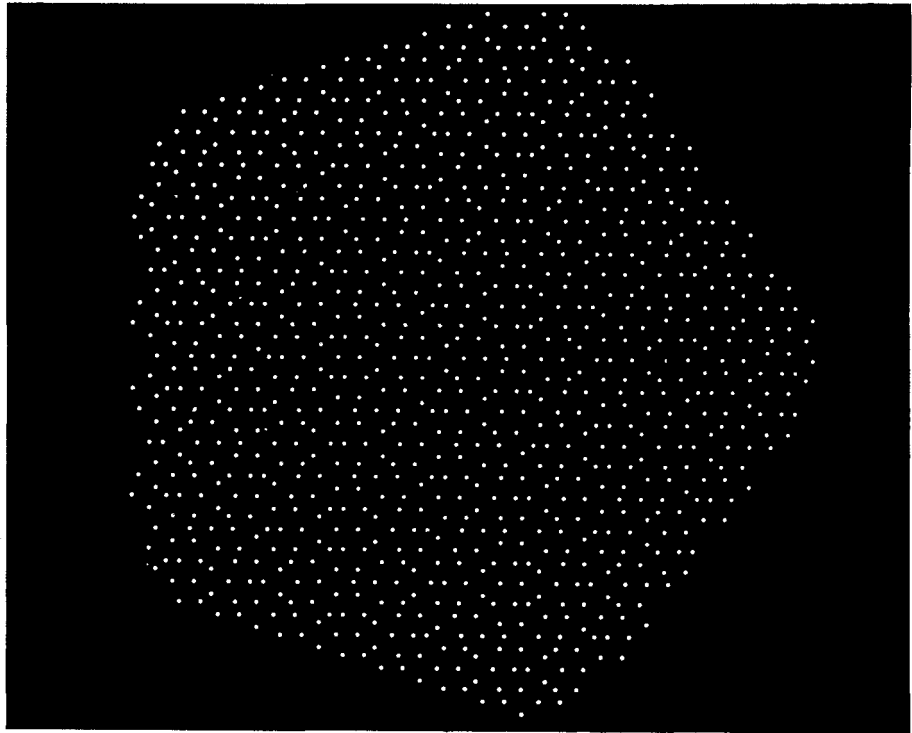


**Figure 8** Two-dimensional quasicrystal, obtained by projections from a five-dimensional hypercubic lattice.

To construct a 2D quasiperiodic lattice, one needs *four* rationally independent vectors; see Levin and Steinhardt [LS 84]. It is more convenient, however, to project a region of the five-dimensional “cubic” lattice onto an appropriately inclined plain. See Figure 8—which was, of course, generated by a computer, since five-dimensional lattices are still out of reach in the tangible world. It is interesting to note that the points in this image correspond to the vertices of an *aperiodic* tiling of the plane by *two* different tiles, the famous Penrose tiling (see Figure 9)—a feat that had long been considered impossible [Pen 74, Mac 82]. (For an aperiodic tiling with just *one* tile, see Figure 10 [Gar 77].)

When a photographic slide with the point pattern of Figure 8 is placed into a laser beam, the diffraction pattern of Figure 11A results, which shows the puzzling fivefold symmetry (which looks like a tenfold symmetry because we cannot see the signs of the scattered amplitudes in the *intensities* recorded photographically). In fact, Figure 11A resembles the diffraction pattern from an actual quasicrystal. Note particularly the self-similarities with the scaling factor  $\gamma$  in

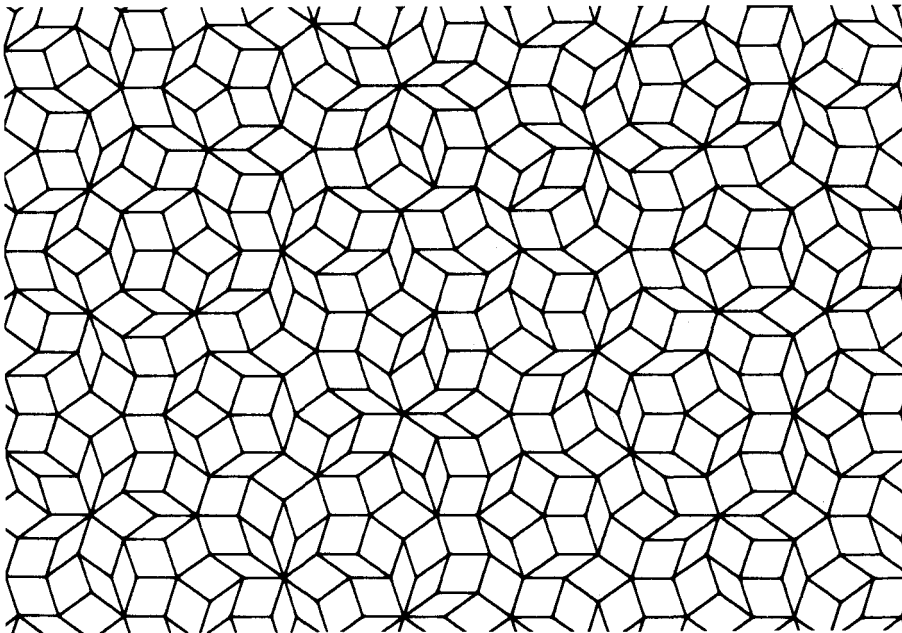


**Figure 9** Penrose tiling: a tiling of the plane with only two different tiles [Mac 82].

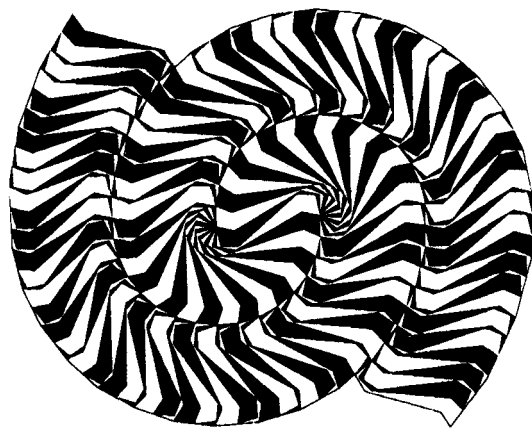


**Figure 10** An aperiodic tiling of the plane by Heinz Voderberg with one tile shown alternately in black or white [Gar 77].

many of the details of the pattern such as the numerous regular pentagons of different sizes.

The experiment just described is amenable to a "live" demonstration before sizable audiences using large television monitors for the display and a lensless TV camera for capturing the diffraction pattern.<sup>2</sup> By increasing the brightness of the diffraction pattern (by turning up the laser intensity), more and more diffraction spots can be made visible until the entire monitor screen is filled. Parts A, B, and C of Figure 11 show the diffraction pattern at three progressively higher intensities. In this manner, one of the crucial differences between quasicrystal diffraction patterns and those of periodic crystals can be demonstrated most convincingly: diffraction patterns of quasicrystals, while consisting of delta functions just like those of periodic crystals, consist of a (countably) *infinite* collection of delta functions that are everywhere dense—in contrast to the isolated diffraction spots of periodic crystals! The original quasicrystal patterns looked like those of periodic crystals only because they were obtained with a relative low incident intensity.

To generate a three-dimensional quasi-periodic lattice, one projects a six-dimensional cubic lattice onto three dimensions [KD 86].

## More Forbidden Symmetries

Having tasted a first forbidden fruit of fivefold symmetry, we might ask whether there are quasicrystals with other outlawed symmetry axes that can be distilled from self-similar iterated maps. There are indeed.

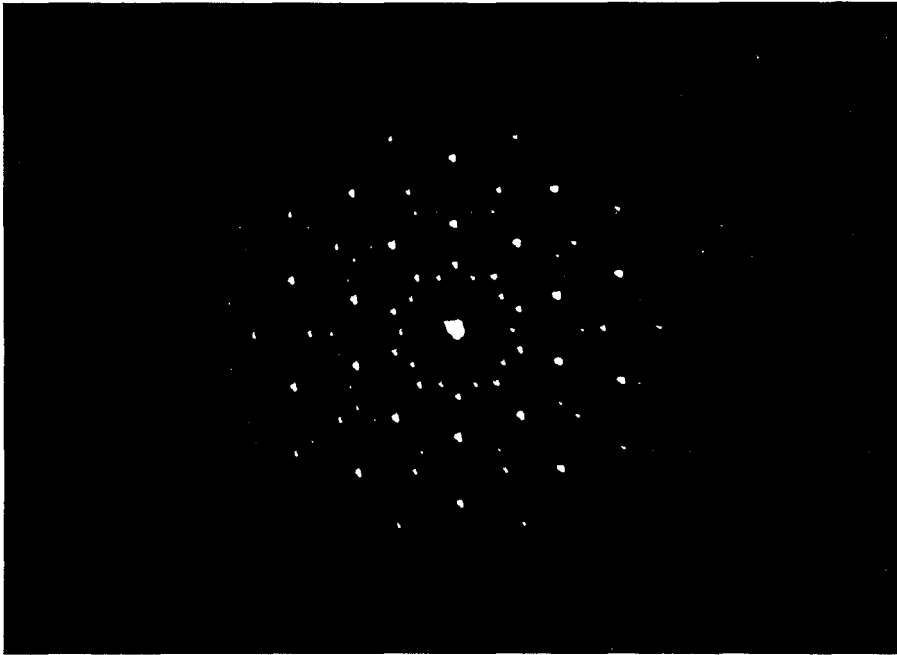
The mapping  $0 \rightarrow 1$ ,  $1 \rightarrow 10$ , which generates the rabbit sequence, is intimately related to the continued fraction for the golden mean  $\gamma$ :

$$\gamma = \frac{1}{1 +} \frac{1}{1 +} \frac{1}{1 +} \dots$$

which is customarily written as  $[1, 1, 1, \dots]$  or, since the continued fraction is periodic, simply as  $[\overline{1}]$ . Note that the period length equals 1. The continued fraction expansion for  $\gamma$  follows immediately from its definition as the positive root of the quadratic equation  $x^2 + x = 1$ , which can also be written as  $x = 1/(1+x)$ . Using this form of the defining equation for  $\gamma$  recursively results in the foregoing continued fraction expansion for  $\gamma$ . (Note that, because  $|1+\gamma| > 1$ , the recursion converges.)

---

2. I am grateful to Hans Werner Strube for the computer-generated "quasicrystal" and to Heinrich Henze for the brilliant laser diffraction patterns.



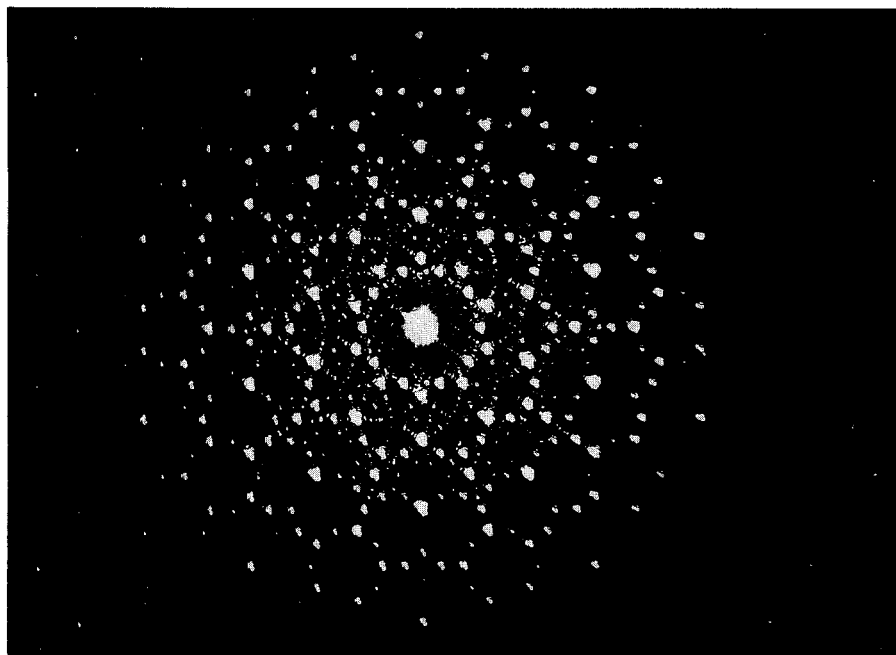
(A)

**Figure 11** (A) Laser diffraction pattern with fivefold symmetry of quasicrystal shown in Figure 8. (B) Laser diffraction pattern at higher laser intensity showing an increased number of diffraction spots. (C) Diffraction pattern at still higher intensity showing a nearly dense pattern of diffracted energy.

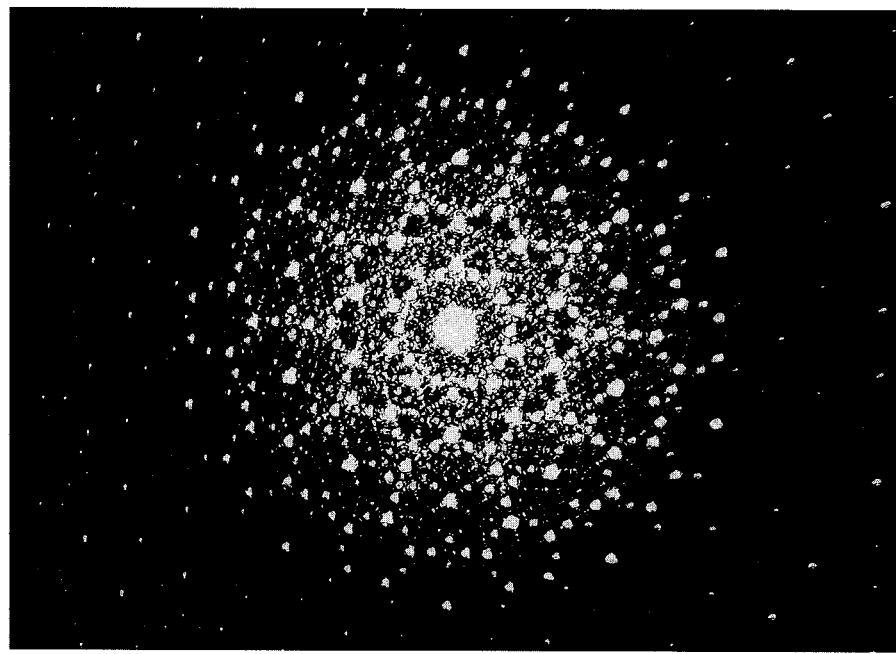
Could it be that iterated mappings related to the lesser “*silver* means,”  $\tau_N^\pm$ , can be pressed into service to generate self-similar lattices? The silver means  $\tau_N^\pm$  are defined by the equation  $1/\tau_N^\pm = N \pm \tau_N^\pm$ ; that is, they are all those quadratic irrational numbers that can be expressed by periodic continued fractions with period length 1 and  $\pm 1$  as the numerator.<sup>3</sup> It can be shown that

3. The *noble means*, another generalization of the golden mean, are defined as all those numbers whose continued fraction expansions end in infinitely many 1s. They distinguish themselves both in the present case and in the quasiperiodic route to chaos of nonlinear dynamic systems. In this nomenclature the golden mean is but the noblest of the noble means.

Cassini's divisions in the rings of Saturn are a manifestation of what happens when, instead of noble numbers, simple rational numbers reign: rocks and ice particles constituting the rings, whose orbital periods are in simple rational relation with the periods of the moons of Saturn, are simply swept out of their paths by the resonance effects between commensurate orbital periods. In fact, the very stability of the solar system depends on the nobility of the orbital period ratios.



(B)



(C)

$\tau_2^+ = [2, 2, 2, \dots] = \sqrt{2} - 1$  generates a quasicrystal with the crystallographically forbidden eightfold symmetry, while  $\tau_4^- = 2 - \sqrt{3}$  underlies a likewise forbidden twelvefold symmetry axis. Both eight- and twelvefold symmetry have recently been observed experimentally [INF 85, INF 88, CLK 88].

In addition to the golden mean  $\gamma = \tau_1^+$ , all  $\tau_N^\pm$ , where  $N$  is the  $n$ th Lucas number and the sign superscript in  $\tau_N^\pm$  equals  $(-1)^n$ , generate quasicrystals with a fivefold symmetry [Schr 90]. The Lucas numbers  $L_n$  obey the same recursion as the Fibonacci numbers, but start with  $L_1 = 1$  and  $L_2 = 3$ . The Lucas numbers  $1, 3, 4, 7, 11, 18, \dots$ , too, are related to the golden mean  $\gamma$ . In fact, for  $n \geq 2$ ,  $L_n$  is given by  $\gamma^{-n}$  rounded to the nearest integer.

# P

## eriodic and Quasiperiodic Structures in Space—The Route to Spatial Chaos

*A great truth is a truth whose opposite is also a great truth.*

—NIELS BOHR

In the preceding chapter we saw that, in addition to crystals with perfectly periodic lattices, there are *quasicrystals* whose spatial structure is *quasiperiodic*. In one-dimensional models, this quasiperiodicity can be described by two *incommensurate* frequencies involving the golden mean or other quadratic irrational numbers continued whose fraction expansions have a short period length.<sup>1</sup> And, of course *amorphous* substances with no discernible periodic structure have always been known.

At the time of their discovery in 1984, quasicrystals came as a real surprise: only a very sparse sampling of scientists had foreseen the possibility of a spatial structure—other than liquid crystals—intermediate between amorphous glasses and regular crystals. Yet, the surprises are not over.<sup>2</sup> There is still another spatial structure lurking between quasiperiodicity and amorphous disorder: spatial chaos.

The existence of spatial chaos should not really come as a surprise to anyone familiar with temporal chaos, considering that space and time are mere components of a unified space-time. Whatever can happen in time could also happen in space

1. Periodic continued fractions with long periods involving large integers would give rise to unrealistic quasicrystals with molecular interactions much too complicated to be believable.

2. "It's not over until the fat lady sings," as P. W. Anderson remarked on St. Patrick's Day in 1987 in New York City at the "Woodstock" meeting of the American Physical Society on the new high- $T_c$  ("room temperature in Alaska") superconductors.

(and vice versa). In the time domain, we have long been acquainted with periodic, quasiperiodic, and random phenomena:

- The motion of a swing is periodic.
- The phases of the moon at midnight every Sunday, say, are quasiperiodic; they are governed by two (as yet) incommensurate frequencies: the moon's orbit around the earth and the earth's elliptic orbit around the sun.
- The hiss of air escaping from a punctured bicycle tire can be considered a random noise. Thermal motion is another example of a random process.<sup>3</sup>

Yet, more recently, physicists have come to appreciate a fourth kind of temporal behavior: *deterministic chaos*, which is aperiodic, just like random noise, but distinct from the latter because it is the result of deterministic equations. In dynamic systems such chaos is often characterized by small fractal dimensions because a chaotic process in phase space typically fills only a small part of the entire, energetically available space.

Taking a cue from chaos in the time domain, we should expect to find chaos entrenched also in the space domain. In fact, *turbulence* is now considered a case of spatial chaos, albeit a very complicated one. In this chapter we first focus on a particularly simple case of spatial quasiperiodicity and chaos, with important analogies in the time domain: a one-dimensional Ising spin model of magnetism.

## Periodicity and Quasiperiodicity in Space

Imagine a one-dimensional system of electron spins  $s_i = +1$  or  $s_i = -1$  positioned at equal intervals along a single spatial dimension, as considered by Bak and Bruinsma [BB 82]. In the presence of an external magnetic field  $H$ , the energy  $E$  of the system is given by

$$E = - \sum_i H s_i + \sum_{i \neq j} J_{ij} s_i s_j \quad (1)$$

where  $J_{ij}$  is an antiferromagnetic interaction ( $J_{ij} > 0$ ) between spins  $s_i$  and  $s_j$  that

---

3. If our ears were a bit more sensitive and if there were no distracting sounds, we would hear the thermal motion of the air molecules: a constant hissing, the perception of which would offer no added survival value to ourselves or the species. In fact, such a super-ear would be an evolutionary liability, considering the extra expense to the species to develop, protect, and maintain it.

decays with increasing spatial distance  $|i - j|$  according to the power law

$$J_{ij} = |i - j|^{-\alpha} \quad (2)$$

with  $\alpha = 2$ , for example.

The fact that  $J_{ij}$  is positive means that adjacent spins would like to have *opposite* sign (to minimize the energy  $E$ ). This is why an interaction like that in equation 2 is said to be *antiferromagnetic*. (In a “ferromagnet,” adjacent spins prefer to align themselves in the *same* direction, creating a strong external magnetic field, such as that of a horseshoe magnet.)

With adjacent spins having opposite signs, spins at alternating locations, of course, have the same value, giving a positive, though smaller, contribution to the energy  $E$  (for  $\alpha > 0$ ). Thus, without an external field  $H$ , the minimum energy is obtained by a fraction  $w = \frac{1}{2}$  of spins pointing up. Setting  $s_0 = +1$  as an initial condition, we have

$$s_{2k} = +1 \quad \text{and} \quad s_{2k+1} = -1 \quad (3)$$

which is a perfectly periodic antiferromagnetic arrangement.

## The Devil's Staircase for Ising Spins

For nonzero values of the external magnetic field  $H$ ,  $w = \frac{1}{2}$  may no longer give the minimum energy  $E$ . In fact, for  $H \rightarrow \infty$  all spins would turn up, so that  $w$ , the fraction of up-spins, would go to 1. But how?

For small changes of  $H$  (and zero temperature), no spins will flip; they are *locked* into their given configuration. In fact, for each rational  $w = p/q$  there is a *range* of  $H$  values,  $\Delta H(p/q)$ , for which  $w$  remains fixed. As a result, the plot of  $w$  versus  $H$  looks like a devil's staircase; see Figure 1 [BB 82, BB 83]. Indeed, the staircase is “complete,” like the one we shall encounter later in this chapter in connection with the mode locking of two oscillators. *Complete* means that the rational plateaus in Figure 1 add up to the entire  $H$  interval. Irrational values of  $w$  occur at values of  $H$  that form a thin Cantor set, whose fractal dimension  $D$  can be determined analytically for power-law interactions of the form  $J_{ij} = |i - j|^{-\alpha}$ :

$$D = \frac{2}{1 + \alpha} \quad (4)$$

The plateau for  $w = \frac{1}{2}$  (see Figure 1) has a relative length of 0.44, and the two intervals for  $w \neq \frac{1}{2}$  are equal:  $r_1 = r_2 = 0.28$ . If the devil's staircase for the one-

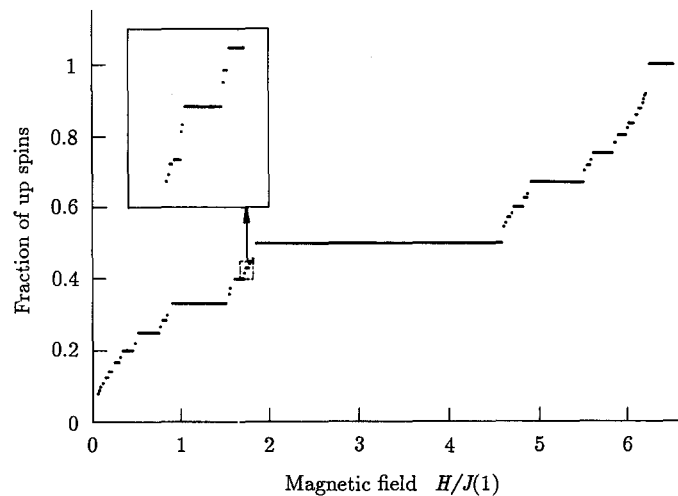


**Figure 1** Fraction of up-spins as a fraction of magnetic field for an Ising spin glass [BB 82].

dimensional Ising “antiferromagnet” were exactly self-similar, the Hausdorff dimension would equal

$$D = \frac{\log N}{\log (1/r)} = \frac{\log 2}{\log (1/0.28)} = 0.54$$

Since, according to equation 4,  $D = 0.6$  for  $\alpha = 2$ , the staircase cannot be exactly self-similar. However, the plateau at  $w = \frac{1}{3}$  (and the one at  $w = \frac{2}{3}$ , with  $r_1 = 0.47$  and  $r_2 = 0.18$ , implies a fractal dimension  $D = 0.59$ , which is obtained from the formula for unequal remainders,  $r_1 \neq r_2$ :

$$r_1^D + r_2^D = 1$$

Thus, it is not unreasonable to expect the devil’s staircase of Figure 1 to be asymptotically self-similar or self-affine. This is also suggested by the 10-times magnified portion of staircase shown in the insert in Figure 1. The largest plateau in the insert corresponds to  $w = \frac{3}{7}$ .

## Quasiperiodic Spatial Distributions

The devil’s staircase for Ising spins, not being precisely self-similar, is at best asymptotically self-similar. How do we approach such a staircase to test its self-similarity? Figure 1 suggests that the larger the denominator  $q$  in  $w = p/q$ , the smaller the locked plateau.

The physical situation would lead to the same conclusion. After all,  $w$  is the period length of the spin configuration, and intuition tells us that the larger the period length, the more tenuous the configuration, and hence the smaller the plateau.

How are the spins arranged for  $w \neq \frac{1}{2}$ ? The answer is about the simplest formula imaginable to satisfy basic symmetries. Suppose  $w = p/q$ , where  $p$  and  $q$  are *coprime* integers (i.e., their largest common divisor equals 1).<sup>4</sup> Then  $p$  of every  $q$  spins should point up. More precisely,  $p$  of every  $q$  consecutive spins should be up. Thus, the spin pattern must be periodic with period length  $q$ . Within each period, precisely  $p$  spins are up and  $q - p$  spins are down—but which are up and which are down? Obviously, for  $w = \frac{3}{7}$ , for example, having three adjacent spins point up and the next four down is not a minimum-energy solution. For a lower energy, the up and down spins must be better intermingled. But how? Detailed theoretical analysis shows that, with the initial condition  $s_0 = +1$ , the locations  $u_k$  of the up spins are given by the simple formula

$$u_k = \left\lfloor \frac{k}{w} \right\rfloor \quad k = \dots, -2, -1, 0, 1, 2, 3, 4, 5, \dots \quad (5)$$

where the floor function  $\lfloor a \rfloor$  is the largest integer not exceeding  $a$ .

With  $w = \frac{1}{2}$ , equation 5 tells us that the position of the  $k$ th up spin is  $2k$ , in agreement with equation 3.

The corresponding locations  $d_k$  of the down spins are given by the set of integers complementary to the set  $u_k$ :

$$d_k = \left\lceil \frac{k}{1-w} \right\rceil - 1 \quad (6)$$

where the ceiling ("gallows") function  $\lceil a \rceil$  means the smallest integer not smaller than  $a$ .

For  $w = p/q = \frac{3}{7}$ , for example, equation 5 tells us that the up spins are at location

$$u_k = \dots, -5, -3; 0, 2, 4; 7, 9, 11; \dots \quad (7)$$

while the down spins, according to equation 6, are to be found at locations

$$d_k = \dots, -4, -2; -1, 1, 3, 5; 6, 8, 10, 12; \dots \quad (8)$$

As can be seen, both sets  $u_k$  and  $d_k$  are periodic with period  $q = 7$ , in the sense

---

4. In number theory, this frequent condition is rendered as  $(p, q) = 1$ . In general,  $(p, q) = m$  means that  $m$  is the largest common divisor of  $p$  and  $q$ .

that if  $u_k = n$  for some  $k$ , then, for some other  $k' (= k + 3)$ ,  $u_{k'} = u_k + 7$ . Similarly, for  $k' = k + 4$ ,  $d_{k'} = d_k + 7$ . The locations  $u_k$  and  $d_k$  together cover all the integers, each integer exactly once. (A simple proof for irrational  $w$  is given in my book on number theory [Schr 90].)

Equations 5 and 6 distribute the up- and down-spins as uniformly as possible under the given constraints—something we already guessed for a minimum-energy “antiferromagnet.” In fact, equation 7 shows that for  $w = \frac{3}{7}$ , the three spacings per period between the up-spins are 2, 2, 3. The spacing pattern for the four down-spins per period for  $w = \frac{3}{7}$  is—according to equation 8—2, 2, 2, 1. In general, it can be shown that, since the spacings have to be integers and add up to the period length  $q$  for both up- and down-spins, the spacings generated by equations 5 and 6 have in fact the least variance.

There is a close connection between these stable spin patterns and the motion in phase space of simple conservative dynamic systems with two degrees of freedom, such as two coupled oscillators. Depending on the nonlinear coupling strength, the motion will be periodic, quasiperiodic, or chaotic. If the two oscillator frequencies are commensurate, that is, if they are locked into a rational frequency ratio  $p/q$ , then the phase space trajectory of the system on the surface of a torus (an “inner tube”) will be periodic with period  $q$ . The trajectory will close after  $p$  cycles around the torus’s second dimension. Thus, a plane cut (called a *Poincaré section*) normal to the first dimension of the torus will be pierced by  $q$  distinct points with angles  $\theta_1, \theta_2, \dots, \theta_q$ .

To simplify the description even further, we can replace the angles  $\theta_k$  by their signs: a plus sign if  $0 \leq \theta_k < \pi$ , say, and a minus sign for  $\pi \leq \theta_k < 2\pi$ . Setting  $\theta_0 = 0$ , the successive five angles (modulo  $2\pi$ ) are  $\theta_k/2\pi = 0, \frac{3}{5}, \frac{1}{5}, \frac{4}{5}, \frac{2}{5}$ . The corresponding sign sequence, also called the *symbolic dynamics*, is  $+ - + - +$ . This is precisely the spin pattern of our antiferromagnetic Ising spin system locked in an up-spin ratio of  $w = \frac{3}{5}$ . Indeed, equation 5 gives the locations for the up-spins for  $k = 1, 2, 3$  at  $u_k = 1, 3$ , and 5. Thus, the spin pattern is  $+ - + - +$ . Because of the close analogy between toroidal trajectories winding around a torus in phase space and (quasi) periodic or chaotic spatial patterns (spins and quasicrystals, for example), people often refer to the ratio  $w$  as a *winding number*.

For irrational  $w$ , the spin pattern will be quasiperiodic rather than periodic. For example, for  $w = (\sqrt{5} - 1)/2$ , the golden mean, the up-spins, according to equation 5, will be at locations

$$u_k = 1, 3, 4, 6, 8, \dots \quad \text{for } k = 1, 2, 3, \dots$$

and the down spins, according to equation 6, will be at

$$d_k = 2, 5, 7, 10, 13, \dots$$

Note that the differences  $d_k - u_k = k$ . Each pair  $(u_k, d_k)$  forms a so-called Beatty pair, a winning combination in a game of Fibonacci nim (see page 307).

## Beatty Sequence Spins

If the energetically favorable proportion of up-spins equals  $w$ , which in general will be different from  $\frac{1}{2}$ , the locations  $u_k$  of the individual up-spins are given by the *Beatty sequence* (equation 5). The locations of the down-spins are given by the *complementary Beatty sequence* (equation 6).

Instead of the Beatty sequences for the *locations* of the up- and down-spins, we can give a simple formula for the spin values themselves. For irrational  $w$  we have

$$s_m = \text{sgn} [w - \langle (m+1)w \rangle_1] \quad (9)$$

where  $\text{sgn}$  is the algebraic sign function and  $\langle \rangle_1$  stands for the fractional part.

For the golden mean,  $w = (\sqrt{5} - 1)/2$ , the sequence of spin signs is  $+ - + + - + - + + - \dots$ , which can also be obtained from the iterated “rabbit” map (see Chapter 13)

$$\begin{array}{rcl} - & \rightarrow & + \\ + & \rightarrow & + - \end{array} \quad (10)$$

Starting with a single minus sign yields the following successive generations and their lengths  $L_i$ :

—	$L_1 = 1$
+	$L_2 = 1$
+ —	$L_3 = 2$
+ — +	$L_4 = 3$
+ — + + —	$L_5 = 5$

and so on. An equivalent rule to generate generation  $n$  is to append generation  $n-2$  to generation  $n-1$ . Note that, as a consequence, the length  $L_n$  of the  $n$ th generation obeys the recursion  $L_n = L_{n-1} + L_{n-2}$ . With  $L_1 = L_2 = 1$ , this results in the Fibonacci numbers  $L_n = 1, 1, 2, 3, 5, 8, 13, \dots$ .

The relative number of up-spins in generation  $n$  equals  $L_{n-1}/L_n$ , which approaches the golden mean  $(\sqrt{5} - 1)/2 = 0.618 \dots$ , as it should.

The Beatty sequence for  $w = (\sqrt{5} - 1)/2$  leads to a one-dimensional analogue of a *quasicrystal* with a fivefold rotational symmetry (see Chapter 13). Such a symmetry is forbidden for *periodic* crystals, but was observed in 1984 when the first quasicrystal was discovered.

The mapping in equation 10 is closely related to the continued fraction (CF) expansion of the golden mean  $(\sqrt{5} - 1)/2 = [1, 1, 1, \dots] = [\overline{1}]$ . For another simple continued fraction with period length equal to 1, that of  $w = \sqrt{2} - 1 = [\overline{2}]$ , the corresponding mapping that generates the spins according to

equation 9, namely,  $-- + - + -- + - + - + \dots$ , is

$$\begin{aligned} - &\rightarrow - + \\ + &\rightarrow - + - \end{aligned} \tag{11}$$

which, starting with a single minus sign, gives the following successive generations:

$$\begin{aligned} - &L_1 = 1 \\ - + &L_2 = 2 \\ - + - + - &L_3 = 5 \\ - + - + - + - + - + &L_4 = 12 \end{aligned}$$

and so on. The alternate rule for generating generation  $n$  is to repeat generation  $n - 1$  twice and append generation  $n - 2$ . Beginning with  $-$  and  $- +$ , this yields the generations just shown, which grow in length  $L_n$  according to the recursion  $L_{n+1} = 2L_n + L_{n-1}$ . With  $L_1 = 1$  and  $L_2 = 2$ , this gives the successive lengths 1, 2, 5, 12, 29, 70, 169. Note that  $L_{n-1}/L_n$  approaches the value of  $w = \sqrt{2} - 1$ . Also, the relative number of up-spins approaches, as it should,  $w = \sqrt{2} - 1$ . In fact, of the  $L_n$  spins in generation  $n$ , precisely  $L_{n-1}$  are up and  $L_n - L_{n-1} = L_{n-1} + L_{n-2}$  are down. The ratio  $L_{n-1}/L_n$  approaches  $w$  as quickly as possible (for given bounds on the denominators). Note that, according to these lengths, the ratio  $70/(29 + 70) = 70/99 = 0.70707 \dots$ , for example, should be a good approximation to  $1/\sqrt{2} = 0.70710 \dots$ , as it is indeed.

When  $w = \sqrt{2} - 1$  is used in equation 9, it will generate the same sequence as the iterated mapping in equation 11. Equations 5 and 6, with  $w = \sqrt{2} - 1$ , will generate the corresponding *locations* of the up- and down-spins.

In the context of quasicrystals, the quadratic irrational number  $\sqrt{2} - 1 = [\bar{2}]$  leads to a one-dimensional model of a quasicrystal with a “forbidden” eightfold rotational symmetry, first described by Wang, Chen, and Kuo [WCK 87].

Similarly, the spin sequence for  $w = [\bar{3}] = (\sqrt{13} - 3)/2$  in equation 9,

$$-- + - - + - - + - \dots$$

can also be generated by the iterated mapping

$$\begin{aligned} - &\rightarrow - - + \\ + &\rightarrow - - + - \end{aligned} \tag{12}$$

Equivalently, starting with the two initial generations  $-$  and  $-- +$ , generation  $n > 2$  is generated by repeating generation  $n - 1$  three times and appending generation  $n - 2$ . It follows directly that the length  $L_n$  of the  $n$ th

generation obeys the recursion  $L_n = 3L_{n-1} + L_{n-2} = 1, 3, 10, 33, 109, 360, \dots$  and  $L_{n-1}/L_n$  approaches  $w = [\bar{3}]$ .

Does the mapping in equation 12 tell us that the number of up-spins in generation  $n$ ,  $m_n^+$ , divided by the total number of spins,  $L_n = m_n^+ + m_n^-$ , approaches the desired ratio  $w = [\bar{3}]$ ? It does indeed. First we observe from mapping 12 that each spin (either up or down) in generation  $n-1$  generates precisely one up-spin in generation  $n$ . Therefore  $m_n^+ = L_{n-1}$ . Thus, the relative number of up-spins equals  $L_{n-1}/L_n$ , which, as we already saw, approaches

$$[\bar{3}] = \frac{(\sqrt{13} - 3)}{2} = 0.3027756 \dots$$

The convergence is quite rapid, too. For example,

$$\frac{L_5}{L_6} = \frac{109}{360} = 0.3027777 \dots$$

In general, the spin pattern for  $w$  equal to a periodic CF with period length 1,  $w = [\bar{n}]$ , is given by the iteration

$$\begin{aligned} - &\rightarrow (-)^{n-1} + \\ + &\rightarrow (-)^{n-1} + - \end{aligned} \tag{13}$$

where  $(-)^{n-1}$  means a sequence of  $n-1$  minus signs.

For  $w = [\bar{n}]$ , we have the relation

$$\frac{1}{w} = n + w$$

The positive solution of this quadratic equation yields

$$\tau_n^+ = \frac{\sqrt{n^2 + 4} - n}{2}$$

which is called a *silver mean* because  $\tau_n^+$ , like the golden mean, has a periodic continued fraction with period length equal to 1. For the special case of  $n = 1$ , silver turns into gold and we get the golden mean  $w = \tau_1^+ = \gamma = (\sqrt{5} - 1)/2$ .

If we relax the condition that the terms of the continued fraction have to be positive, then we get a second family of silver means, defined by

$$\frac{1}{\tau_n^-} = n - \tau_n^- \quad n = 2, 3, \dots$$

with the unique root in the interval  $[0, 1]$

$$\tau_n^- = \frac{n - \sqrt{n^2 - 4}}{2}$$

and the continued fraction expansion

$$\tau_n^- = [n-, n-, n-, \dots]$$

Spin patterns for these silver means, too, can be generated by simple iterated mappings. For example, for  $n = 4$ , we have  $\tau_4^- = 2 - \sqrt{3} = 0.268 \dots$ . With this  $\tau_4^-$  in equation 5, we find the up-spins at  $u_k = 3, 7, 11, 14, 18, \dots$ . Thus, the pattern of spins for  $\tau_4^-$  is

$$- \quad - + - \quad - - + - - - + - - + - , \quad - - + - - - + \dots \quad (14)$$

To find the spin-mapping law, we have to compute the approximants of the continued fraction:  $\frac{1}{4}, 1/(4 - \frac{1}{4}) = \frac{4}{15}, \frac{15}{56}$ , and so on, where the denominators (4, 15, 56, ...) are the period lengths. The length of the  $n$ th generation  $L_n$  ( $n > 1$ ) is given by  $4L_{n-1} - L_{n-2}$ , starting with  $L_0 = 0$  and  $L_1 = 1$ . Marking off subsequences of these lengths by commas (see spin pattern 14) reveals the iteration law

$$\begin{aligned} - &\rightarrow - - + - \\ + &\rightarrow - - + \end{aligned}$$

which, starting with a single minus sign, produces the following successive generations:

$$\begin{aligned} - & \qquad \qquad \qquad L_1 = 1 \\ - - + - & \qquad \qquad \qquad L_2 = 4 \\ - - + - - - + - - - + - - + - & \qquad \qquad \qquad L_3 = 15 \end{aligned}$$

and so on, in uncanny agreement with spin pattern 14.

The silver mean  $\tau_4^- = 2 - \sqrt{3}$  is the basis for generating quasicrystals with a forbidden twelvefold symmetry, which were discovered in 1988 [CLK 88].

All silver means  $\tau_N^+$  ( $\tau_N^-$ ), where  $N$  equals an even- (odd-) index Lucas number, belong to the irrational number field  $\mathbb{Q}(\sqrt{5})$  and lead to fivefold symmetric quasicrystals. The Lucas numbers,  $L_n = 2, 1, 3, 4, 7, 11, 18, \dots$ , are defined by the same recursion as the Fibonacci numbers:  $L_n = L_{n-1} + L_{n-2}$ , but with the initial condition  $L_0 = 2$ ,  $L_1 = 1$ . For  $n > 1$ ,  $L_n$  can be obtained by rounding  $\gamma^{-n}$  to the nearest integer.

It is a fair guess that the general mapping law for  $\tau_n^-$  is given by

$$\begin{aligned} - &\rightarrow (-)^{n-2} + - \\ + &\rightarrow (-)^{n-2} + \end{aligned} \quad (15)$$

where  $(-)^{n-2}$  stands for a sequence of  $n-2$  minuses. The reader may wish to prove this and the following equivalent law: beginning with the first two generations  $-$  and  $(-)^{n-2} + -$ , generation  $k$  is obtained by repeating the previous generation  $(n-1)$  times and appending generation  $k-1$ , from whose beginning generation  $k-2$  has been eliminated.

## The Scaling Laws for Quasiperiodic Spins

Equation 9 allows us to calculate the sign of any spin directly without recursion. For example, for  $w = (\sqrt{13} - 3)/2$ , the 1000th spin is  $+$ . On the other hand, the very fact that, for  $w$  equal to a periodic continued fraction of the form  $[\bar{n}]$ , our antiferromagnetic Ising spins can be calculated recursively by an iterated mapping suggests that these spin patterns must have some scaling invariance. And indeed they have—in fact, they enjoy numerous self-similarities.

Let us focus on the spin pattern for the winding number  $w$  equal to the golden mean. In  $\{0, 1\}$  notation this is the “rabbit” sequence:

$$\underline{1} \ 0 \ 1 \ \underline{1} \ 0 \ \underline{1} \ 0 \ 1 \ \underline{1} \ 0 \ 1 \ \underline{1} \ 0 \dots \quad (16)$$

The infinite rabbit sequence reproduces itself if, for every 1 we encounter (beginning on the left), we hop ahead two places and strike out the third bit. For every 0, we hop only one place and eliminate the second bit. The digits retained by this mad hopping and striking-out scheme are underlined in sequence 16, and the decimated sequence does reproduce the original rabbit sequence. The pattern of long and short underscores also corresponds to the rabbit sequence, albeit by construction. And, maddeningly, the *struck-out* (nonunderlined) digits *also* reproduce the original rabbit sequence. Can the reader show why?

What the hopping scheme really does is to map  $101 \rightarrow 10$  and  $10 \rightarrow 1$ , as can be seen from sequence 16. This “block-renaming” scheme, which we have encountered before, is in effect the reverse of the mapping  $1 \rightarrow 10 \rightarrow 101$ , which is the next iteration of the original mapping ( $0 \rightarrow 1 \rightarrow 10$ ).

The block renaming  $101 \rightarrow 10$  and  $10 \rightarrow 1$  corresponds to a simple scaling of the index  $k$  by a factor  $w$ . Specifically, in the formula for the up-spins (equation 5),  $k$  is replaced by  $k' = k/w$  and the spin pattern is laterally transposed by one unit:

$$u_{k'} = u_{k/w} - 1 = \left\lfloor \frac{k}{w^2} \right\rfloor - 1$$

However, according to equation 6,  $\lfloor k/w^2 \rfloor = \lfloor k/(1-w) \rfloor = \lfloor k/(1-w) \rfloor - 1$  are the locations of the original *down*-spins  $d_k$ . Thus, we see that in the scaled spin pattern, obtained by the block-renaming renormalization, the retained up-spins are one site to the left of the original down-spins. Indeed, as we can see from expression 16, the surviving up-spins are precisely those that have a 0 as a right neighbor. All other up-spins “die” in the construction.

We leave it to the reader to show that the surviving *down*-spins are to be found one site to the left of the original up-spin doublets 11 (whose density, like that of the surviving down-spins, is  $w^3 = \sqrt{5} - 2 = 0.236 \dots$ ).

## Self-Similar Winding Numbers

The scaling law for the antiferromagnetic Ising spins can also be derived from the formula (equation 9) that generates the spins in the  $\pm 1$  notation:

$$s_m = \operatorname{sgn} [w - \langle (m+1)w \rangle_1]$$

Obviously, there is no change in the spin  $s_m$  if we add any integer—for example,  $n(m+1)$ —to the contents of the fractional-part brackets  $\langle \rangle_1$ :

$$s_m = \operatorname{sgn} [w - \langle (m+1)(w+n) \rangle_1] \quad (17)$$

For  $w$  equal to the golden mean, we have  $w+1=1/w$ . Hence, with  $n=1$ ,

$$s_m = \operatorname{sgn} \left[ w - \left\langle (m+1) \frac{1}{w} \right\rangle_1 \right]$$

which tells us that the index  $m+1$  can be formally scaled by the factor  $1/w^2$  without changing the spin pattern.

What other winding numbers show this kind of self-similarity? Equation (17) shows that for all  $w$  for which  $(w+n)=1/w$  we can scale  $m+1$  by a factor of  $1/w^2$ . Here  $n$  can be a positive or negative integer. (Note that  $\langle \alpha \rangle_1 := \alpha - \lfloor \alpha \rfloor$  lies in the interval  $[0, 1)$ , so that for  $\alpha = -4.7$ , for example,  $\langle \alpha \rangle_1 = \langle -4.7 \rangle_1 = 0.3$ .) For positive  $n$ , these winding numbers are precisely those whose continued fraction expansion is periodic and has period length 1:

$$w = \tau_n^+ := [\tilde{n}] \quad n > 0$$

In fact, this equation can be written as

$$w = \frac{1}{n+w} \quad (18)$$

which is the relationship we need for the scaling invariance of equation 17.

The solution of the quadratic equation 18 for positive  $w$  is

$$w = \tau_n^+ = \frac{\sqrt{n^2 + 4} - n}{2} \quad n > 0$$

as already stated.

For negative  $n$ , the two roots of this equation are outside the “legal” interval  $(0, 1)$  for  $w$ . However, we can still get a self-similar solution, namely, for

$$w = \tau_n^- := [\bar{n}] \quad n < -1$$

The solution of this equation that lies in  $(0, 1)$  is

$$w = \tau_n^- = -\frac{\sqrt{n^2 - 4} + n}{2} \quad n < -2 \quad (19)$$

The numbers  $\tau_n^+$  and  $\tau_n^-$  are the *silver means*, another generalization of the golden mean that we have previously encountered.

How does the scaling law for the spin-generating formula in equation 5 translate into a scaling law for the up-spins? In other words, what change in equation 5 is necessary so that it gives the locations of the up-spins surviving the block-decimation process for  $n > 1$ ?

## Circle Maps and Arnold Tongues

Next to the quadratic map, discussed in Chapter 12, another nonlinear law plays an important role for modeling a great many natural phenomena, the famous *circle map*:

$$\theta_{n+1} = \theta_n + \Omega - \frac{K}{2\pi} \sin(2\pi\theta_n) \quad (20)$$

Here  $K$  is a “coupling constant,” which regulates the degree of nonlinearity; in fact, for  $K = 0$ , equation 20 is linear. The variable  $\theta_n$  represents an angle, usually in the phase space of a dynamic system. The average increment per iteration of  $\theta_n$  is called the *dressed winding number*, defined as

$$w := \lim_{n \rightarrow \infty} \frac{\theta_n - \theta_0}{n} \quad (21)$$

The parameter  $\Omega$  in equation 20 is called the *bare winding number*. This curious nomenclature stems from the fact that the phase space in question is often a

torus around which the trajectory *winds* its way. In a typical application, the *bare* winding number represents a frequency ratio, such as the resonant frequency of an oscillator, a swing, say, divided by the frequency of a periodic force acting on the resonator. The *dressed* winding number  $w$  represents the frequency ratio, usually a rational number  $w = P/Q$ , into which the system has been “locked” by some nonlinear coupling. Of course, for  $K = 0$ ,  $w = \Omega$  and there is no mode locking to rational winding numbers  $w$ . But for  $K = 1$ , yielding the *critical* circle map, the mode-locked regions cover the entire  $\Omega$  interval (see Figure 7 in Chapter 7), leaving only a Cantor set of  $\Omega$  values unlocked. The locked regions are called *Arnold tongues* after their discoverer, the Russian mathematician V. I. Arnol'd.

The critical circle map has a *cubic inflection point* for  $\theta_n = 0$  and can be approximated by

$$\theta_{n+1} = \Omega + \frac{2\pi^2}{3} \theta_n^3 \quad (22)$$

for  $|\theta_n| \leq 1$ . Most of the results obtained for the critical circle map are in fact *universally* valid for all maps with a zero-slope cubic nonlinearity. This universality corresponds to the universality of the results for unimodal maps with a quadratic maximum. Together the quadratic map and the cubic map model many nonlinear phenomena, characterized by either a symmetric (even) nonlinearity or an *anti*-symmetric (odd) nonlinearity.

For  $K > 1$ , the circle map is nonmonotonic and the Arnold tongues overlap each other, giving rise to chaotic motion. Just as the transition to chaos in the quadratic map can be studied by period-doubling bifurcations, the route to chaos in the critical circle map too is analyzed in terms of orbits with increasing period lengths. But here the preferred period lengths are equal to the Fibonacci numbers  $F_n$  and the dressed winding numbers  $w$  (or  $1 - w$ ) are ratios of adjacent Fibonacci numbers. With  $n$  going to infinity, these winding numbers approach the golden mean.

Even the most important symbolic dynamics of these two prototypical nonlinearities are similar to each other, as we shall see later in this chapter.

Figure 6 in Chapter 7 shows the dressed winding number  $w = P/Q$  as a function of the bare winding number  $\Omega$  for the critical circle map. It is a devil's staircase with horizontal plateaus at *all* rational values of  $w$  (as opposed to the devil's staircase based on the original Cantor set, which has plateaus only for  $w = P/Q$  with  $Q = 2^n$ ). Although not exactly self-affine, like the Cantor staircase, the mode-locking staircase shows an approximate self-affinity, as seen in the inset.

The widths of the plateaus obviously have a tendency to decrease with increasing value of  $Q$ , which is the period length of the frequency-locked motion. This is intuitively clear, because modes lock preferentially into frequency ratios involving small integers, such as the ratio of planet Mercury's orbital frequency around the sun to its spin frequency around itself, which equals  $\frac{2}{3}$ .

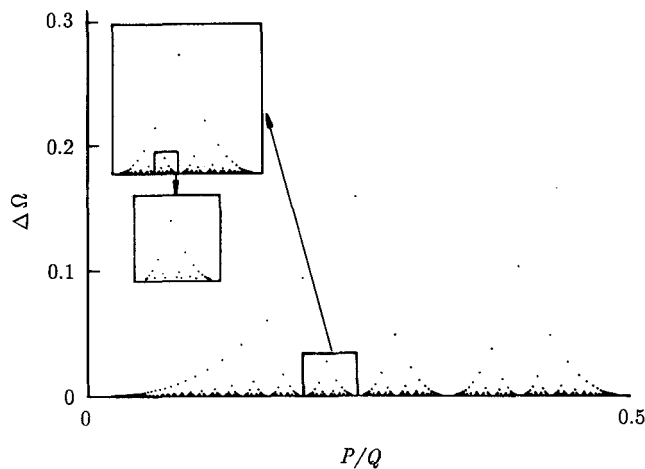


**Figure 2** Width of frequency-locked intervals as a function of frequency ratio. Note self-similarity revealed by successive magnifications ratio [JBB 84].

Figure 2 shows the width of the plateaus  $\Delta\Omega$  as a function of  $P/Q$ , calculated by Jensen, Bak, and Bohr [JBB 84]. Again there is a great deal of self-similarity, as shown in the insets. The scaling of  $\Delta\Omega$  with  $Q$  found by these authors has an exponent  $\log(\Delta\Omega)/\log Q \approx 2.292$ .

The fractal defined by those values of  $\Omega$  for which no mode locking takes place is in fact a *multifractal*, with  $D_q$  ranging from  $D_{-\infty} \approx 0.924$  down to  $D_\infty = 0.5$ . As explained in Chapter 9,  $D_{-\infty}$  corresponds to the thinnest region of the fractal, which here is located around  $\Omega$  equal to the golden mean  $\gamma$ , the most difficult frequency ratio to mode-lock. Shenker found the lengths  $r_n$  to scale asymptotically as  $F_n^{-\delta} \sim \gamma^{n\delta}$ , with  $\delta = 2.1644 \dots$ , for  $\Omega_n = F_{n-1}/F_n$ ,  $n \rightarrow \infty$ , called the golden-mean route to chaos [She 82]. With the probabilities given by  $p_n \sim \gamma^{2n}$  and  $r_n \sim \gamma^{n\delta}$ , one finds

$$D_{-\infty} = \lim_{n \rightarrow \infty} \frac{\log p_n}{\log r_n} = \frac{2}{\delta} \approx 0.924$$

The most concentrated region of the mode-locking fractal lies just to the right of the locked interval for the frequency ratio 0 (near  $\Omega = 1/2\pi$ ) as it is approached by the frequency ratios  $1/Q$ , with  $Q \rightarrow \infty$ . This is the so-called harmonic series, which is comparatively easy to mode-lock. For the harmonic series, changes in dressed winding numbers are asymptotically proportional to the square root of the changes in the bare winding number—that is,  $p_n \sim r_n^{1/2}$ . Thus,  $D_\infty = 0.5$  exactly.

The entire multifractal spectrum  $f(\alpha)$  was calculated from 1024 mode-locked intervals by Cvitanović, Jensen, Kadanoff, and Procaccia [CJKP 85]. The maximum of  $f(\alpha)$  equals approximately 0.868 and corresponds to the Hausdorff dimension  $D_0$  of the multifractal underlying the mode-locking staircase.

## Mediants, Farey Sequences, and the Farey Tree

In order to calculate the dimensions  $D_q$  of the mode-locking fractal and its multifractal spectrum  $f(\alpha)$ , some order has to be imposed on the rational numbers  $P/Q$  representing different frequency ratios. One such ordering is used in the standard proof that the rational numbers (as opposed to the irrational numbers) form a countable set. Here we need a different ordering, one that better reflects the physics of mode locking.

Suppose the parameter  $\Omega$  in equation 20, the bare winding number, is such that the dressed winding number falls somewhere between  $\frac{1}{2}$  and  $\frac{2}{3}$  without actually locking into either one. What is the most likely locked-in frequency ratio for a nonlinear coupling strength just below the value that would cause mode locking at  $\frac{1}{2}$  or  $\frac{2}{3}$ ? It seems reasonable that it should be a frequency ratio  $P/Q$  in the interval  $(\frac{1}{2}, \frac{2}{3})$  with  $Q$  as small as possible.

Indeed, this is precisely what happens in dynamic systems modeled by the circle map. Adjust the nonlinear coupling strength  $K$  and the bare winding number  $\Omega$  to a point just below the crossing of the two Arnold tongues for the locked frequency ratios  $\frac{1}{2}$  and  $\frac{2}{3}$ . The dressed winding number  $w$  for this point in the  $\Omega$ - $K$  plane must be rational because  $K > 1$ . In fact, the rational value  $P/Q$  that  $w$  assumes is given by  $\frac{1}{2} < P/Q < \frac{2}{3}$  with  $Q$  as small as possible.

This raises an interesting mathematical question with a curious but simple answer: What is the ratio following  $\frac{1}{2}$  and  $\frac{2}{3}$  with the *smallest* denominator? If you ask a kindergartner to add  $\frac{1}{2}$  and  $\frac{2}{3}$ , he or she may well add numerators and denominators separately and write

$$\frac{1}{2} + \frac{2}{3} = \frac{3}{5}$$

and in so doing will have discovered the looked-for “locked-in” fraction with the smallest denominator.<sup>5</sup>

---

5. This is somewhat reminiscent of S. N. Bose (1894–1974), the celebrated Indian physicist, who, in deriving photon statistics, “forgot” to take account of the photon’s (nonexistent) distinguishability. When *Nature* (not nature) turned his paper down, Bose wrote to Einstein, who saw the light and recognized Bose’s “mistake” as the long-sought-after answer in the statistical physics of light. Bose’s name has become enshrined ever since in the *Bose-Einstein* distribution, *bosons* (integer-spin particles, such as the photon) and *Bose condensation*, which gives us superconductivity and other macroscopic marvels of the microscopic quantum world.

What can such a strange strategy for forming intermediate fractions possibly mean? Physically, the frequency ratio  $1/2$  of two oscillators can be represented by a pulse (1) followed by a “nonpulse” (0) of the faster oscillator during every period of the slower oscillator. Thus, the frequency ratio  $1/2$  is represented by the sequence  $101010\dots$  or simply  $\overline{10}$ . Similarly, the frequency ratio  $2/3$  is represented by two 1s repeated with a period of three:  $\overline{110}$ .

Now, to form an intermediate frequency ratio, we simply *alternate* between the frequency ratios  $1/2$  (i.e.,  $\overline{10}$ ) and  $2/3$  (i.e.,  $\overline{110}$ ), yielding  $\overline{10110}$ , which represents the frequency ratio  $3/5$  (3 pulses during 5 clock times). So, in averaging frequency ratios, taking *mediants*, as this operation is called, is not such a strange thing after all.

In general, given two reduced fractions  $P/Q$  and  $P'/Q'$ , the desired intermediate fraction is given by

$$\frac{P''}{Q''} = \frac{P + P'}{Q + Q'}$$

and is called the *mediant* by number theorists. In a penetrating analysis of Diophantine equations, John Horton Conway showed that numerators and denominators can be interpreted as the components of a two-dimensional *vector* and that the intermediate fraction with the lowest denominator is obtained by componentwise vector addition [unpublished, personal communication, 1989]. Thus, for example, the mediant of  $\frac{5}{13}$  and  $\frac{2}{5}$  equals  $\frac{7}{18}$  (the revolutionary frequency ratio that Jupiter and Pallas selected for their gravitationally coupled orbits around the sun). (As it happens, there is not a single fraction between  $\frac{5}{13}$  and  $\frac{2}{5}$  with a denominator smaller than 18.) For this to be true, the two parent fractions must be sufficiently close. More precisely, they must be *unimodular*. The *modularity* of two reduced fractions  $P/Q$  and  $P'/Q'$ , which measures their closeness for our purposes, is defined as the absolute difference  $|QP' - PQ'|$ , and unimodular fractions are those for which  $|QP' - PQ'|$  equals 1.

The mediant of two fractions has the same modularity with its two parents as the parents have between them: modularity is another hereditary trait. Inheritance is a pivotal property, in self-similarity, including the self-similarities found in mode locking.

Mediants occur naturally in *Farey sequences*. A Farey sequence is defined as the sequence of fractions between 0 and 1 of a given largest denominator (called the *order* of the sequence). Thus, the Farey fractions of order 5 are (in increasing magnitude):

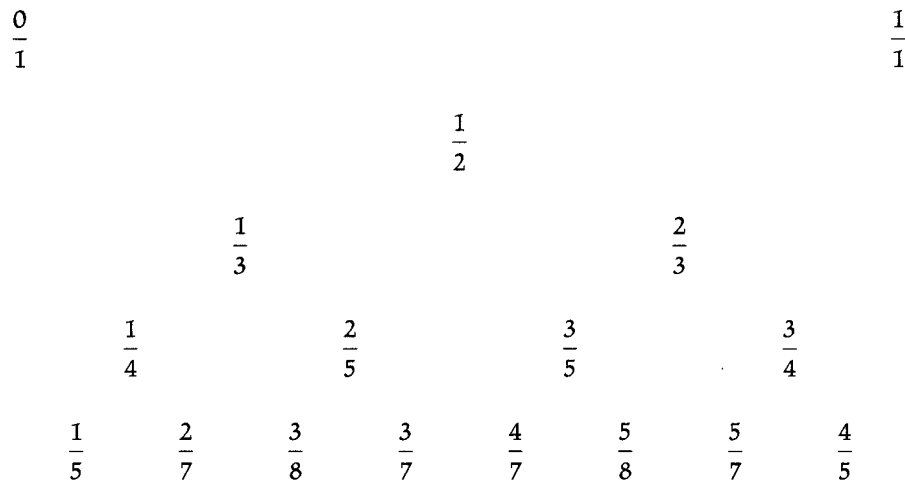
$$\frac{0}{1}, \frac{1}{5}, \frac{1}{4}, \frac{1}{3}, \frac{2}{5}, \frac{1}{2}, \frac{3}{5}, \frac{2}{3}, \frac{3}{4}, \frac{4}{5}, \frac{1}{1}$$

Notice that each fraction is the mediant of its two neighbors. The modularity between all adjacent fractions equals 1, but they are not uniformly spaced.

However, Riemann's famous hypothesis, concerning the zeros of his zeta function, guarantees that the spacings between adjacent fractions are relatively uniform [Schr 90].

While Farey sequences have many useful applications and nice properties, such as classifying the rational numbers according to the magnitudes of their denominators (in fact, there are entire books listing nothing but Farey fractions), they suffer from a great irregularity: the number of additional fractions in going from Farey sequences of order  $n - 1$  to those of order  $n$  equals the highly fluctuating Euler's function  $\phi(n)$ , defined as the number of positive integers smaller than and coprime with  $n$ . For example,  $\phi(5) = 4$ ,  $\phi(6) = 2$ , and  $\phi(7) = 6$ . A much more regular order is infused into the rational numbers by *Farey trees*, in which the number of fractions added with each generation is simply a power of 2.

Starting with two fractions, we can construct a Farey tree by repeatedly taking the mediants of all numerically adjacent fractions. For the interval  $[0, 1]$ , we start with  $\frac{0}{1}$  and  $\frac{1}{1}$  as the initial fractions, or "seeds". The first five generations of the Farey tree then look as follows:



Each rational number between 0 and 1 occurs exactly once somewhere in the infinite Farey tree. The tree's construction reflects precisely the interpolation of locked frequency intervals in the circle map by means of mediants. The Farey tree is therefore a kind of mathematical skeleton of the Arnold tongues.

The location of each fraction within the tree can be specified by a binary address, in which 0 stands for moving to the left in going from level  $n$  to level  $n + 1$  and 1 stands for moving to the right. Thus, starting at  $\frac{1}{2}$ , the rational number  $\frac{3}{7}$  has the binary address 011. The complement of  $\frac{3}{7}$  with respect to 1 (i.e.,  $\frac{4}{7}$ ) has the complementary binary address: 100. This binary code for the rational numbers is useful in describing coupled oscillators.

Note that any two *numerically* adjacent fractions of the tree are unimodular. For example, for  $\frac{4}{7}$  and  $\frac{1}{2}$ , we get  $2 \cdot 4 - 1 \cdot 7 = 1$ .

Some properties of the Farey tree are particularly easy to comprehend in terms of continued fractions, which for numbers  $w$  in the interval  $[0, 1]$  look as follows:

$$w = \cfrac{1}{a_1 + \cfrac{1}{a_2 + \cfrac{1}{a_3 + \dots}}}$$

but are more conveniently written as  $w = [a_1, a_2, a_3, \dots]$ , where the  $a_k$  are positive integers. Irrational  $w$  have nonterminating continued fractions. For quadratic irrational numbers the  $a_k$  will (eventually) repeat periodically. For example,  $1/\sqrt{3} = [1, 1, 2, 1, 2, 1, 2, \dots] = [1, \overline{1, 2}]$  is preperiodic and has a period of length 2;  $1/\sqrt{17} = [8]$  has period length 1 and  $1/\sqrt{61}$  has period length 11. (It is tantalizing that no simple rule is known that predicts period lengths in general.)

Interestingly, for any fraction on level  $n$  of the Farey tree, the sum over all its  $a_k$  equals  $n$ :

$$\sum_k a_k = n \quad n = 2, 3, 4, \dots$$

We leave it to the reader to prove this equation (by a simple combinatorial argument, for example).

There is also a direct way of calculating, from each fraction on level  $n - 1$ , its two neighbors or direct descendants on level  $n$ . First write the original fraction as a continued fraction in two different ways, which is always possible by splitting off a 1 from the final  $a_k$ . Thus, for example,  $\frac{2}{5} = [2, 2] = [2, 1, 1]$ . Then add 1 to the last term of each continued fraction; this yields  $[2, 3] = \frac{3}{7}$  and  $[2, 1, 2] = \frac{3}{8}$ , which are indeed the two descendants of  $\frac{2}{5}$ .

Conversely, the close parent of any fraction (the one on the adjacent level) is found by subtracting 1 from its last term (in the form where the last term exceeds 1, because  $a_k = 0$  is an illegal entry in a continued fraction). The other (distant) parent is found by simply *omitting* the last term. Thus, the two parents of  $\frac{3}{7} = [2, 3]$  are the close parent  $[2, 2] = \frac{2}{5}$  and the distant parent  $[2] = \frac{1}{2}$ . (But which parent is greater, in general—the close or the distant one? And how are mediants calculated using only continued fractions?)

Interestingly, if we zigzag down the Farey tree from its upper right ( $\frac{1}{1} \rightarrow \frac{1}{2} \rightarrow \frac{2}{3} \rightarrow \frac{3}{5} \rightarrow \frac{5}{8}$ , and so on), we land on fractions whose numerators and denominators are given by the Fibonacci numbers  $F_n$ , defined by  $F_n = F_{n-1} + F_{n-2}$ ;  $F_0 = 0$ ,  $F_1 = 1$ . In fact, on the  $n$ th zig or zag, starting at  $\frac{1}{1}$ , we reach the fraction  $F_{n+1}/F_{n+2}$ , which approaches the golden mean  $\gamma = (\sqrt{5} - 1)/2 = 0.618 \dots$  as  $n \rightarrow \infty$  [Schr 90]. (Starting with  $\frac{0}{1}$  we land on

the fractions  $F_n/F_{n+2}$ , which converge on  $\gamma^2 = 1 - \gamma$ .) The binary address of  $\gamma$  in the Farey tree is 101010 . . . .

The continued fraction expansions of these ratios  $F_n/F_{n+1}$  have a particularly simple form. For example,

$$\frac{F_3}{F_4} = \frac{2}{3} = [1, 1, 1]$$

and in general

$$\frac{F_n}{F_{n+1}} = [1, 1, \dots, 1] \quad (\text{with } n \text{ 1s})$$

Obviously, continued fractions with small  $a_k$  converge relatively slowly to their final values, and continued fractions with only 1s are the slowest converging of all. Since

$$\gamma = \lim_{n \rightarrow \infty} \frac{F_n}{F_{n+1}} = [1, 1, 1, \dots] = [\bar{1}]$$

where the bar over the 1 indicates infinitely many 1s, the golden mean  $\gamma$  has the most slowly converging continued fraction expansion of all irrational numbers. The golden mean  $\gamma$  is therefore sometimes called (by physicists and their ilk) "the most irrational of all irrational numbers"—a property of  $\gamma$  with momentous consequences in a wide selection of problems in nonlinear physics, from the double swing to the three-body problem.

Roughly speaking, if the frequency ratio of two coupled oscillators is a rational number  $P/Q$ , then the coupling between the driving force and the "slaved" oscillator is particularly effective because of a kind of a resonance: every  $Q$  cycles of the driver, the same physical situation prevails so that energy transfer effects have a chance to build up in resonancelike manner. This resonance effect is strong, of course, particularly if  $Q$  is a *small* integer. This is precisely what happened with our moon: resonant energy transfer between the moon and the earth by tidal forces slowed the moon's spinning motion until the spin period around its own axis locked into the 28-day cycle of its revolution around the earth. As a consequence the moon always shows us the same face, although it wiggles ("librates") a little.

Similarly, the frequency of Mercury's spin has locked into its orbital frequency at the rational number  $\frac{3}{2}$ . As a consequence, one day on Mercury lasts two Mercury *years*. (And one day—in the distant future, one hopes—something strange like that may happen to Mother Earth!)

The rings of Saturn, or rather the gaps between them, are another consequence of this resonance mechanism. The orbital periods of any material (flocks of ice and rocks) in these gaps would be in a rational resonance with some periodic force (such as the gravitational pull from one of Saturn's "shepherding"

moons). As a consequence, even relatively weak forces have a cumulatively significant effect over long time intervals, accelerating any material out of the gaps.

For rational frequency ratios with large denominators  $Q$ , such a resonance effect would, of course, be relatively weak, and for *irrational* frequency ratios, resonance would be weaker still or absent.

For strong enough coupling, however, even irrational frequency ratios might be affected. But there is always one irrational frequency ratio that would be least disturbed: the golden mean, because, in a rational approximation to within a certain accuracy, it requires the largest denominators  $Q$ . This property is also reflected in the Farey tree: on each level  $n$  the two fractions with the largest denominators are the ones that equal  $F_{n-1}/F_{n+1}$  and  $F_n/F_{n+1}$ , which for  $n \rightarrow \infty$  approach  $\gamma^2 = 0.382 \dots$  and  $\gamma = 0.618 \dots$ , respectively. (Conversely, the fractions with the smallest  $Q$  on a given level of the Farey tree are from the harmonic series  $1/Q$  and  $1 - 1/Q$ .)

Another way to demonstrate the unique position of the golden mean among all the irrational numbers is based on the theory of rational approximation, an important part of number theory. For a good rational approximation, one expands an irrational number  $w$  into a continued fraction and terminates it after  $n$  terms to yield a rational number  $[a_1, a_2, \dots, a_n] = p_n/q_n$ . This rational approximation to  $w$  is in fact the best for a given maximum denominator  $q_n$ . For example, for  $w = 1/\pi = [3, 7, 15, 1, 293, \dots]$  and  $n = 2$ , we get  $p_n/q_n = 7/22$ , and there is no closer approximation to  $1/\pi$  with a denominator smaller than 22.

Now, even with such an optimal approximation as afforded by continued fractions, the differences for the golden mean  $\gamma$

$$\left| \gamma - \frac{p_n}{q_n} \right|$$

exceed  $c/q_n^2$  (where  $c$  is a constant that is smaller than but arbitrarily close to  $1/\sqrt{5}$ ) for *all* values of  $n$  above some  $n_0$ . And this is true only for the golden mean  $\gamma$  and the “noble numbers” (defined as irrational numbers whose continued fractions end in all 1s). Thus, in this precise sense, the golden mean (and the noble numbers) keep a greater distance from the rational numbers than does any other irrational number. Small wonder that the golden mean plays such an important role in synchronization problems.

The golden mean is also visible in visual perception (see Figure 3). For a computer-generated image of a “sunflower” using the *golden angle*  $\Delta\phi = 360^\circ \gamma \approx 225.5^\circ$  as the angular increment in the placement  $(r_n, \phi_n)$  of successive seeds, where

$$(r_n, \phi_n) = (c \cdot r_{n-1}, \phi_{n-1} + \Delta\phi)$$

we get a realistic image of the sun flower’s seed pattern, which uses the golden

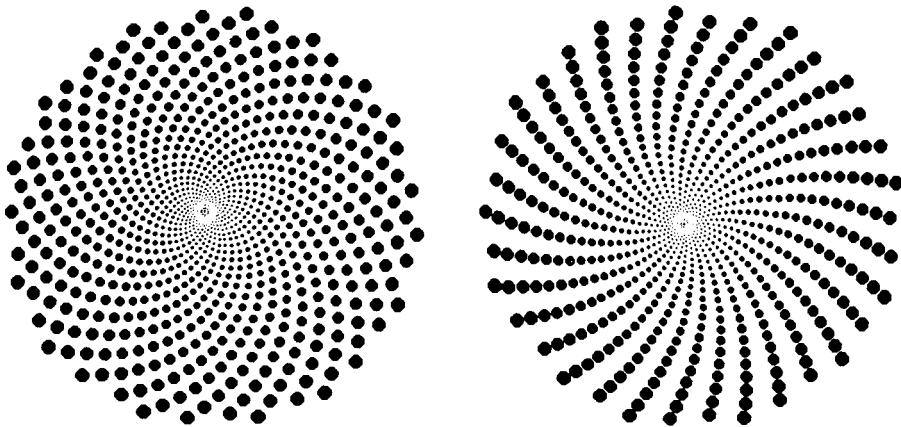


**Figure 3** The golden angle in visual perception. (Courtesy T. Gramss, after [RS 87])

angle in its construction (the left part of Figure 3) [RS 87]. But for angular increments  $\Delta\phi$  that differ by just 0.04 percent from the golden angle ( $222.4^\circ$ ), the human eye perceives pronounced spirals (the right part of Figure 3)—a psychovisual mode-locking phenomenon!

## The Golden-Mean Route to Chaos

For the critical circle map

$$\theta_{n+1} = \theta_n + \Omega - \frac{1}{2\pi} \sin(2\pi\theta_n) \quad (23)$$

the sequence of the locked-in frequency ratios  $P/Q$  equal to the ratio of successive Fibonacci numbers  $F_{n-1}/F_n = [1, 1, \dots, 1]$  is in many respects the most interesting route to aperiodic behavior and deterministic chaos of the variable  $\theta_n$ . In the transition to chaotic motion, these frequency ratios and equivalent ones, such as  $F_{n-2}/F_n = [2, 1, 1, \dots, 1]$ , are usually the last to remain unaffected as the degree of nonlinear coupling is increased. *Chaotic* means, as always, that initially close values of  $\theta$  will diverge exponentially so that all predictability is lost as the system evolves in time.

In the Farey-tree organization of the rational numbers, introduced in the previous section, the ratios  $F_{n-1}/F_n$  or  $F_{n-2}/F_n$  lie on a zigzag path approaching

the golden mean  $\gamma$  or its square,  $1 - \gamma = \gamma^2$ , respectively. Each fraction is the mediant of its two predecessors. For example, the sequence  $F_{n-2}/F_n$ , beginning with  $\frac{0}{1}$  and  $\frac{1}{2}$ , equals  $\frac{1}{3}, \frac{2}{5}, \frac{3}{8}, \frac{5}{13}, \frac{8}{21}, \dots$ . The corresponding continued fractions, beginning with  $\frac{1}{2}$ , keep adding 1s: [2], [2, 1], [2, 1, 1], [2, 1, 1, 1], [2, 1, 1, 1, 1], and so on to  $[2, \overline{1}] = \gamma^2$ .

The parameter value  $\Omega_n$  that gives a dressed winding number equal to the frequency ratio  $F_{n-2}/F_n$  has to be determined numerically. A simple calculator program that adjusts  $\Omega$  so that, for  $\theta_0 = 0$ ,  $\theta_{F_n} = F_{n-2}$  yields the following approximate parameter values:

$$\begin{aligned}\Omega(\frac{1}{2}) &= 0.5 \\ \Omega(\frac{1}{3}) &\approx 0.3516697 \\ \Omega(\frac{2}{5}) &\approx 0.4074762 \\ \Omega(\frac{3}{8}) &\approx 0.3882635 \\ \Omega(\frac{5}{13}) &\approx 0.3951174 \\ \Omega(\frac{8}{21}) &\approx 0.3927092 \\ \Omega(\frac{13}{34}) &\approx 0.3935608\end{aligned}$$

and so on, converging to  $\Omega_\infty \approx 0.3933377$ .

These parameter values give rise to superstable orbits because the iterates  $\theta_n$  include the value  $\theta_n = 0$  for which the derivative of the critical circle map vanishes. These  $\Omega$  values therefore correspond to the superstable values  $R_n$  of the quadratic map, and  $\Omega_\infty$  corresponds to  $R_\infty$ .

Is there a universal constant, corresponding to the Feigenbaum constant, which describes the rate of convergence of the parameter values  $\Omega_n := \Omega(F_{n-2}/F_n)$  to  $\Omega_\infty$  as  $n$  goes to infinity? Numerical evidence suggests that there is, and that the differences between successive values of  $\Omega_n$  scale with an asymptotic factor:

$$\frac{\Omega_{n-1} - \Omega_n}{\Omega_n - \Omega_{n+1}} \rightarrow \delta$$

with  $\delta = -2.8336 \dots$ , which thus corresponds to the Feigenbaum constant 4.6692  $\dots$  (The minus sign signifies that successive differences alternate in sign.)

Other self-similar scaling behaviors can be observed in the iterates of the variable  $\theta_n$ . For example, for  $\Omega = \Omega(F_{n-2}/F_n)$  the differences  $\theta_{F_{n-1}} - F_{n-3}$  converge to 0 in an asymptotically geometric progression:

$$\theta_{F_{n-1}} - F_{n-3} \approx \alpha^n$$

with  $\alpha = -1.288575 \dots$ , which corresponds to the scaling parameter  $-2.5029 \dots$  for the iterated variable of the quadratic map.

Both  $\alpha$  and  $\delta$  are universal for maps with a zero-slope cubic inflection point. This result follows from a renormalization theory for the golden-mean transition to chaos of such maps. The functional equation of the fixed-point function for the renormalized cubic map is

$$f(x) = \alpha f(\alpha f(x/\alpha^2))$$

(The corresponding functional equation for the period-doubling transition of the quadratic map looks rather similar:  $g(x) = \alpha g(g(x/\alpha))$ ; see page 274).

Another similarity between these two prototypical transitions to chaos is in their symbolic dynamics. For  $\Omega = \Omega(F_{n-2}/F_n)$  and  $K = 0$ ,

$$\theta_n = \theta_0 + n \frac{F_{n-2}}{F_n}$$

We consider  $\theta_n \bmod 1$  in the interval  $(-0.5, 0.5]$  and write  $L$  for  $\theta_n < 0$ ,  $C$  for  $\theta_n = 0$ , and  $R$  for  $\theta_n > 0$ . For  $\theta_0 = 0$ , we then get the following symbolic dynamics as  $n \rightarrow \infty$ :

*CRLRRLRLRRLRRL ...*

Following the initial  $C$ , this sequence is, of course, none other than the familiar rabbit sequence in which 1 has been replaced by  $R$  and 0 by  $L$ . For  $K = 1$ , the actual iterates are different from those for  $K = 0$ , but the symbolic dynamics are given by the same sequence.

As we know from the discussion of quasicrystals in Chapter 13, this sequence can be constructed from the iteration  $0 \rightarrow 1$ ,  $1 \rightarrow 10$  or, in our present alphabet,  $L \rightarrow R$ ,  $R \rightarrow RL$ . Again there is a great similarity with the period-doubling transition for which the symbolic dynamics are generated from the iteration  $L \rightarrow RR$ ,  $R \rightarrow LR$ . In fact, these two transitions were treated by a unified renormalization theory by Procaccia, Thomae, and Tresser [PTT 87].

For finite  $n$ , the symbolic dynamics can be obtained from the formula for Ising spin positions (see pages 323–324). Thus, for the dressed winding number  $P/Q = 3/8$ , the positions of the  $L$ 's are given by equation 6 for the down-spins with  $1 - w = 3/8$ , namely, 2, 5, 7. Thus, the superstable orbit with frequency ratio  $3/8$  is  $CRLRRLRL$ , which is the initial eight-term segment of the infinite sequence.

For the winding number  $P/Q = 2/5$ , the dynamics computed in this manner are  $CRLRL$ , which differs in the last letter from the corresponding letter in the infinite sequence. In general, for  $Q = F_{2k+1}$ , the last letter is  $L$  and not  $R$ , as in the infinite sequence. However, this minor blemish is self-inflicted. It is easily removed by considering  $\theta_n \bmod 1$  not in the interval  $(-0.5, 0.5)$  but in the slightly shifted interval  $(-x, 1 - x)$ , where  $x \approx 0.4461583$  is the solution of the transcendental equation  $x = \Omega_\infty + (\sin 2\pi x)/2\pi$ .

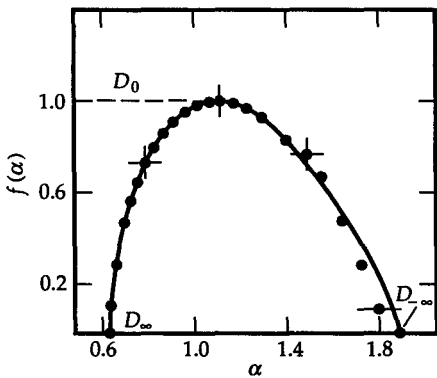


**Figure 4** Multifractal spectrum of the critical circle map at the golden-mean winding number [JKLPS 85].

The aperiodic iterates  $\theta_n$  of the critical circle map, for the dressed winding number equal to the golden mean  $\gamma$ , form a multifractal with a spectrum of singularities  $f(\alpha)$  shown in Figure 4. The same spectrum obtains for all equivalent numbers, that is, all those irrational numbers whose continued fraction ends in all 1s, the so-called *noble numbers* (see Appendix B). This spectrum was computed from the periodic orbit with period length  $Q = 2584 = F_{18}$ . The distances  $r_k = \theta_{k+F_1} - \theta_k \bmod 1$  were taken as the length scales of the multifractal, and  $p_k$  was set equal to  $1/2854$ . The dimension  $D_{-\infty}$  for the most rarefied region was already obtained by Shenker from the abovementioned scaling exponent  $\alpha = -1.288575 \dots$  as

$$D_{-\infty} = \frac{\log \gamma}{\log (-1/\alpha)} \approx 1.898$$

The most concentrated region of the multifractal scales as  $\alpha^3$ , giving the smallest dimension  $D_\infty$  as  $D_{-\infty}/3 \approx 0.6327$  [She 82].

A selection of the applications related to spatial or temporal mode locking and chaos are listed in the references. These relate to acoustics [LP 88], solar system dynamics [Las 89, WPM 83, AS 81], physical chemistry [BB 79], astrophysics [HLSTLW 86], solid-state electronics [MM 86, BBJ 84, GW 87, CMP 87], cardiology [CJ 87], turbulence [JKLPS 85, FHG 85], and nonlinear mechanical oscillators [AL 85, Moo 84].

# P

## ercolation: From Forest Fires to Epidemics

*Observation always involves theory.*

—EDWIN HUBBLE

*The function of an expert is not to be more right than other people, but to be wrong for more sophisticated reasons.*

—DAVID BUTLER

Percolation permeates nature and man-made devices in many modes. In a coffee percolator, water seeps, or percolates, through the ground beans to emerge as drinkable coffee at the output spout.

To remain at the breakfast table, when you boil an egg long enough, its protein bonds will link up, and before too long the bonds will percolate through the entire egg to solidify it—so that you can eat it safely with a spoon and without spillage.

By contrast—and happily—an *epidemic* does not always percolate through an entire population. There is a *percolation threshold* below which the epidemic has died out before most of the *people* have. And an undercooked egg, too, is below the percolation threshold.

On a grander scale, percolation theory, eloquently expounded by Dietrich Stauffer [Sta 85], has something to offer for a better understanding of the formation of galaxies and clusters of galaxies. And at the other extreme, percolation has infiltrated even one of the tiniest scales: atomic nuclei. Their fragmentation is now being analyzed as a percolation process [Cam 86].

Another famous and preferred paradigm for percolation is a forest fire. If we ignite a few trees, will the whole forest burn down, or will most trees still be standing by the time the fire has stopped?

At the percolation threshold (clearly exceeded in the 1988 conflagrations in Yellowstone National Park), statistical self-similarities abound, and it is these self-similarities that make the mathematical treatment tractable and lead to simple scaling laws at or near the threshold.

Percolation theory is also a good preparation for the study of more complicated physical phenomena, such as phase transitions in magnetic materials and in thermodynamics in general. For example, the correlation length of the spin directions in a dilute “ferromagnet” becomes infinite at the percolation threshold, called the *critical* or *Curie* point in physics. This means that *clusters* of magnetic domains as large as the sample appear. In fact, clusters of *all* sizes, or length scales, arise, and these clusters are self-similar. In the entire range, from atomic distances to the size of the sample, clusters look similar and become stochastically indistinguishable when scaled to the same size.

Below the percolation threshold (*above* the Curie point for magnets), clusters of only finite size exist: the coffee does not drip through, and the chunk of iron is only “paramagnetic.” But above the percolation threshold (below the Curie point), infinite clusters are common, with well-known consequences, depending on the application: a forest fire will spread to the other end of the forest, epidemics become pandemics, and iron (ironically?) becomes a ferromagnet. And near the percolation threshold, self-similarity reigns supreme!

Let us take a closer look at one of the hotter paradigms in percolation theory: forest fires, often fought but still ablaze.

## Critical Conflagration on a Square Lattice

Assume, for simplicity, that a forest can be modeled as a square point lattice in which the lattice points are independently occupied by trees with probability  $p < 1$  (see Figure 1). Now ignite the lowest row of trees and watch how the fire spreads as a digital clock ticks along in discrete time.

We assume that a burning tree will ignite all nearest-neighbor trees after one unit of time. After one more time unit of burning, a tree is burned out.

Elaborate computer simulations [Sta 85] have confirmed the obvious: below a critical tree density,  $p_c$ , the fire dies out before reaching the other edge of the forest, the uppermost rows in Figure 1. By contrast, for  $p > p_c$ , the fire will reach the far edge (and would threaten more trees if the forest were longer).

While  $p \ll p_c$  would be a very safe forest and  $p \approx 1$  a natural powder keg, the most interesting things happen *near the percolation threshold*, that is, for  $p \approx p_c$  or for

$$\varepsilon := \frac{p - p_c}{p} \ll 1$$

It turns out that for  $\varepsilon \ll 1$ , the crucial variables obey simple scaling laws reflecting the self-similarity of percolation near the threshold, or *critical point* (to borrow a term from the physics of phase transitions).

Let us call the number of trees in the  $n$ th row of the lattice that have burned down at time  $t$ , divided by the average number of trees per row,  $Z(n, t, \varepsilon)$ . Here  $n$  and  $t$  are assumed to be large compared to 1. Numerous numerical analyses [Sta 85] have suggested that near the threshold (i.e.,  $\varepsilon \ll 1$ ), the *order parameter*  $Z$  is a (generalized) homogeneous function of its arguments:

$$Z(n, t, \varepsilon) = \frac{Z(\lambda^{a_n} n, \lambda^{a_t} t, \lambda^{a_\varepsilon} \varepsilon)}{\lambda} \quad n \gg 1, t \gg 1, \varepsilon \ll 1 \quad (1)$$

That is,  $Z$  is some *universal* function that scales as shown, with three *scaling exponents*:  $a_n$ ,  $a_t$ , and  $a_\varepsilon$  [Gri 89]. What else can we say about this important function? If we wait long enough (i.e., as  $t \rightarrow \infty$ ) and go far enough away (as  $n \rightarrow \infty$ ), equation 1 becomes

$$Z(\infty, \infty, \varepsilon) = \frac{Z(\infty, \infty, \lambda^{a_\varepsilon} \varepsilon)}{\lambda} \quad (2)$$

Postulating a power-law dependence of  $Z(\infty, \infty, \varepsilon)$  on  $\varepsilon$ :

$$Z(\infty, \infty, \varepsilon) = \text{const} \cdot \varepsilon^\beta \quad (3)$$

we obtain, from equation 2,  $\varepsilon^\beta = (\lambda^{a_\varepsilon} \varepsilon)^\beta / \lambda$ , or  $a_\varepsilon = 1/\beta$ . The exponent  $\beta$  is called a *critical exponent*, and we have just succeeded in relating it to one of the scaling exponents,  $a_\varepsilon$ .

Next, we introduce two more parameters: a characteristic length (e.g., the correlation length)  $\xi$ , and a characteristic time  $\theta$ . Both  $\xi$  and  $\theta$  are known to diverge to infinity as  $\varepsilon$  goes to 0 according to simple power laws:

$$\xi = \text{const} \cdot \varepsilon^{-\nu} \quad (4)$$

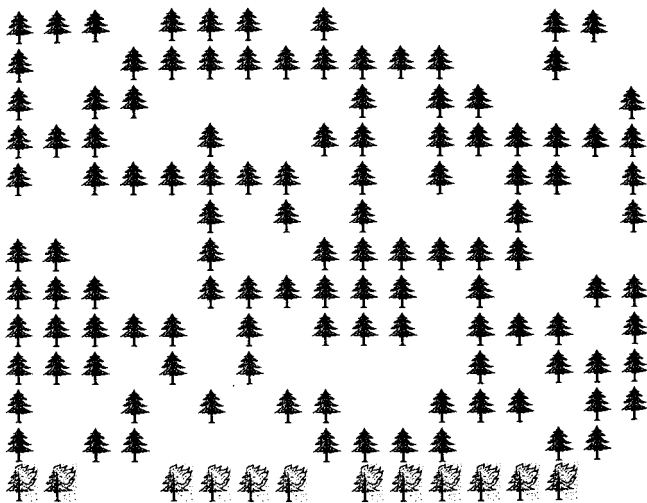
and

$$\theta = \text{const} \cdot \varepsilon^{-\delta} \quad (5)$$

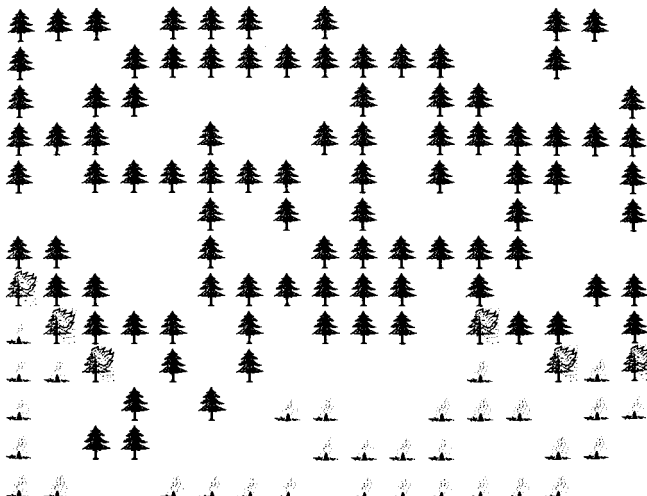
We subsume the dependence of  $Z(n, t, \varepsilon)$  on  $\varepsilon$  into the characteristic quantities and write, tentatively,

$$Z(n, t, \varepsilon) = n^x g\left(\frac{n}{\xi}, \frac{t}{\theta}\right) \quad (6)$$

where the function  $g$  depends only on two variables. The exponent  $x$  must equal  $-\beta/\nu$  for the original scaling law (equation 1) to hold.

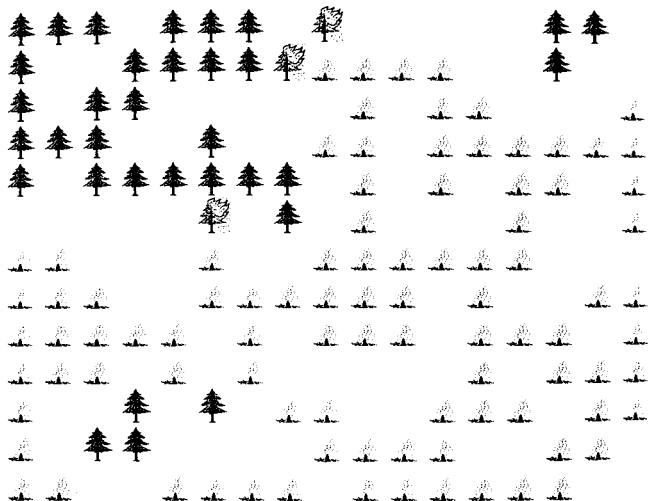


(A)

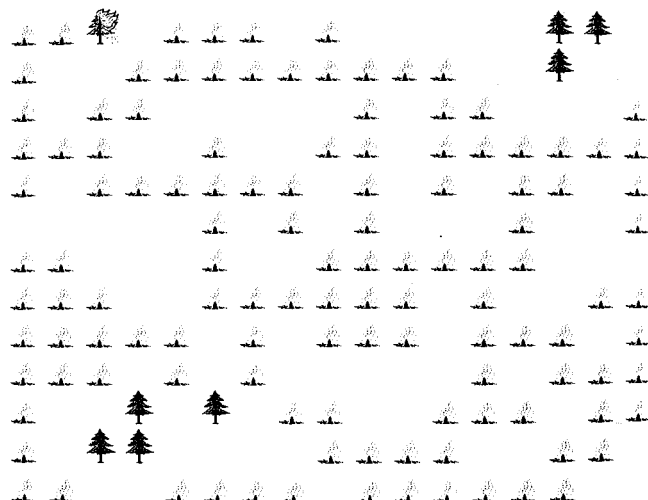


(B)

**Figure 1** (A) Square lattice randomly occupied by trees at percolation threshold. Lowest row of trees has been ignited. (B) A little later: nearby trees have caught fire. (C) The conflagration has reached the upper edge of the forest. (D) The fire has died out, and so have most of the trees. (Courtesy of H. Behme).



(C)



(D)

**Figure 1** Continued

We have now related all three scaling exponents in equation 1 to three critical exponents:  $\beta$ ,  $v$ ,  $\delta$ , which describe how  $Z$  and the length and time parameters,  $\xi$  and  $\delta$ , scale with  $\varepsilon$  near the critical point ( $\varepsilon \ll 1$ ).

Defining a characteristic number of burned-down trees,

$$\zeta := n^{-\beta/v}$$

we can write equation (6) as

$$\frac{Z(n, t, \varepsilon)}{\zeta} = g\left(\frac{n}{\xi}, \frac{t}{\theta}\right) \quad (7)$$

which is the most symmetric and useful way of expressing the power-law dependence of  $Z$  on  $n$  and  $t$  and, with equations 3 to 5, on  $\varepsilon$ . These equations tell us, for example, that as we change  $p$ , that is,  $\varepsilon$ , the new values of  $Z(n, t, \varepsilon)$  can be obtained from the *same* “universal” function  $g$  by multiplication with  $n^{-\beta/v}$  and scaling  $n$  and  $t$  with  $\varepsilon^{-v}$  and  $\varepsilon^{-\delta}$ , respectively.

## Universality

*For quite a while I have set for myself the rule if a theoretician says “universal” it just means pure nonsense.*

—WOLFGANG PAULI

The “critical exponents”  $v$  and  $\delta$  must be determined analytically, or by computer simulation, and the critical reader is invited to try this on his or her home computer. The surprising result is that, for a wide variety of problems in physics, chemistry, biology, and many other disciplines, the critical exponents do *not* depend upon the details of the situation but, typically, only on the dimensionality of the embedding space (e.g., two dimensions for a square lattice) and the “degrees of freedom” of the variable considered—for example, 2 in the case of a spin (or tree) system where spins (trees) are either up or (burned) down.

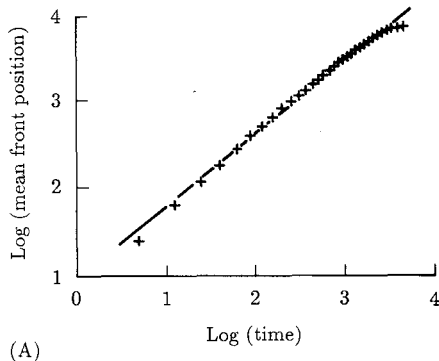
This kind of universality is one of the liveliest themes in contemporary physics, giving rise to many burning questions, such as, How does a specified random walk diverge on a *fractal* lattice, like the Sierpinski gasket, for example, near the critical point (percolation threshold)? How is electricity conducted on fractal networks? or, How does the *speed* of a forest fire depend on the density  $p$  of the trees?

According to equations 4, 5, and 7,  $Z/\zeta$  has a fixed value if  $n$  changes with time  $t$  as

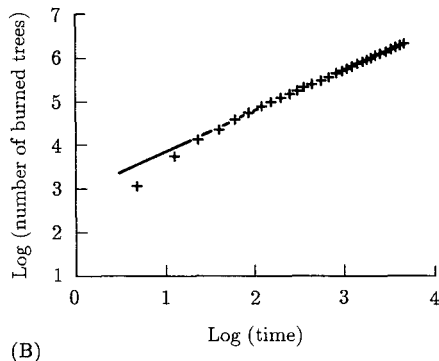
$$n = \text{const} \cdot t^{v/\delta}$$

Thus, the mean propagation speed of the fire defined, for example, by observing the progress in time of the fire's front scales as  $t^{v/\delta - 1}$ . By counting newly ignited trees in a computer simulation (to conserve forests and oxygen), the ratio of two of the critical exponents,  $v/\delta$ , can easily be determined [ASS 86].

Figure 2A shows one of the results of a simulation by Albinet and coworkers in which the mean position of the fire's cutting edge is plotted versus time in log-log coordinates. In this simulation, the lattice had a size of 200 times 200 points and the density of trees was at the critical value for a square lattice,  $p_c \approx 0.593$ . Thus, there were a total of 23,720 trees to burn or not to burn.



(A)



(B)

**Figure 2** (A) Mean position of a fire's cutting edge as a function of burning time. Straight line, based on power-law postulate, has slope 0.87. (B) Number of burned trees as a function of time. Slope is 0.79 [ASS 86].

The straight line conforms to the power-law postulate, and its slope,  $v/\delta$ , equals 0.87. Thus, not surprisingly, the fire spreads faster than a diffusion process (slope 0.5), but slower than on a fuse cord (slope 1.0).

The deviations from the straight line for very short times are residual effects of how the fires were laid, and those for very long times are size effects due to "saturation" (where all trees have burned down).

The total number of burned trees,

$$N_b(t, \varepsilon) = \text{const} \cdot \sum_n Z(n, t, \varepsilon)$$

scales as  $t^{(v-\beta)/\delta}$ . Thus simple unrestrained counting gives the ratio of  $(v - \beta)/\delta$ , or  $\beta/\delta$  once  $v/\delta$  has already been determined. Figure 2B shows the result of a computer experiment. Again, after initial effects have died out, the number of burned-down trees as a function of time is a straight line in a log-log plot with a slope of  $(v - \beta)/\delta = 0.79$ .

The third critical exponent,  $\beta$ , is determined by exploiting equation 3, that is, counting the dead trees after the fire has stopped. The simulation results turned (burned?) out to be rather prone to sampling error:  $\beta = 0.12 \pm 0.03$ ; the theoretical value [Sta 85] is  $\beta = \frac{5}{36} \approx 0.139$ .

The exponent  $\beta$  is rather small, as would be expected if the fraction of trees that eventually burn down does not depend on  $\varepsilon$  as strongly as the speed of the fire does.

Another exponent that can be calculated analytically is  $v$ , which governs the correlation length (equation 4); it equals  $\frac{4}{3}$  exactly. With  $v = \frac{4}{3}$  and  $v/\delta = 0.87$ , the critical *time* exponent  $\delta$  equals 1.533, close to the value found by Peter Grassberger [Gra 85]. Thus, as  $\varepsilon$  goes to zero, characteristic times diverge more rapidly than the correlation lengths. This makes sense, because for  $p$  smaller than but near  $p_c$ , that is,  $\varepsilon \ll 1$ , there may be a long period of time in which the fire keeps burning after its outer perimeter has stopped advancing much further. As firefighters know all too well, fires spread backward as well as forward.

It is interesting to note that all critical exponents,  $v$ ,  $\delta$ , and  $\beta$ , were found to be independent of the size of the interacting neighborhood; their values are indistinguishable for the following cases: 4 nearest neighbors on the square lattice, 8 nearest and next-nearest neighbors, and 24 neighbors in a  $5 \times 5$  square.

This invariance illustrates what is meant by *universality*; the critical exponents depend only on the embedding dimension ( $d = 2$ ) and the degrees of freedom (also 2) for all three coordination numbers studied.

However, the critical *densities*  $p_c$  do differ. Experimental values are  $p_c = 0.592745$ , 0.407355, and 0.168, respectively, for these three different coordination numbers. This is not surprising, because if a fire can jump not just to the nearest trees, but also to the second-, third-, fourth-, and fifth-nearest neighbors, wider gaps can exist in the forest without stopping the fire.

## The Critical Density

In Figure 3, the average termination times of the fire  $t_\infty$  are plotted against the tree density  $p$  for a 300 by 300 square lattice. The divergence near  $p = p_c \approx 0.593$  is quite pronounced and follows the theoretical expectation  $t_\infty = \text{const} \cdot |e|^{-\tau}$  with  $\tau \approx 1.5$  [Sta 85].

Similar behavior, with the same value for  $\tau$ , is found for triangular lattices, except that  $p_c \approx 0.5$ , in accordance with the exact theoretical prediction for the critical density,  $p_c = 0.5$ .

The triangular lattice is one of the lattices for which an analytical value is available. The Bethe lattice (see Chapter 16), called a Cayley tree in graph theory, is another instance: for  $z$  nearest neighbors, the percolation threshold  $p_c$  equals precisely  $1/(z - 1)$ . It is clear from Figure 3 that computer experiments with varying  $p$  are a good way to determine  $p_c$ : at the critical point  $p = p_c$ , many parameters show a sharp peak. In physics such peaks (of specific heat or magnetic susceptibility, for example) as a function of temperature signal second-order phase transitions. Indeed, percolation is a phase transition, albeit much cleaner and clearer than the “average” thermodynamic phase transition, which can be very “mean” to treat indeed.

## The Fractal Perimeters of Percolation

Does the forest fire advance in a straight front like a Greek phalanx, or is its cutting edge more fingerlike? The front is in fact fractal, complete with a Hausdorff

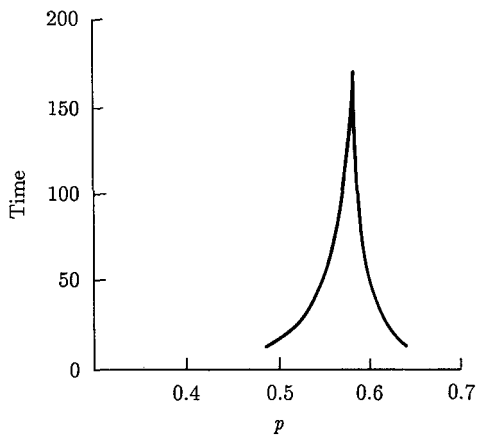


**Figure 3** Average termination time of fires as a function of tree density. Note divergence near critical density  $P \approx 0.593$ . [Sta 85].

dimension  $D$  that lies between 1 and 2. A seemingly related phenomenon is *invasion percolation*, also known as “fingering” in oil exploration, where it has been much touted, especially when oil became “temporarily” scarce in the 1970s (see Chapter 9). However, fingering results from an instability at the interface of two liquids. By contrast, the fractal fire front stems from a connectivity paradigm: the adjacency of trees.

## Finite-Size Scaling

What does computer simulation of forest fires teach us about the fractal dimension  $f$  of the perimeter? If we define the perimeter as the number  $F$  of burned sites which border an unburned site and plot this number as a function of the size of the lattice  $L$ , we find a simple power law, called *finite-size scaling* [Sta 85]:

$$F = \text{const} \cdot L^f$$

with  $f = 1.75$  for all three neighborhoods—a value uncomfortably close to 2 for a *perimeter*, which, topologically, has only one dimension. (Note, though, that our definition of *perimeter* includes the boundaries of internal pockets of unburned trees.)

Another fractal dimension,  $\bar{d}$ , describes the total number  $M$  of burned trees. If all trees burned down, or even if just a fixed fraction of trees burned down,  $M$  would be proportional to the total number of trees or the area of the lattice:  $M = \text{const} \cdot L^2$ . But that is not what happens near the percolation threshold. In fact, we find another power law describing the finite-size scaling:

$$M = \text{const} \cdot L^{\bar{d}} \quad (8)$$

with  $\bar{d} \approx 1.9$ , somewhat less than 2 because pockets of unburned trees persist. After the fire has stopped, the *burned-down* trees form a kind of two-dimensional sponge (or Swiss cheese) with many holes on many scales.

Stauffer [Sta 85] also cites an interesting relationship for the difference between the fractal dimension  $\bar{d}$  and the embedding dimension  $d$ , and the critical exponents  $\beta$  and  $v$ :

$$d - \bar{d} = \frac{\beta}{v} \quad (9)$$

For  $d = 2$ ,  $\beta = \frac{5}{36}$ , and  $v = \frac{4}{3}$ , this relation gives  $\bar{d} = \frac{91}{48}$ , in excellent agreement with the experimental data; see Figure 4.

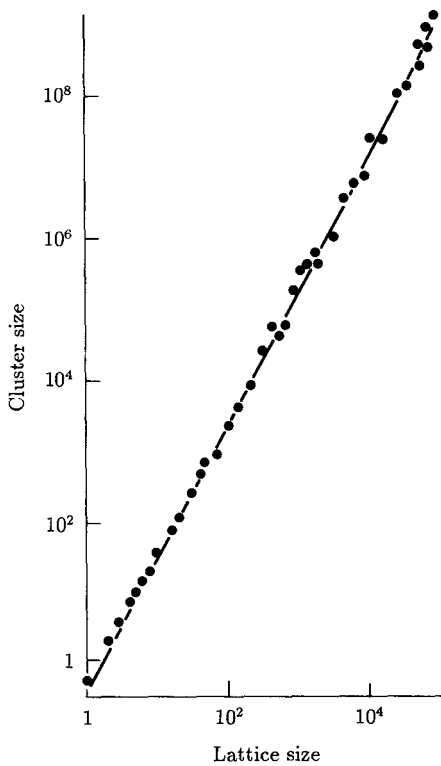


**Figure 4** Size of largest cluster at the percolation threshold of the triangular lattice plotted against lattice size. The slope of the straight line corresponds to the theoretical fractal dimension  $\frac{91}{48}$  [Sta 85].

Of course, far from the critical point there is little dependence of the number of burned-down trees on  $\varepsilon$ . Thus, the exponent  $\beta$  (see equation 3) would tend to zero so that, with equation 9,  $\bar{d} \rightarrow d$ , as expected, because forest fires are fractal only near the critical point  $\varepsilon \ll 1$ .

In fact, far from the critical point, the correlation length is much, much smaller than the forest (or the magnet). Thus,  $M$  does not vary as  $L^{\bar{d}}$ , as in equation 8, with a fractal exponent  $\bar{d}$ , but in a completely "Euclidean" manner:  $M = \text{const} \cdot L^d$ , where  $d$  is the Euclidean dimension of the embedding space. In short: Percolation is a fractal phenomenon only near the critical point; above or below, it shows classical Euclidean behavior.

Still another fractal dimension,  $\tilde{d}$ , can be defined by the penetration time  $t_\infty$  as a function of forest size  $L$ :

$$t_\infty = \text{const} \cdot L^{\tilde{d}}$$

Numerical evidence confirms this power law and gives  $\tilde{d} \approx 1.16$ , in close agreement with the expectation that characteristic times scale as lengths raised to the power  $v/\delta = 1.159$ .

While we have focused our attention on forest fires, much the same laws govern the spread of epidemics, the formation of galaxies, nuclear fragmentation, and countless other phenomena [Kes 87].

Percolation is a widespread paradigm. Percolation theory can therefore illuminate a great many seemingly diverse situations. Because of its basically geometric character, it facilitates the analysis of intricate patterns and textures without needless physical complications. And the self-similarity that prevails at critical points permits profitably mining the connection with scaling and fractals.

# P

## hase Transitions and Renormalization

*Is nature trying to tell us something by  
using only renormalizable interactions?*

—HEINZ PAGELS

The concepts of renormalization and self-similarity are closely related. In fact, renormalization is one of the most fruitful applications of self-similarity. In physics, renormalization theories have shed light on nonlinear dynamics and the mysteries of phase transitions in areas ranging from freezing to ferromagnetism, spin glasses, and self-organization [Hak 78].

Where do the puzzling fractional exponents, describing behavior near critical points, come from, and why are they so often identical in widely different situations? And what is the reason behind the small integers in these exponents? All this has been greatly clarified in the last two decades by Leo Kadanoff, Michael Fisher, and others, and especially by Kenneth Wilson, who has won the Nobel Prize in physics for his work. One of the more spectacular phase transitions that are now completely transparent is *critical opalescence*, in which a translucent medium, at the critical point, becomes optically opaque as a result of a “soft mode” that scatters light much as thick smoke does in a smoke-filled foyer.

Here we shall touch only very lightly on the subject, but hope, nevertheless, to convey some of the spirit by the sprinklings that follow.

### A First-Order Markov Process

A *Markov process* is a stochastic process in which present events depend on the past only through some finite number of generations. In a *first-order* Markov process, the influential past is limited to a *single* earlier generation: the present can be fully accounted for by the *immediate* past.

Such processes are often represented by state diagrams, such as that shown in Figure 1, with various transition probabilities. Thus, in the simple first-order Markov source depicted in Figure 1, if +1 was the last symbol generated by the source, we are in the left state, labeled +, and  $p$  is the probability of generating another +. This is indicated by the curved arrow that starts and ends at the left state.

With probability  $1 - p$  the source will emit the symbol  $-1$  and thus jump to the right state, labeled  $-$ . In this state, the source will emit another  $-1$  with probability  $q$  and thus remain in the right state. With probability  $1 - q$ , the source will emit a  $+1$  and jump back to the left state.

For  $p = q$ , the entropy  $H_M$  of such a Markov source is

$$H_M = -p \log_2 p - (1-p) \log_2 (1-p) \quad \text{bits per output symbol}$$

which happens to be the same as the entropy  $H(p)$  of a *memoryless* binary source with probabilities  $p$  and  $1 - p$  for the two possible outputs. This agreement is easily verified by modeling the first-order Markov source with  $p = q$  as a zero-order (memoryless) source “kicking” a polarity reversal switch (i.e., changing + to  $-$  or  $-$  to +) with probability  $1 - p$  and *not* kicking the switch with probability  $p$ . The outputs from these two sources can be reversibly transformed into each other (except for an overall sign change) and therefore must have the same entropy.

## Self-Similar and Non-Self-Similar Markov Processes

For  $p = q$ , the Markov source depicted in Figure 1, emits  $+1$  or  $-1$  with equal probability. For  $p = \frac{1}{2}$ , successive outputs are independent: the machine has turned into a memoryless honest-coin flipper.<sup>1</sup> The output sequence is an example of a statistically self-similar process: strike out every other symbol, and the decimated sequence is statistically indistinguishable from the original sequence, because we again have independent  $+1$ s and  $-1$ s, each occurring with probability  $\frac{1}{2}$ .

For  $p \neq \frac{1}{2}$ , however, self-similarity no longer holds. Adjacent samples are correlated, and when we skip symbols the remaining symbols will have an absolutely smaller correlation.

In fact, another look at Figure 1 reveals that, for  $p = q > \frac{1}{2}$ , a like symbol is more likely than an unlike one to follow a given symbol. For  $p = q < \frac{1}{2}$ , the situation is reversed: symbols prefer to alternate.

---

1. Not to be confused with the forgetful but honest coin-flipper.

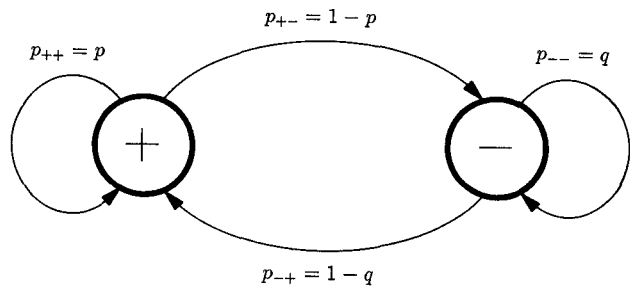


**Figure 1** First-order Markov source with two states (+ and -) and four transition probabilities.

The correlation  $C_m$  between two symbols  $s_n$  and  $s_{n+m}$  from the source in Figure 1 with  $p = q$  is given by

$$C_m = \lim_{N \rightarrow \infty} \frac{1}{N} \sum_{n=1}^N s_n s_{n+m} \quad (1)$$

Since our Markov source is stationary and ergodic for  $0 < p < 1$ , we can replace the “time” average in equation 1 by an ensemble expectation value, symbolized by angular brackets:

$$C_m = \langle s_n s_{n+m} \rangle$$

For  $C_1$  we obtain, by averaging over the four distinct possibilities (+ +, + -, - +, - -),

$$C_1 = \frac{1}{2}[p - (1 - p) - (1 - p) + p] = 2p - 1$$

For  $p = \frac{1}{2}$ ,  $C_1 = 0$ , as expected. Note that  $C_1 < 0$  for  $p < \frac{1}{2}$ .

Here is a typical “random” sequence, generated by this inveterate stochastic generator while writing this (without mechanical or electronic assistance):

+ + - + - - - + - + - - + - + + + + -

By coincidence, this sequence has equal numbers of + and -. The sample correlation is  $-\frac{3}{19}$ , giving an estimate for the probability parameter  $p = \frac{8}{19} \approx 0.42$ . Considering that my intent was to generate a sequence with  $p = \frac{1}{2}$ , I fell about 16 percent short—a typical human failing. Most *human* random number generators can be characterized as Markov sources with  $p < \frac{1}{2}$  when they are trying to generate independent binary events. People have the greatest trouble being really random; they almost always alternate too much (a common shortcoming

that was judiciously exploited in Claude Shannon's "outguessing machine" [Sha 53], described in pages 149–150).

## The Scaling of Markov Outputs

Since, in a first-order Markov process, the present is fully accounted for by the immediately preceding past, one obtains for the correlation coefficients

$$C_m = C_1^m = (2p - 1)^m$$

or, introducing a new parameter  $\beta$  defined by

$$e^{-\beta} = 2p - 1 \quad \text{for} \quad p \geq \frac{1}{2} \quad (2)$$

we have

$$C_m = e^{-\beta m}$$

Let us delete every other output symbol from our Markov source. The result can be viewed as the output of another Markov source with a different parameter  $p$  (for  $p \neq \frac{1}{2}$ ). The correlation,  $C_m^{(2)}$ , of the decimated process is the square of that of the original process:

$$C_m^{(2)} = C_{2m} = C_m^2 = e^{-2\beta m}$$

Thus, we see that our parameter  $\beta$  has doubled, which means (see equation 2) that the new transition probability has changed from  $p$  to  $p^{(2)}$  given by  $2p^{(2)} - 1 = (2p - 1)^2$ , or

$$p^{(2)} = 2p^2 - 2p + 1$$

The aforementioned value  $p = \frac{8}{19} \approx 0.42$  then changes to  $p^{(2)} \approx 0.51$ . If we again take every other sample (every fourth term of the original sequence), we get  $C_m^{(4)} = C_{4m} = C_m^4$  and  $p^{(4)} = 0.5003$  for  $p = 0.42$ . As we leave out more and more intermediate samples,  $p^{(2^n)}$ , for  $n \rightarrow \infty$ , approaches  $\frac{1}{2}$ , the value for independent samples, from above.

Thus, while the output of our Markov source is not self-similar (except for  $p = 0.5$  or 1 for nonnegative  $C_1$ ), scaling the *index* of the output sequence  $s_k$  by an integer  $r$ , to yield the decimated sequence  $s_{rk}$ , is equivalent to taking the output of another Markov source with a rescaled parameter  $\beta^{(r)}$ , where  $\beta^{(r)} = r\beta$ . Thus, the parameter  $\beta$  scales exactly as the index.

The physical significance of  $1/\beta^r$  is a *correlation length*, which goes to zero as  $r$  becomes larger and larger, reflecting again the fact that “skipping” samples makes the correlation smaller. In other contexts, the parameter  $\beta$  can also be identified with a temperature (as we will see shortly).

Together with periodic symmetries, as manifest in spatial rotations and other periodic phenomena, the scaling symmetry we just encountered is now one of the most important symmetries in physics and other fields. In fact, the ingenious Maurits Escher (1898–1972) has combined these two fundamental symmetries in several of his graphical representations.

In physics, rescaling has led to the by now ubiquitous *renormalization theories*. In a typical application, one might want to derive, from fundamental principles, the *critical exponent*  $\alpha$  of the specific heat  $c(T)$ , say, near a critical temperature  $T_c$ . Measurements may suggest a simple power law like

$$c(T) - c(T_c) \approx |T - T_c|^{-\alpha}$$

In such problems it has been found again and again that the exponent  $\alpha$  does not depend on the specific situation, but may be the same for very different physical systems like water, helium, xenon, or any other fluid near its liquid-gas critical point.<sup>2</sup> These are then said to fall into the same *universality class*, which typically depends on only a few pure *numbers*: the dimensionality of the space in which the phenomenon takes place and the number of degrees of freedom of the order parameter.

Of course, most physical systems are so complicated that one has to rely on simple models of reality. For example, for spin systems, an easy model is the one named after the German-born physicist Ising (originally, and appropriately it may seem, pronounced “easing”). In the Ising model, spins have only two possible values (“up” or “down”), and usually only adjacent spins are assumed to interact (“nearest-neighbor coupling”).

The first-order Markov source that we studied in this chapter corresponds to the one-dimensional Ising model. This Ising model has two “critical temperatures”:  $T_c = 0$ , in which all spins are aligned (corresponding to the fully correlated case in the Markov model with  $\beta = 0$ ), and  $T_c = \infty$ , in which the spins are totally disordered (corresponding to the case  $\beta = \infty$ ).

For the three-dimensional (3D) Ising model, computer simulations give, for the average spontaneous magnetization,

$$\bar{M} \sim (T_c - T)^\beta \quad \text{for} \quad T < T_c$$

---

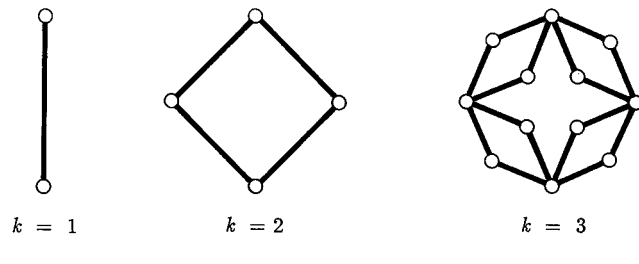
2. Under carefully controlled conditions, one can also push liquids beyond the critical point, resulting in “supercritical” liquids, which have numerous useful applications. Supercritical water, for example, can be used to extract caffeine from coffee beans without altering the taste, unlike-chemical solvents.

with  $\beta = 0.325$ , the same exponent found for all other 3D systems with only one degree of freedom of the order parameter (spin up or down, in the Ising model).

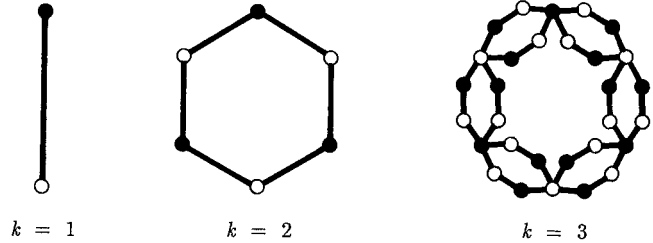
## Renormalization and Hierarchical Lattices

For renormalization to be applicable to an atomic lattice, the lattice must scale in the sense that the Koch flake and other fractals scale. To construct lattices having this property, one begins with an initiator—for example, just two spin sites ( $k = 1$ )—and a generator ( $k = 2$ ); see Figure 2A. The next iteration yields the “lattice” shown for  $k = 3$ . Such self-similar lattices are described as *hierarchical* in this context [DDI 83, PR 86a, b].

For an antiferromagnetic lattice, one has to distinguish the two spins at the endpoints of the initiator (open and filled circles in Figure 2B). The generator



(A)



(B)

**Figure 2** (A) Initiator, generator, and next generation of hierarchical lattice for ferromagnetic spin interactions. (B) Initiator, generator, and next generation of hierarchical lattice for antiferromagnetic interactions [PR 86a].

for the antiferromagnetic hierarchical lattice (a hexagon) is necessarily more complicated than the generator for the ferromagnetic lattice (a rhombus).

The fact that such hierarchical lattices do not exist in nature has not prevented physicists from playing endless computer games with them; they are great fun! And while the playing continues, everybody is waiting for even faster supercomputers and parallel processors to be able to study more realistic models. (In their spare time, these number crunchers can then factor giant integers, like the 100-digit monster that was reported on the front page of the *New York Times* on October 12, 1988, to have been cracked to yield its two prime factors, 41 and 60 digits long.)

Given that hierarchical lattices are defined recursively and exhibit self-similarity, it is not surprising that they can be characterized by a fractal dimension. However, the hoped-for universality has not materialized: hierarchical lattices with identical connectivities and fractal dimensions have been constructed whose phase transitions have different critical exponents [Hu 85].

In 1952, in one of the more daring attacks on phase transitions, Yang and Lee introduced complex numbers to represent such physical variables as temperature and magnetic field strength [YL 52]. Later it was found that the Julia sets of the renormalization transformation of hierarchical models are identical with the sets of complex zeros that Yang and Lee had worked with [PPR 85]. Similar Julia sets were obtained for the zeros of the partition function of Ising models on self-similar fractal lattices [SK 87]. These fractal Julia sets, like those of the quadratic map (Chapter 12), exhibit visually appealing self-similarities, which are engendered by the recursive construction of the underlying lattices. They are celebrated in Peitgen and Richter's *The Beauty of Fractals* [PR 86a].

## The Percolation Threshold of the Bethe Lattice

Another type of hierarchical lattice is the Bethe lattice (see Figure 3), known in graph theory as a Cayley tree. In a Cayley tree each node has the same number  $z$  of branches or bonds. Thus, the size of the neighborhood grows *exponentially* with "diameter," as opposed to a power-law growth for physical lattices—fractal or nonfractal. It is therefore not surprising that in some respects the Bethe lattice behaves as if its number of dimensions were infinite. But the infinite Bethe lattice, being hierarchical, permits calculating both the percolation threshold and the probability  $P$  that a given lattice site is connected to infinity, by a beautifully simple similarity argument.

Starting at an arbitrary site and proceeding to one of its  $z$  neighbors, we find  $z - 1$  new bonds or branches emanating from the neighbor (see Figure 4). Each of these  $z - 1$  branches leads to a neighbor, which is occupied with probability  $p$ . Thus, on average there are  $(z - 1)p$  new occupied neighbors to which the path can be continued. If this number is smaller than 1, the probability of

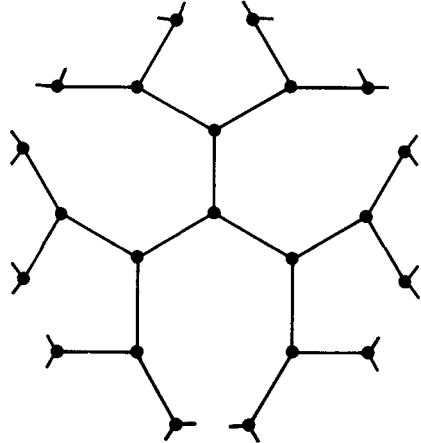


**Figure 3** Cayley tree, called Bethe lattice by physicists. Here each node has exactly three bonds [Sta 85].

finding a connected path of a given length decreases exponentially with length. On the other hand, if  $(z - 1)p$  exceeds 1, there is a positive probability that an infinite path exists. Thus, the percolation threshold  $p_c$  (for either sites or bonds) is given by

$$p_c = \frac{1}{z - 1} \quad (3)$$

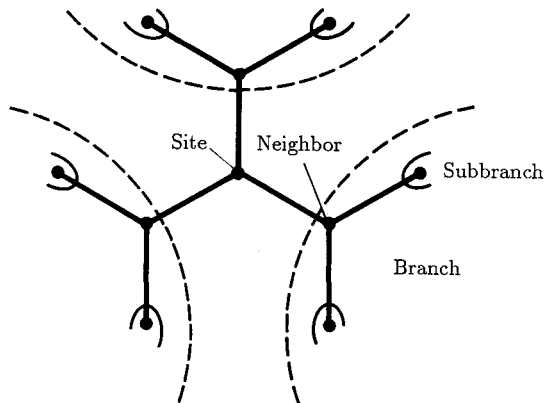


**Figure 4** Hierarchical neighborhoods: branches and subbranches in a Bethe lattice [Sta 85].

which for  $z = 3$  equals  $\frac{1}{2}$ , as for site percolation on a triangular lattice or bond percolation on a square lattice [Sta 85].

However, the probability  $P$  that a *given* lattice site is connected to infinity does not equal 1. After all, there is a finite probability  $(1 - p)^z$  that its  $z$  neighbors are unoccupied. What is the probability  $P$  that a given site does belong to an infinite cluster for  $p > p_c$ ? (For  $p < p_c$ ,  $P$  is obviously equal to zero.)

Let  $Q$  be the probability that a given site is *not* connected to infinity through *one* fixed branch originating from this site. The probability that *all*  $z - 1$  sub-branches from a neighbor site are not connected to infinity equals  $Q^{z-1}$ . (Because of the statistical independence of the occupation probabilities, the probabilities  $Q$  are simply multiplied.) Thus,  $pQ^{z-1}$  is the probability that the neighbor is occupied but not connected to infinity. With probability  $1 - p$  the neighbor is not even occupied, in which case it provides no link to infinity even if it is well connected. Thus, we find the fundamental relation

$$Q = 1 - p + pQ^{z-1} \quad (4)$$

which for  $z = 3$  has two solutions:

$$Q = 1 \quad \text{and} \quad Q = \frac{1-p}{p}$$

The probability  $p - P$  that a given site is occupied but not connected to infinity equals  $pQ^z$ . Thus,

$$P = p(1 - Q^z) \quad (5)$$

or, for  $z = 3$ ,

$$P = p \left( 1 - \left( \frac{1-p}{p} \right)^3 \right)$$

At the percolation threshold  $p = p_c = \frac{1}{2}$ , this relation gives  $P = 0$ , demonstrating that although an infinite cluster exists, it is infinitely dilute.

The ratio  $P/p$  is plotted as the solid line in Figure 5, together with  $P/p$  for the triangular lattice (dashed line). Note the steep rate of increase of  $P/p$  for the triangular lattice. For example, for  $p = 0.6$ , the probability  $P$  that a given Bethe lattice site is a member of an infinite cluster equals 0.422, while for the triangular lattice the probability  $P$  that an *occupied* site is a member of an infinite cluster is practically 1.

The solution  $Q = 1$  of equation 4, which, with equation 5, gives  $P = 0$ , obviously corresponds to  $p < p_c$ . Indeed, for  $z = 2$ , for which equation 3 gives  $p_c = 1$ , the only solution of equation 4 for  $p < 1$  is  $Q = 1$ , that is,  $P = 0$ .

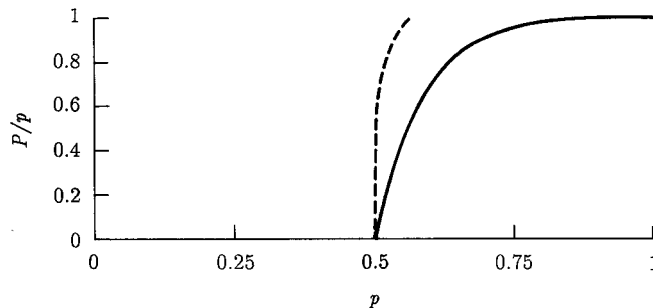


**Figure 5** Strength  $P$  of the infinite network plotted against concentration  $p$  in the Bethe lattice (solid line), and in the triangular lattice (dashed line) [Sta 85].

For  $P$  near but above  $p_c = \frac{1}{2}$ ,  $P$  increases with  $p$  according to the relation

$$P = 6(p - p_c) \quad p > p_c \quad (6)$$

Thus, the critical exponent  $\beta$  of  $P$  equals 1.

Below the percolation threshold, the *mean cluster size*  $S$  can be calculated in a similar manner, giving

$$S = p \frac{1 + p}{1 - 2p}$$

[Sta 85], or, for  $p$  near but below  $p_c = \frac{1}{2}$ ,

$$S = \frac{3}{8}(p_c - p)^{-1} \quad p < p_c \quad (7)$$

Hence, the critical exponent for the cluster size is equal to  $-1$ .

Equations 6 and 7 reflect the behavior, for the Bethe lattice with  $z = 3$ , of two important “order parameters,”  $P$  and  $S$ , near a critical point, the percolation threshold  $p = p_c$ . This behavior is characterized by two simple power laws with exponents 1 and  $-1$ , respectively. Such behavior is now often described as “algebraic,” as opposed to logarithmic, exponential, or other transcendental behavior.

Another, early instance in which the Bethe lattice has resulted in an *exactly solvable model* is Anderson localization, an important phenomenon in disordered systems [And 58]. For its discovery, Philip Anderson was awarded the 1977 Nobel Prize in physics. Disordered systems are now a central theme and the subject of intense study in several fields of physics, such as spin glasses and neural networks.

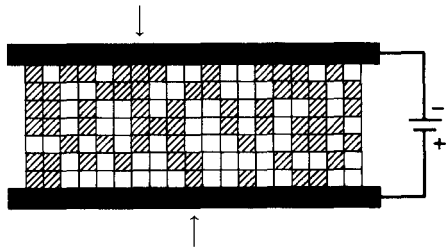


**Figure 6** Random resistor network with one conducting path (arrows) between two copper bars [Sta 85].

There are other lattices for which, different exponents may be found although the behavior is still algebraic. For example, on the square lattice,  $P$  varies as  $(p - p_c)^\beta$  with a critical exponent  $\beta = \frac{5}{36}$ . The very value of this exponent is an indication that its theoretical derivation is anything but trivial.

An important application of percolation theory [Sta 85, Kes 87, Gri 89] is the conductance  $\Sigma$  of random resistor networks (see Figure 6). Of course, for  $p < p_c$ , the conductance is zero. But even for  $p > p_c$  it grows rather slowly with  $p$ , compared with the growth of the probability  $P$  that a given site is a member of an infinite cluster. The reason is that most sites in an infinite cluster near the percolation threshold belong not to the "backbone" but to dangling dead ends that do not contribute to the conductance.

## A Simple Renormalization

The fundamental requirement for renormalization to work is self-similarity. Since many critical phenomena in physics show self-similar behavior near the critical point (the percolation threshold, or the Curie temperature, for instance), these phenomena are therefore amenable to a renormalization-theoretic treatment, yielding the critical exponents for the correlation length  $\xi$  and other important parameters.

Following Stauffer [Sta 85], we shall illustrate the renormalization method for a case for which an exact answer is known: the triangular lattice (see Figure 7). For this lattice, the *bond* percolation threshold  $p_c$  equals precisely  $\frac{1}{2}$  and the correlation length exponent  $v$  is believed to be  $\frac{4}{3}$ . Let us see whether we can derive  $p_c$  and  $v$  by a space renormalization of the lattice.

For this purpose, we replace three adjacent lattice sites in the triangular lattice by a "supersite" (the open circles in Figure 7). Suppose the occupation probability of the original sites is  $p$ . What is the corresponding probability,  $p'$ , of a supersite? We consider a supersite occupied if its original sites form a

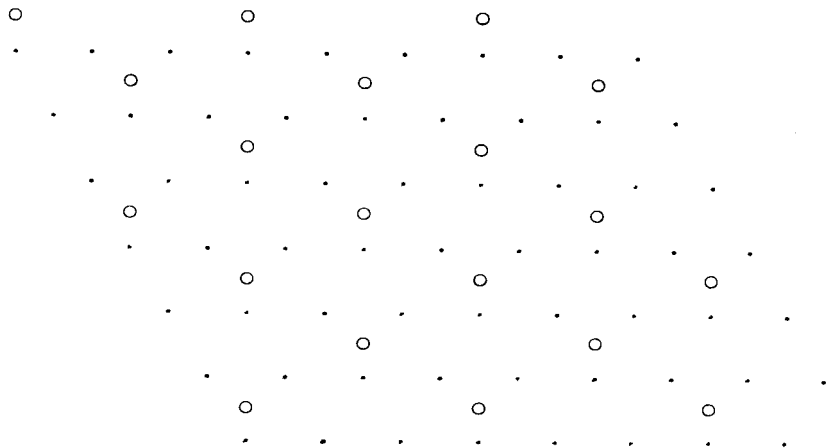


**Figure 7** Space normalization of the triangular lattice.“Supersites” (open circles) each replace three adjacent sites and again form a triangular lattice [Sta 85].

“spanning cluster,” that is, if *at least* two out of its three sites are occupied. The probability that all three sites are occupied is  $p^3$ , and the probability that exactly two out of three sites are occupied equals (3)  $p^2(1 - p)$ . Thus,

$$p' = p^3 + 3p^2(1 - p) \quad (8)$$

At a critical point  $p = p_c$ , we should have  $p' = p$ . Hence, with equation 8, we find three critical points  $p_c = 0, \frac{1}{2}$ , and 1, of which only  $p_c = \frac{1}{2}$  is nontrivial. This renormalization result corresponds precisely to the known site percolation threshold for the triangular lattice. Renormalization seems to work! But will we be as lucky with the correlation-length exponent  $\nu$ ?

The correlation length  $\xi$  near a critical point is given by

$$\xi = c|p - p_c|^{-\nu} \quad (9)$$

where  $c$  is a constant. In the renormalized lattice we have

$$\xi' = bc|p' - p_c|^{-\nu} \quad (10)$$

where  $b$  is the length scaling factor between lattice and superlattice. If we set  $\xi = \xi'$ , equations (9) and (10) give

$$\nu = \frac{\log b}{\log [(p' - p_c)/(p - p_c)]} \quad (11)$$

Expanding equation 8 about the fixed point  $p = p_c = \frac{1}{2}$  gives

$$p' = p_c + \frac{3}{2}(p - p_c) + \dots$$

or

$$\frac{p' - p_c}{p - p_c} = \frac{3}{2}$$

With  $b = 3^{1/2}$  (see Figure 7), equation (11) yields, to first order in  $(p - p_c)$ ,

$$\nu = \frac{\log 3^{1/2}}{\log (3/2)} = 1.355$$

which is reassuringly close to the exact value  $\nu = \frac{4}{3}$ .

Another powerful approach to renormalization is *conformal mapping* [Car 85]. Like self-similar scaling, conformal mapping preserves angles. Its usefulness results from the conformal invariance—real or assumed—of the system under study. Mirroring a given space at a fixed sphere is a well-known example of a conformal mapping. In the plane, any analytic function defines a local conformal mapping at points where its derivative does not vanish. As an instance of conformal invariance in physics, we might mention Maxwell's famous equations, which were revealed as such in 1909—several decades after their conception.

Here we reluctantly leave renormalization theories and phase transitions to transit to the self-similarities engendered by *cellular automata*.

# C ellular Automata

*Truth is much too complicated to allow anything but approximations.*

—JOHN VON NEUMANN

Cellular automata were originally conceived by Konrad Zuse and Stanislaw Ulam and put into practice by John von Neumann to mimic the behavior of complex, spatially extended structures [TM 87]. As early as the early 1940s, Zuse thought of “computing spaces,” as he suggestively called them, as discrete models of physical systems. Ulam’s proposal came in the late 1940s, shortly after his invention, with Nicholas Metropolis, of the Monte Carlo method. (The astonishingly broad scope of Ulam’s mind can be sampled in the selection from his works titled *Sets, Numbers, and Universes* [Ula 74].) An anthology surveying the present state of cellular automata was edited by Stephen Wolfram [Wol 86].

A one-dimensional cellular automaton consists of a row of *cells*, each cell containing some initial numbers, and a set of *rules* specifying how these numbers are to be changed at every clock time. Suppose in the initial state of the automation all cells are filled with 0s, except a single cell which is occupied by a 1:

... 01000000 ...

And suppose the rule states that the number in each cell is to be replaced by the sum of itself and its left neighbor. Thus, after one clock time, the state of the automaton will be as follows:

... 01100000 ...

Another clock time later the state will be

... 01210000 ...

followed by

... 01331000 ...

... 01464100 ...

and so on. Such cellular automata are in fact computers, and cellular computers are being put to increasing use in calculating intricate functions because they are naturally amenable to fast parallel processing. In the example just given, the cellular computer calculates the binomial coefficients that appear in the expansion of the powers of binomials such as  $(a + b)^4$ , which equals  $a^4 + 4a^3b + 6a^2b^2 + 4ab^3 + b^4$ .

Cellular automata come in one, two, or many dimensions. To calculate a two-dimensional fluid flow, one uses cellular automata that are two-dimensional arrays of cells, each cell filled with a number (representing fluid density, for example) that changes at clock times in accordance with fixed rules acting on a neighborhood of cells. These rules embody local interactions between neighboring cells, reflecting the dynamics of the system under study.

Instead of forming a *square* lattice, the cells can form a hexagonal pattern, for example; and the "numbers" in each cell can in fact be vectors, representing the velocity of a fluid or gas at each lattice point (see Figure 1). Such cellular

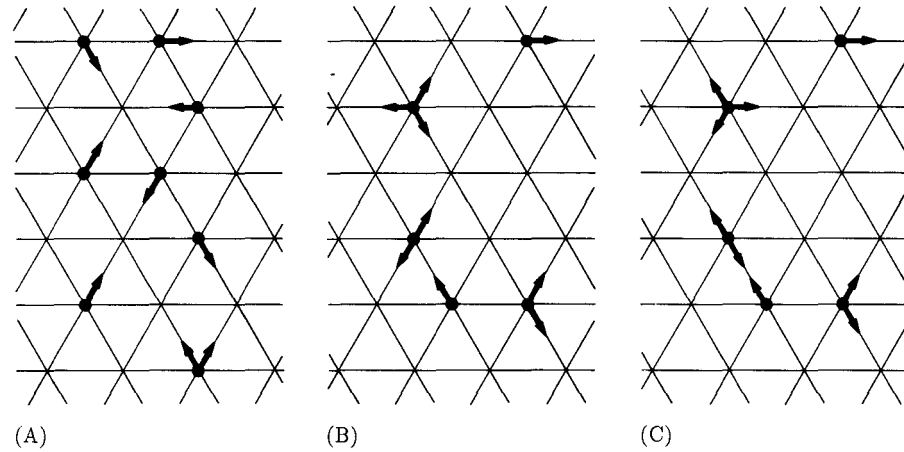


**Figure 1** Hydrodynamic flow modeled by a cellular automaton ("lattice gas"). Parts A, B, and C show successive stages in the history of the gas. The arrows show the directions of the particle velocities.

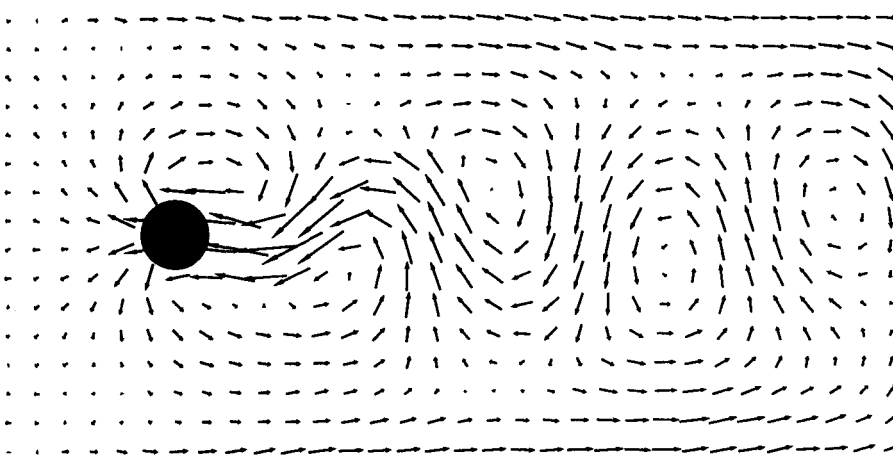


**Figure 2** Flow behind a moving cylinder simulated by a lattice gas [SW 86].

automata, called *lattice gas* models by physicists, have been used to great advantage to simulate otherwise intractable flow problems [SW 86, MBVB 89]. Figure 2 shows the flow behind a cylinder moving from right to left through a viscous gas, exhibiting the well-known vortex shedding behind the obstacle. Such fluid-flow phenomena are still studied by physical experiments in wind tunnels and ship-model basins. But they are now increasingly being analyzed by computer simulations based on cellular automata.

Since typical cellular automata employ repetitive application of fixed rules, we should expect to find self-similarities—as we did with so many other iterative procedures. And indeed, many cellular automata do produce self-similar patterns, often of considerable visual appeal.

## The Game of Life

The best-known cellular automaton is probably John Horton Conway's game of "Life" [Gar 70]. "Life" describes the growth and decline of a population of cells according to rather simple rules—rules that nevertheless lead to a rich zoo of creatures with truly astounding behavior [BCG 82].

In "Life" as conceived by Conway, each cell is either dead (0) or alive (1) and changes its state according to the states in its immediate neighborhood including its own state. Specifically, at each clock time ("tick"), a cell that is alive will stay alive when it is surrounded by precisely two or three live cells among its eight neighbors on a square lattice. If more than three neighbors are alive, the cell will feel overcrowded and "suffocate" to death. If fewer than two neighbors

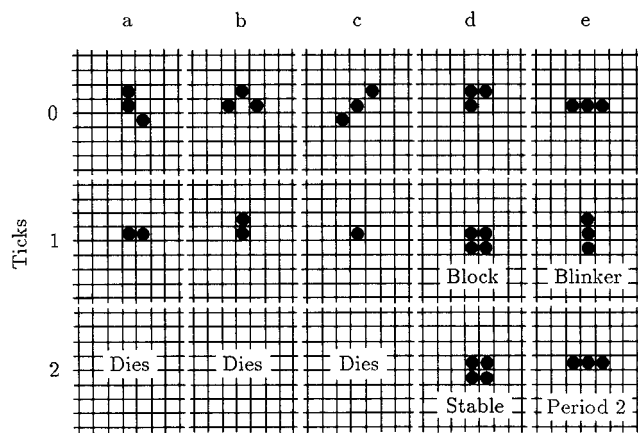


**Figure 3** Conway's "Life": the fates of five triplets [Gar 83].

are alive, the cell will die from loneliness. On the other hand, a dead cell will come to life when surrounded by exactly three live neighbors (two parents and a midwife, so to speak). Figure 3 illustrates the fates of five different triplets. The plethora of patterns generated by these simple rules is beyond belief. Figures 4 to 8 show a sparse sampling of stationary, periodic, disappearing, and surviving "organisms."

Conway's set of rules, or *law*, is but one of many imaginable. For binary-valued cells and a neighborhood of eight cells acting on a center cell, there are  $2^8 \approx 10^{154}$  different "life"-like laws, of which, it seems, only one, the one decreed by Conway, really comes to life.

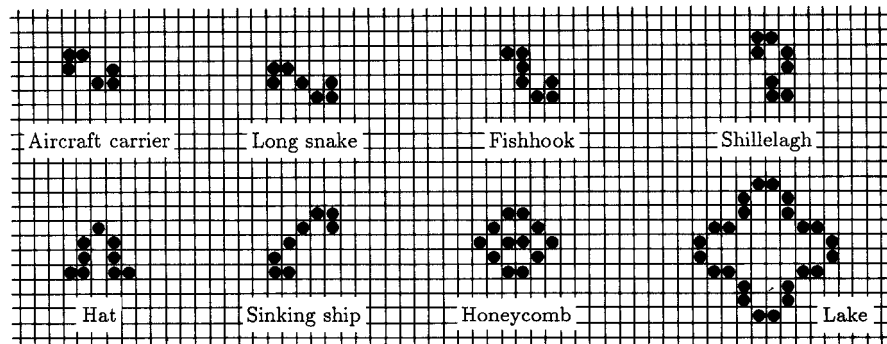


**Figure 4** Six still "Life" forms [Gar 83].

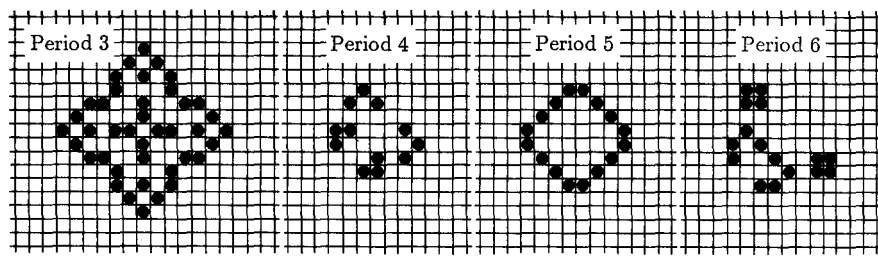


**Figure 5** Four periodic patterns of "Life" [Gar 83].

## Cellular Growth and Decay

Consider a two-dimensional cellular automaton in which a cell again has two possible states, 0 and 1, as in the game of "Life," but has only *four* neighbors, East, West, South, and North, acting on it. The present state of a cell  $C$  and its neighborhood EWSN is given by a 5-bit string, for example, EWSNC = 11000. The next state of  $C$ , say  $C = 1$ , is given by the prevailing rule  $11000 \rightarrow 11001$  (see Figure 9). A complete set of rules, called a *law*, is given by a table of the 32 possible states and the subsequent values of the center cell  $C$  (see Figure 10). For binary-valued cells and four acting neighbors there are  $2^{32} \approx 4$  billion possible different laws.

Figure 11 illustrates the variety of patterns obtained from the fixed law of Figure 10 called HGLASS for different initial conditions [TM 87].

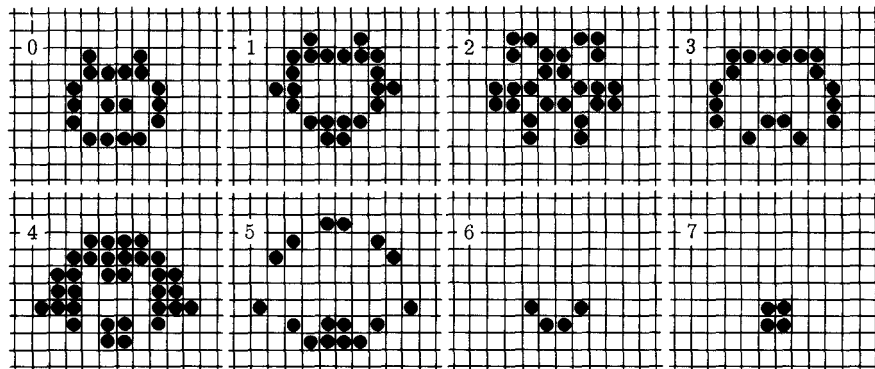


**Figure 6** The Cheshire cat (0) leaves a grin (6) that turns into a permanent paw print [Gar 83].

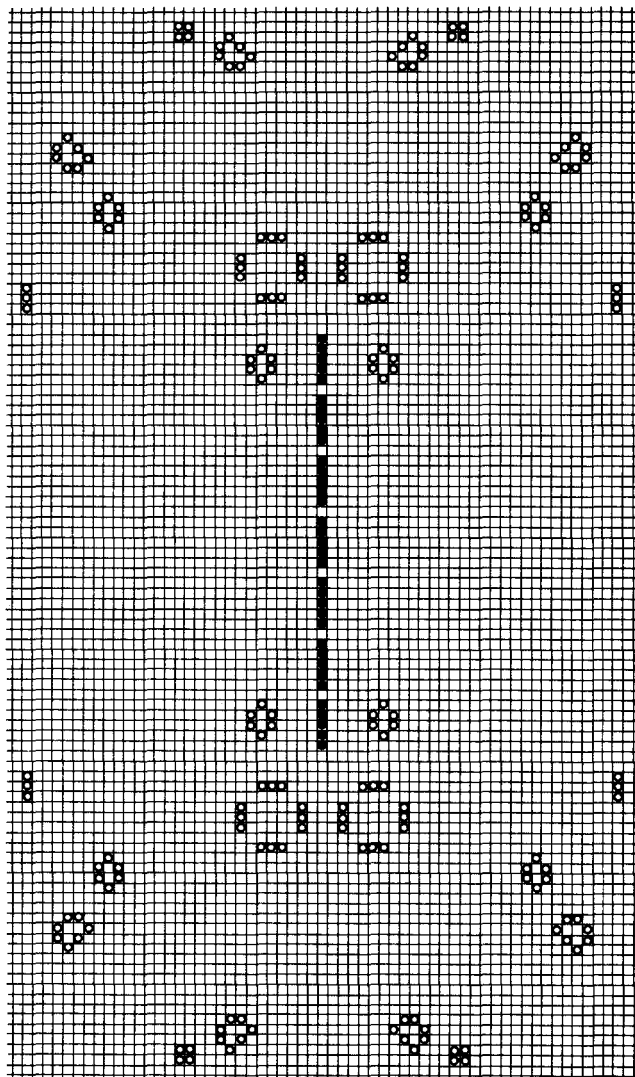


**Figure 7** Initial pattern (solid dots) and final state (open circles) of  $7 \times 5$  bits [Gar 83].

A particularly simple law assigns to  $C$  the sum modulo 2, that is, the *parity*, of the five cells of the neighborhood. Starting with a small square of 1s, floating in a sea of 0s, the patterns that have evolved after some 50 and 100 steps are shown in Figure 12. Are there any self-similarities? Indeed there are. In fact it can be shown that any initial pattern on a uniform background reproduces itself and surrounds itself with four identical copies after a certain number of steps.

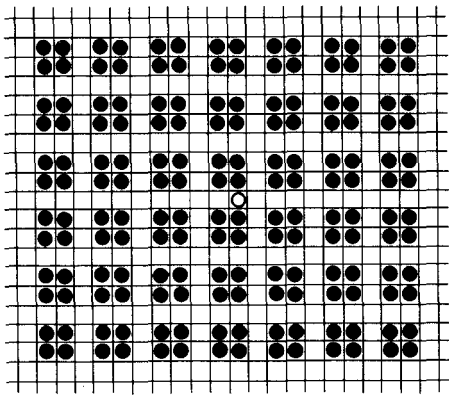


**Figure 8** Killing “Life”: a single “virus” in the position shown (open circle) destroys the entire pattern. In other positions, the virus is eliminated and the pattern repairs itself and survives intact [Gar 83].

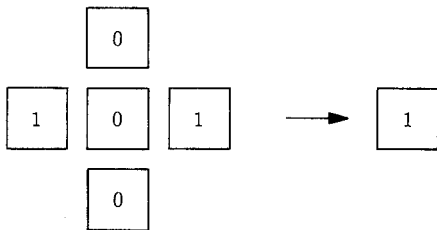
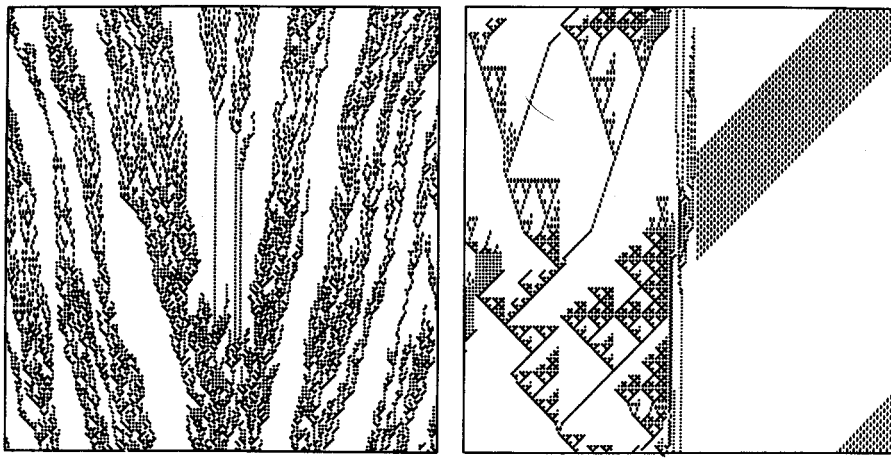


**Figure 9** The center cell is turned on (switches from 0 to 1) by the rule (East, West, South, North, Center) = 11000 → 11001.

| EWSNC | $C_{\text{new}}$ | EWSNC | $C_{\text{new}}$ | EWSNC | $C_{\text{new}}$ | EWSNC | $C_{\text{new}}$ |
|-------|------------------|-------|------------------|-------|------------------|-------|------------------|
| 00000 | 0                | 01000 | 0                | 10000 | 0                | 11000 | 0                |
| 00001 | 1                | 01001 | 0                | 10001 | 0                | 11001 | 1                |
| 00010 | 1                | 01010 | 0                | 10010 | 0                | 11010 | 0                |
| 00011 | 1                | 01011 | 1                | 10011 | 0                | 11011 | 0                |
| 00100 | 0                | 01100 | 0                | 10100 | 0                | 11100 | 0                |
| 00101 | 0                | 01101 | 0                | 10101 | 1                | 11101 | 1                |
| 00110 | 0                | 01110 | 0                | 10110 | 0                | 11110 | 1                |
| 00111 | 0                | 01111 | 0                | 10111 | 0                | 11111 | 1                |

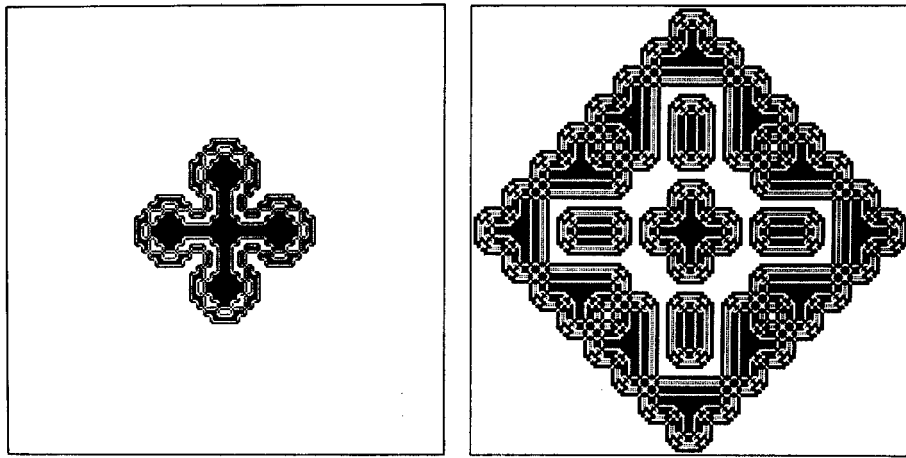
**Figure 10** Table of rules HGLASS, one of 4 billion possible sets of rules.



(A)

(B)

**Figure 11** (A) An HGLASS pattern evolving from random seed. (B) HGLASS pattern resulting from a simple seed [TM 87].



(A)

(B)

**Figure 12** (A) Pattern produced by parity rules from a  $32 \times 32$  square pattern after 50 steps. (B) Parity pattern after 100 steps [TM 87].

And after the same number of steps there will be 25 copies of the original, and so forth *ad infinitum*. Because summation modulo 2 is a linear operation, different patterns can penetrate each other without affecting the future growth. Specifically, any pattern can be obtained by the summation modulo 2 of patterns generated by a single, isolated point.

Another simple law turns a cell on (1) if exactly one of its eight neighbors is alive (1); otherwise it remains unchanged. The resulting growth is a self-similar fractal (Figure 13), whose Hausdorff dimension the reader may wish to calculate.

In still another law, each cell adjusts to the *majority* in its neighborhood: if four or fewer of the neighborhood of nine (including itself) are off, then the center cell will also turn (or stay) off. Otherwise it will turn or stay on. The resulting patterns resemble Ising spin systems at low temperature and are reminiscent of percolation; see Figure 14A for a pattern emerging from an initial configuration of random 1s occupying half the cells.

How sensitive the patterns are to slight amendments in the law is illustrated in Figure 14B, in which either five or fewer than four neighbors in the off state will turn the center cell off. This law, drafted by G. Vichniac, simulates annealing, as evidenced by the consolidation of domains [Vic 86]. These patterns are spatially homogeneous but not self-similar.

To obtain self-similar spin domains, the initial random configuration has to have a *critical "energy"* [Vic 84]. The energy pattern has a *broken symmetry* with magnetic domains on all size scales; see Figure 15.

While all laws passed so far have been of a "strictly enforced" nature, that is deterministic, many cellular automata are subjected to *random* rules to emulate

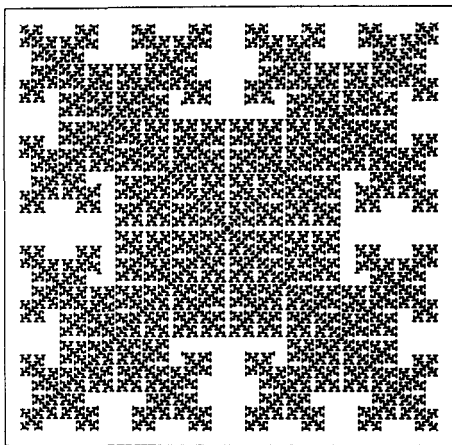
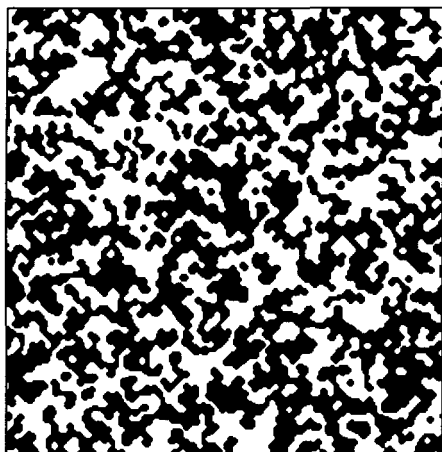


**Figure 13** Self-similar fractal produced by the one-out-of-eight rule [TM 87].



(A)



(B)

**Figure 14** (A) Pattern evolving from 50 percent random 1s by “majority-voting” rule of neighbors. (B) Result of “annealed-majority” rule [Vic 86].

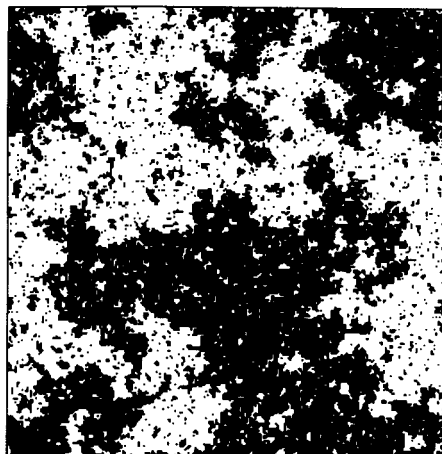


**Figure 15** Equilibrium configuration of Ising spins at the critical temperature shows magnetic domains on all size scales [Vic 84].

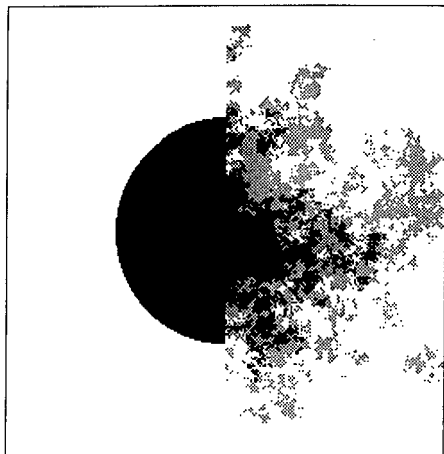


**Figure 16** Exploding disk obtained from "copy random neighbor" rule [TM 87].

diffusion and other stochastic processes. For example, a lenient law may simply say, "Copy from a random neighbor." With one of four neighbors chosen with equal probability, an initial disk will explode as shown in the right half of Figure 16. Diffusion with drift can be simulated by "particles" (1s) that move with probability  $\frac{3}{8}$  either east or south and with probability  $\frac{1}{8}$  west or north (Figure 17).

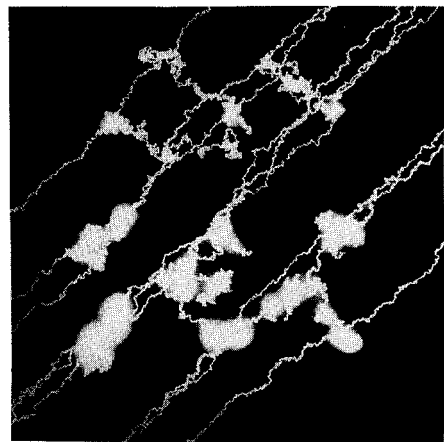


**Figure 17** Diffusion with and without drift: a pretty programming error [Schr 69].

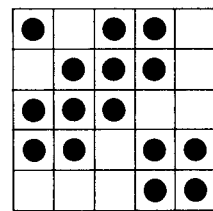
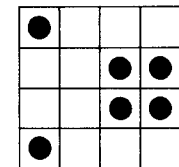


**Figure 18** Odd-parity covers for a  $4 \times 4$  and a  $5 \times 5$  chessboard [Sut 89].

Such cellular automata can be bred into plausible models of genetic drift. Color Plate 9 shows the spatial intermingling for sixteen competing species of genes [TM 87].

A classical problem that can be phrased in the language of cellular automata is the “all-1s” problem [Sut 89]. Each square (cell) of an  $n \times n$  chessboard is equipped with a light bulb and a switch that turns the bulbs in a given neighborhood on (or off, for those that are already on). Starting with a completely dark chessboard, which switches must be activated to light up all bulbs? It is clear that the number of activated buttons in the neighborhood of each square must be odd. This is called an *odd-parity cover*. If the neighborhood of a square consists of the square itself and its four edge-adjacent neighbors, odd-parity covers for a  $4 \times 4$  and a  $5 \times 5$  board are as shown in Figure 18.

What is the solution for an  $8 \times 8$  board? Can the reader design the rules for a cellular automaton that will converge on the proper set of switches, that is, an odd-parity cover for a given neighborhood? Of course, if the odd-parity cover is a “Garden of Eden,” it can never be reached. (A Garden-of-Eden pattern is defined as one that has no predecessor; once lost, it can never be regained.)

## Biological Pattern Formation

Another field where cellular automata have proved their mettle for modeling is pattern formation in plants and animals. The formation of stripes in zebras and numerous other patterns in countless forms of life has been modeled with cellular automata by H. Meinhardt, A. Gierer, and others using combinations of local and long-range autocatalytic and inhibitory interactions [Mei 82].

A simple cellular automaton imitates the design on the shell of the snail *Olivia porphyria* (see Figure 19), characterized by diagonal lines that annihilate each other when they touch. Another mechanism causes a single line to bifurcate to keep the average pigmentation near a given level [MK 87].

Numerous other biological structures, including the formation of arms and legs, have been modeled by cellular automata employing simple self-reinforcing and antagonistic reactions. The variety of shapes thus engendered is truly astonishing.

## Self-Similarity from a Cellular Automaton

Self-similarity arises in many fields in many forms. A set of Russian dolls, all looking alike but each a little smaller than its parent, is perhaps the most widely known example of discrete, if limited, self-similarity. Self-similarity can even be distilled from such a discrete and artless entity as the integers 0, 1, 2, 3, 4, 5, 6, 7, . . . Let us write successive integers, starting with 0, in the binary number system (apparently invented by Leibniz while waiting to see the Pope in the Vatican with a proposal to reunify the Christian churches):<sup>1</sup>

$$0, 1, 10, 11, 100, 101, 110, 111, \dots$$

The sums of the digits for each number form the sequence

$$B(t) = 0, 1, 1, 2, 1, 2, 2, 3, \dots \quad t = 0, 1, 2, \dots$$

which can also be obtained *iteratively* as follows. To obtain the subsequence of length  $2^{n+1}$  from the subsequence of length  $2^n$ , repeat the latter with 1 added to each term. Thus, the initial subsequence of length  $2^0 = 1$  (i.e., 0) generates the subsequence of length  $2^1 = 2$  (i.e., 01) by appending to the initial 0 the number  $0 + 1 = 1$ . In this manner, successive generations of subsequences of length  $2^n$  are generated:

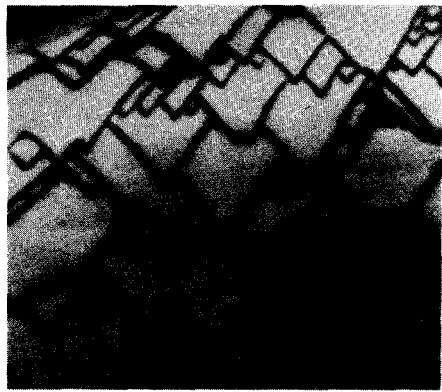
```

0
01
0112
01121223
0112122312232334
:

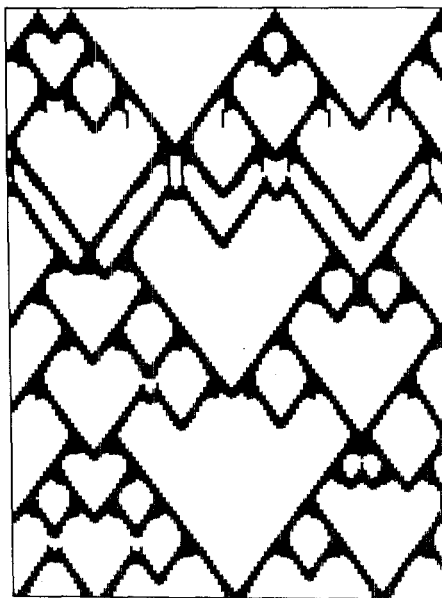
```

---

1. The fact that this system uses only two digits, 0 and 1, is, of course, the reason why computers are so fond of it: a digit is simply and unambiguously represented by the two states of a switch, open or closed—nothing in between.



(A)



(B)

**Figure 19** (A) Detail of the shell of the snail *Olivia porphyria*. (B) Wavelike design generated by a cellular automaton with local and long-range autocatalytic interactions [MK 87].

This generative rule is, of course, a direct consequence of how binary numbers are defined: for  $k < 2^n$  the two integers  $k$  and  $k + 2^n$  differ by precisely a single 1 in their binary notations.

It is interesting and important to note that our iterative rule for generating subsequences is a *fast algorithm*: each iteration *doubles* the length of the subsequences. Their lengths therefore grow *exponentially* with the number of iterations. (By contrast, a *linear* recursion, such as that for the sequence of Fibonacci numbers,  $F_{n+2} = F_{n+1} + F_n$ , adds only one additional term with *each* iteration.)

The infinite sequence  $B(t)$  obtained in this manner is self-similar in the following sense: it reproduces itself when only even-indexed terms are retained, as indicated in the following by underlining:

$$B(t) = \underline{0}, \underline{1}, \underline{2}, \underline{1}, \underline{2}, \underline{2}, \underline{3}, \underline{1}, \underline{2}, \underline{2}, \underline{3}, \underline{2}, \underline{3}, \underline{3}, 4, \dots$$

Thus,  $B(2t) = B(t)$ .

This self-similarity is a near-trivial consequence of the fact that, in the binary system, multiplication by 2 results in a mere left shift of the digits, which, of course, does not change the sum of the digits.

The sequence  $B(t)$  can be converted into a sequence that is self-similar also in the *magnitude* of its terms. In fact, the sequence

$$C(t) = 2^{B(t)} = 1, 2, 2, 4, 2, 4, 4, 8, \dots$$

has the same similarity factor of 2 not only in its index  $t$  but also in its magnitude. The second half of each subsequence of length  $2^{n+1}$  equals twice the first half:

$$C(t + 2^n) = 2C(t) \quad 0 \leq t < 2^n \tag{1}$$

Figure 20 illustrates the sequence  $C(t)$  and its self-similarity. Alternatively,  $C(t)$  can be obtained from the product  $(1 + b_1)(1 + b_2)(1 + b_3)\dots$ , where the  $b_k$  are the bits of the binary expansion of  $t$ .

Interestingly,  $C(t)$  can also be generated by a cellular automaton, and this is important for what follows. Let us ask how many of the binomial coefficients  $\binom{t}{n}$  for a given  $t$  are odd as  $n$  runs from 0 to  $t$ . The answer (I leave the simple inductive proof to the reader) is  $1, 2, 2, 4, 2, 4, 4, 8, \dots = C(t)$ . And the binomial coefficients themselves are generated by one of the simplest cellular automata. (See the introduction to this chapter.)

Note that  $C(t)$  summed to  $t = 2^m - 1$  is equal to  $3^m$ . This follows directly from  $C(0) = 1$  and equation 1.

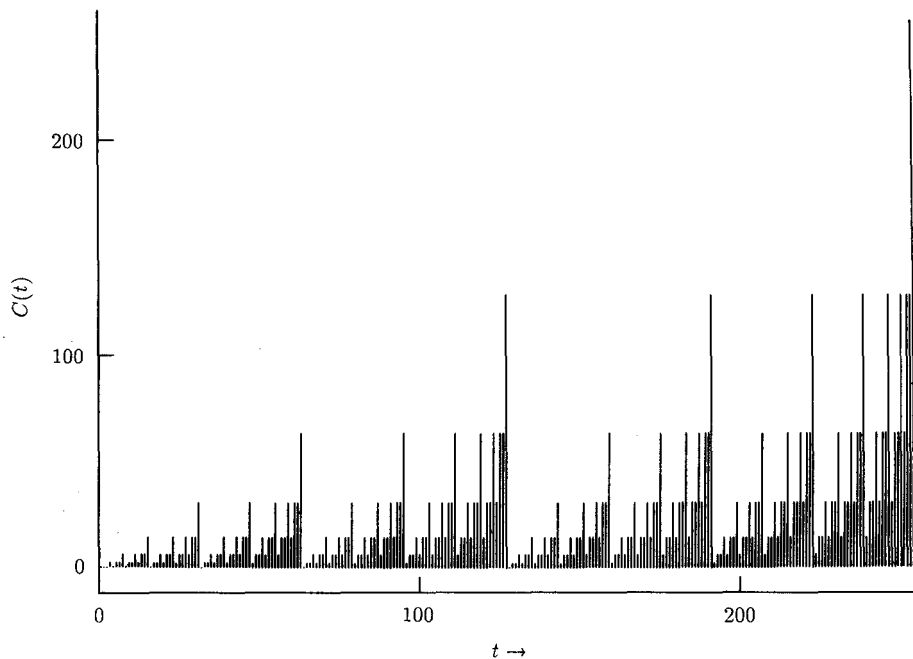


**Figure 20** Self-similar sequence obtained from the binary number system.

## A Catalytic Converter as a Cellular Automaton

Sequences resembling  $C(t)$ , where  $t$  is interpreted as discrete time, have been observed in certain chemical reactions—for example, in catalytic oxidation processes (see Figure 21). Now what on earth could the relation be between a chemical reaction and the sequence  $C(t)$ , that is,  $2$  raised to the sums of digits in the binary representations of successive integers? A simple explanation was found by Andreas Dress, who modeled such catalytic processes by one-dimensional cellular automata [DGJPS 85].

In a one-dimensional cellular automaton, each time epoch is characterized by a sequence of symbols or numbers. And as we learned in the introduction to this chapter, the sequence at time  $t$ ,  $g_t(n)$ , is generated by some law from the sequence at time  $t - 1$ . For example,

$$g_t(n) = g_{t-1}(n) + g_{t-1}(n-1)$$

which, with the initial generation  $g_0(0) = 1$  and  $g_0(n) = 0$  elsewhere, generates the binomial coefficients  $\binom{n}{k}$  as arranged in Pascal's triangle. In Pascal's triangle

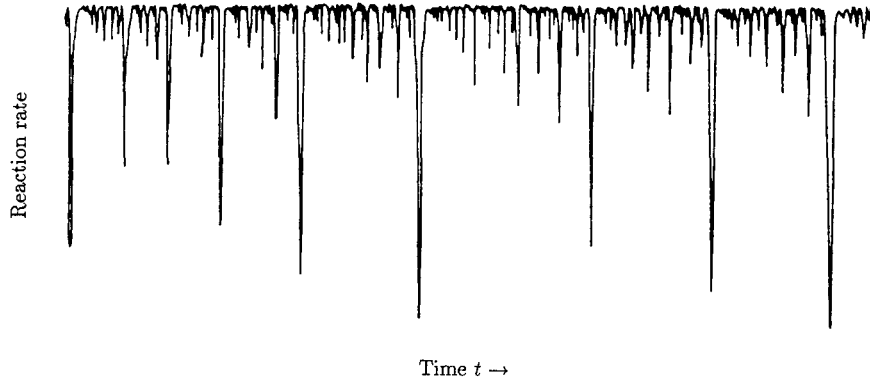


**Figure 21** Chemical reaction rate as a function of time in a catalytic oxidation process [DGJPS 85].

each number is the sum of the two numbers directly above it. Now let us take Pascal's triangle modulo 2. That is, if the binomial coefficient  $\binom{n}{k}$  is odd, then the number is replaced by 1; if it is even, it is replaced by 0. The resulting Pascal's triangle modulo 2 is illustrated in Figure 22. Black cells correspond to 1s and white cells to 0s.

In terms of the chemical reaction modeled by Pascal's triangle modulo 2, Dress assumed that a "molecule," represented by a cell at position  $n$ , becomes "infected" (e.g., oxidized) at time  $t$  if precisely one of its neighbors at positions  $n$  and  $n - 1$  was infected (black) at time  $t - 1$ .

But by construction, the *number* of black squares (1s) at time  $t$  equals  $C(t)$ . Thus,  $C(t)$  describes the chemical reaction rate in the specified catalytic converter, a fact originally suggested by the approximate self-similarity of the reaction as seen in Figure 21.

## Pascal's Triangle Modulo N

The recursive generation of Pascal's triangle of binomial coefficients  $\binom{n}{k}$  from a single 1 is a paradigm of a cellular automaton. While the numbers  $\binom{n}{k}$  themselves become larger and larger with increasing  $t$  and  $0 < n < t$ , their divisibility properties form self-similar patterns. In fact, the even coefficients occupy triangles much like the holes in a Sierpinski gasket (see pages 17–18). The appearance of these triangles follows easily from the fact that the  $\binom{n}{k}$  for  $t = 2^m$  are all even

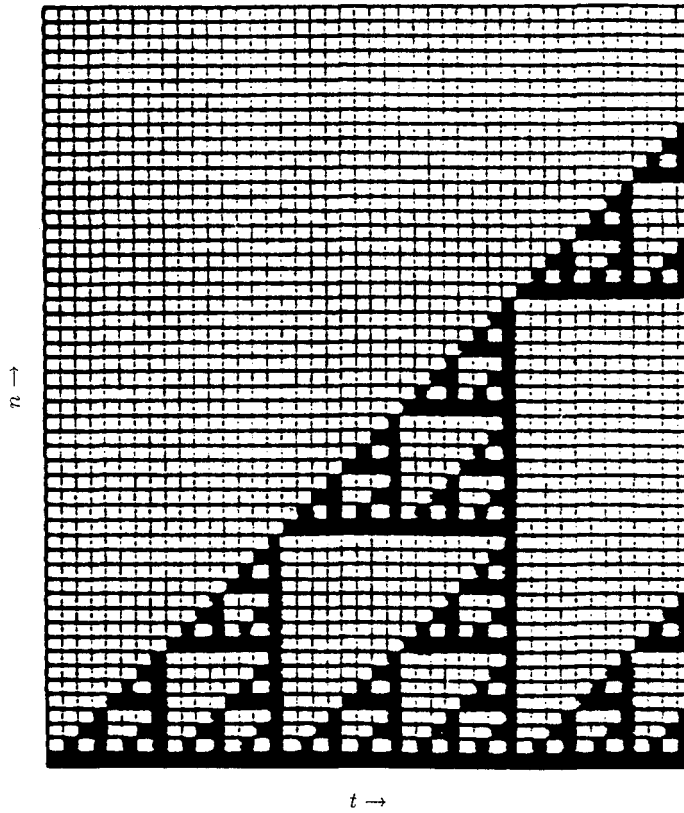


**Figure 22** Pascal's triangle modulo 2: a discrete version of the Sierpinski gasket.

for  $0 < n < t$ . The two 1s for  $n = 0$  and  $n = t$  then progressively "eat up" the even coefficients as  $t$  is increased, until for  $t = 2^{m+1} - 1$  all coefficients are odd.

Similar mechanisms produce self-similar patterns from Pascal's triangle if the binomial coefficients are taken modulo any other prime [Wol 84]. The PC-equipped reader is invited to generate, in cellular-automaton fashion, Pascal's triangle modulo arbitrary prime numbers, powers of primes, and general composite numbers and to observe the resulting self-similarities in one or many colors. What are the Hausdorff dimensions  $D$  of the limiting patterns? The value of  $D$  for Pascal's triangle modulo 2,  $D = \log 3/\log 2$ , can be inferred from the fact that the total number of odd coefficients goes up by a factor of 3 every time the number of lines is doubled, beginning with the first line consisting of a single 1—just as the covered area of the infinite Sierpinski gasket triples for every doubling of the linear dimensions of the cover.

## Bak's Self-Organized Critical Sandpiles

As we have seen in several chapters of this book, many natural phenomena—from flicker noise to the flow of the river Nile—have self-similar power spectra with an  $f^{-\beta}$  frequency dependence. Such processes are called  $1/f$  noise (even if the spectral exponent  $\beta$  is not exactly equal to 1). Such power-law spectra signal the absence of characteristic time scales; there are no such typical times as the half-life in radioactive decay, for example.

The absence of characteristic scales is also evident in the *spatial* aspects of numerous natural events; no characteristic lengths prevail, in contrast to nuclear forces or the mean free path of molecules in a gas.

To account for the ubiquity of such self-similar structures, Per Bak, Chao Tang, and Kurt Wiesenfeld have recently introduced the concept of *self-organized criticality* [BTW 87]. In their paper of that title and subsequent publications [TB 88, BTW 88], Bak and his collaborators argue persuasively that spatially extended dynamic systems evolve spontaneously into barely stable structures of critical states and that this self-organized criticality is the common underlying mechanism for many self-similar and fractal phenomena.

To make their proposal concrete, Bak and his coworkers have constructed several models, including a simple two-dimensional cellular automaton mimicking the flow of sand in a sandpile. If the slope becomes too large at some point  $(x, y)$  in the pile, sand flows to reduce the gravitational force  $z$  at the expense of the forces on the four neighboring points  $(x \pm 1, y)$  and  $(x, y \pm 1)$ . Thus, if the (integer) variable  $z$  exceeds a critical value  $z_c$ , it is updated (synchronously) as follows:

$$\begin{aligned} z(x, y) &\rightarrow z(x, y) - 4 \\ z(x \pm 1, y) &\rightarrow z(x \pm 1, y) + 1 \\ z(x, y + 1) &\rightarrow z(x, y + 1) + 1 \end{aligned}$$

The automaton is started with random initial conditions  $z \gg z_c$ ; the boundary conditions are  $z = 0$ . Once all  $z$  are smaller than  $z_c$ , the evolution of the system stops; it has reached a *minimal stable state*—minimal, because the addition of a single grain of sand may set off an avalanche. In fact, backing Bak, the reader equipped with a personal computer may discover that sand avalanches on all length scales will be triggered by small local perturbations, that is, random additions of sand to a single site. The clusters of sites reached by this physical “domino effect” have power-law size distributions:

$$D(s) \sim s^{-\tau}$$

with  $\tau \approx 1$  for cluster sizes  $s$  ranging up to 500 for a  $50 \times 50$  array and  $\tau \approx 1.35$  for a three-dimensional  $20 \times 20 \times 20$  array [BTW 87].

The *life-times* of these avalanches, too, follow power laws with exponents  $\alpha \approx 0.43$  in two dimensions and  $\alpha \approx 0.9$  in three, corresponding to power-spectrum exponents  $2 - \alpha$  equal to 1.57 and 1.1, respectively.

Tang and Bak also found a power-law behavior of the flow, the correlation length, the largest cluster size, and other parameters if the average value of  $z$  is kept away from its critical value by an "external field" [TB 88]. While the critical exponents they found for these quantities may depend on the details of the system under consideration, they expect the power-law scaling as such to be more universal.

If so, self-organized criticality may lend itself as a generic model for a great variety of scale-invariant phenomena, from glassy systems, magnetic domains, water flow, and turbulence to traffic jams, economic interactions, and earthquakes [BW 90].

And do not the political upheavals in eastern Europe in 1989 also flow from long maintained minimally stable states?

## The Hausdorff Dimension for Unequal Remainders

The following proof was suggested by H. W. Strube.

Let  $I_k \subset [0, 1]$  be the intervals of the generator of a Cantor set  $F$  and  $s_k = |I_k|$  their lengths. (In the original “ternary” Cantor set  $I_1 = [0, \frac{1}{3}]$ ,  $I_2 = [\frac{1}{3}, \frac{2}{3}]$ , and  $s_1 = s_2 = \frac{1}{3}$ .) Define those parts of  $F$  that lie in  $I_k$  as  $F_k$ :

$$F_k := F \cap I_k \quad (1)$$

Let  $N(r)$  and  $N_k(r)$  be the smallest numbers of intervals of radius  $r$  that cover  $F$  and  $F_k$ , respectively. Further, let  $L$  be the length of the *smallest gap* between the  $I_k$ . For  $2r < L$ , we then have

$$N(r) = \sum_k N_k(r) \quad (2)$$

or

$$\sum_k \frac{N_k(r)}{N(r)} = 1 \quad (3)$$

Since  $F_k$  is simply a scaled version of  $F$ , with the scaling factor  $s_k$ , we have  $N_k(s_k r) = N(r)$ , or

$$N_k(r) = N\left(\frac{r}{s_k}\right) \quad (4)$$

Thus, for  $r \rightarrow 0$ , since the Hausdorff dimension  $D$  is also a similarity dimension (that is,  $N(r) \sim r^{-D}$ ),

$$\frac{N_k(r)}{N(r)} \rightarrow s_k^D \quad (5)$$

holds. Introducing this relation into equation 3, one obtains the generalized result

$$\sum_k s_k^D = 1 \quad (6)$$

for the Hausdorff dimension  $D$  of a Cantor set whose generator consists of intervals of arbitrary lengths  $s_k$ .

## Noble and Near Noble Numbers

Noble numbers  $v$  are defined as irrational numbers whose continued fractions end in all 1s. For  $0 < v < 1$ , we have

$$v := [a_1, a_2, \dots, a_n, \overline{1}] \quad (1)$$

where the bar over the 1 indicates an infinite sequence of 1s.

With the help of the golden mean

$$\gamma := [\overline{1}] = 0.618 \dots \quad (2)$$

the noble numbers can be written as "equivalent numbers" [HW 84]:

$$v = \frac{A_n + \gamma A_{n-1}}{B_n + \gamma B_{n-2}} \quad (3)$$

where  $A_k$  and  $B_k$  are the numerator and denominator, respectively, of the  $k$ th approximating fraction ("convergent") of  $[a_1, a_2, \dots, a_n]$ .

For example, a simple noble number, as defined in equation 1, for  $n = 2$ , with  $a_1 = 1$  and  $a_2 = 2$ , is  $v = [1, 2, \overline{1}] = 0.7236 \dots$ . Since the approximating fractions of the nonperiodic "leader"  $[1, 2]$  are equal to  $A_1/B_1 = 1/1$  and  $A_2/B_2 = 2/3$ ,  $v$ , according to equation 3, can also be written as

$$v = \frac{2 + \gamma}{3 + \gamma} \quad (4)$$

In general, because  $\gamma = (\sqrt{5} - 1)/2$ , the noble numbers form a subset of the field  $\mathbb{Q}(\sqrt{5})$ .

I have defined *near noble* numbers as all those real numbers  $\tilde{v}$ ,  $0 < \tilde{v} < 1$ , whose continued fraction expansion is periodic, with period length  $P$ , the period comprising  $(P - 1)$  1s followed by an integer  $n > 1$ :

$$\tilde{v} = [\overline{1, 1, \dots, 1, n}] \quad \text{period length } P \quad (5)$$

where the horizontal bar indicates periodic repetition. A simple near noble number is  $[\overline{1, 2}] = \sqrt{3} - 1$ .

To see which  $\tilde{v}$  have the continued fraction expansion represented in equation 5, we express its periodicity in the following form:

$$\tilde{v} = \left[ 1, 1, \dots, 1, n, \frac{1}{\tilde{v}} \right] \quad (6)$$

where the last term on the right,  $1/\tilde{v}$ , although not an integer, is treated like any other term in a continued fraction expansion. For example,

$$\tilde{v} = [\overline{1, 2}] = \left[ 1, 2, \frac{1}{\tilde{v}} \right] = \frac{1}{1 + (1/2 + \tilde{v})} \quad (7)$$

This is a quadratic equation for  $\tilde{v}$  with the positive solution  $\tilde{v} = \sqrt{3} - 1$ .

Calculating the value of  $\tilde{v}$  from equation 6, we obtain

$$\begin{array}{ccccccccc} & 1 & 1 & 1 & \dots & 1 & & n & 1/\tilde{v} \\ \hline 1 & 0 & 1 & 1 & 2 & \dots & F_{p-2} & F_{p-1} & nF_{p-1} + F_{p-2} & (nF_{p-1} + F_{p-2})\tilde{v}^{-1} F_{p-1} \\ 0 & 1 & 1 & 2 & 3 & \dots & F_{p-1} & F_p & nF_p + F_{p-1} & (nF_p + F_{p-1})\tilde{v}^{-1} F_p \end{array}$$

where the  $F_n$  are the Fibonacci numbers [Schr 90]. From this, we obtain the following quadratic equation for  $\tilde{v}$ :

$$\tilde{v} = \frac{nF_{p-1} + F_{p-2} + \tilde{v}F_{p-1}}{nF_p + F_{p-1} + \tilde{v}F_p} \quad (8)$$

which has the solution

$$\tilde{v} = \frac{n}{2} \left( \sqrt{1 + 4 \frac{nF_{p-1} + F_{p-2}}{n^2 F_p}} - 1 \right) \quad (9)$$

For the special case  $n = 2$ , one obtains

$$\tilde{v} = \sqrt{\frac{F_p + 2F_{p-1} + F_{p-2}}{F_p}} - 1 \quad (10)$$

Applying the recursions  $F_p + F_{p-1} = F_{p+1}$ ,  $F_{p-1} + F_{p-2} = F_p$ , and  $F_p + F_{p+1} = F_{p+2}$ , the final result is

$$\tilde{v} = \sqrt{\frac{F_{p+2}}{F_p}} - 1 \quad (11)$$

For  $P = 3$ , for example, equation 11 yields  $\tilde{v} = \sqrt{\frac{5}{2}} - 1$ , which indeed has a continued fraction expansion of period length 3, the period terminating in a 2:  $\sqrt{\frac{5}{2}} - 1 = [\overline{1, 1, 2}]$ .

Asymptotically, for  $P \rightarrow \infty$  and any fixed  $n$ , our near noble numbers will approach the golden mean  $\gamma = (\sqrt{5} - 1) \approx 0.61803$ . For example, for  $n = 2$

and  $P = 10$ ,  $\tilde{v} \approx 0.61808$ . According to equation 10 or 11, successive values of  $\tilde{v}$  for  $P = 1, 2, 3, \dots$  constitute, in fact, an approach to the golden mean  $\gamma$  through (quadratic) irrational numbers.

A possible sequence for *cubic* irrational numbers is

$$x_n = \left( \frac{F_n}{F_{n+k}} \right)^{1/k} \quad (12)$$

with  $k = 3$ , and  $k > 3$  for quartic and higher-degree irrational numbers.

# References

Single-author publications are identified by the first letters of the author's name followed by the year of publication. Multiple-author works are identified by the first letter of each author's name. Identical author codes are listed in the order of appearance in the text and distinguished by lowercase letters following the year.

- [AAMA 82] W. Alvarez, F. Asaro, H. V. Michel, and L. W. Alvarez: Iridium anomaly approximately synchronous with terminal eocene extinctions. *Science* **216**, 886–888.
- [Agu 76] M. Agu: A nonstationary time-series having  $1/f$ -type power spectrum. *J. Phys. Soc. Japan* **40**, 1510–1511.
- [AH 48] R. A. Alpher and R. Herman: Evolution of the universe. *Nature* **162**, 774–775.
- [AL 85] P. Alstrøm and M. T. Levinsen: Fractal structure of the complete devil's staircase in dissipative systems described by a driven damped-pendulum equation with a distorted potential. *Phys. Rev. B* **32**, 1503–1511.
- [Alv 87] L. W. Alvarez: *Adventures of a Physicist* (Basic Books, New York).
- [And 58] P. W. Anderson: Absence of diffusion in certain random lattices. *Phys. Rev.* **109**, 1492–1505.
- [Arn 89] V. I. Arnold: *Mathematical Methods of Classical Mechanics* (Springer, Berlin).
- [AS 81] J. E. Avron and B. Simon: Almost periodic Hill's equation and the rings of Saturn. *Phys. Rev. Lett.* **46**, 1166–1168.
- [ASS 86] G. Albinet, G. Searby, and D. Stauffer: Fire propagation in a 2-D random medium. *J. Physique* (Paris) **47**, 1–7.
- [ASSW 66] B. S. Atal, M. R. Schroeder, G. M. Sessler, and J. E. West: Evaluation of acoustic properties of enclosures by means of digital computers. *J. Acoust. Soc. Am.* **40**, 428–433.
- [AZLPAGNCFFMS-SBCGHHKSW 89] M. E. Ander, M. A. Zumberge, T. Lautzenhiser, R. L. Parker, C. L. V. Aiken, M. R. Gorman, M. M. Nieto, A. P. R. Cooper, J. F. Ferguson, E. Fisher, G. A. McMechan, G. Sasagawa, J. M. Stevenson, G. Backus, A. D. Chave, J. Greer, P. Hammer, B. L. Hansen, J. A. Hildebrand, J. R. Kelty, C. Sidles, and J. Wirtz: Test of Newton's inverse-square law in the Greenland ice cap. *Phys. Rev. Lett.* **62**, 985–988.

- [Bar 1509] A. Barclay: *The Ship of Fools*. (Translation from the original Alsatian German of *Das Narrenschiff*, 1494, by Sebastian Brant; an exposition of abuses within the church and precursor of the Protestant Reformation.)
- [Bar 88] M. Barnsley: *Fractals Everywhere* (Academic Press, San Diego).
- [Bas 90] T. A. Bass: *The Newtonian Casino* (Longman, New York).
- [BB 79] J. von Boehm and P. Bak: Devil's stairs and the commensurate-incommensurate transition in CeSb. *Phys. Rev. Lett.* **42**, 122–125.
- [BB 82] P. Bak and R. Bruinsma: One-dimensional Ising model and the complete devil's staircase. *Phys. Rev. Lett.* **49**, 249–251.
- [BB 83] R. Bruinsma and P. Bak: Self-similarity and fractal dimension of the devil's staircase in the one-dimensional Ising model. *Phys. Rev.* **B27**, 5824–5825.
- [BB 87] J. M. Borwein and P. B. Borwein: *Pi and the AGM—A Study in Analytic Number Theory and Computational Complexity* (Wiley, New York).
- [BBB 89] J. M. Borwein, P. B. Borwein, and D. H. Bailey: Ramanujan, modular equations, and approximations to pi, or how to compute one billion digits of pi. *Am. Math. Monthly* **96**, 201–219.
- [BBFT 89] P. G. Bizetti, A. M. Bizetti-Sona, T. Fazzini, and N. Taccetti: Search for a composition-dependent fifth force. *Phys. Rev. Lett.* **62**, 2901–2904.
- [BBJ 84] T. Bohr, P. Bak, and M. H. Jensen: Transition to chaos by interaction of resonances in dissipative systems. II. Josephson junctions, charge-density, and standard maps. *Phys. Rev. A* **30**, 1970–1981.
- [BCG 82] E. R. Berlekamp, J. H. Conway, and R. K. Guy: *Winning Ways for Your Mathematical Plays*, vol. 2 (Academic Press, New York), chapter 25.
- [Ber 62] L. L. Beranek: *Music, Acoustics and Architecture* (Wiley, New York).
- [Ber 79] M. V. Berry: Difractals. *J. Phys. A* **12**, 781–797.
- [Bil 83] P. Billingsley: The singular function of bold play. *Am. Sci.* **71**, 392–397.
- [BPS 87] J. Bahcall, T. Piran, and S. Weinberg (eds.): *Dark Matter in the Universe* (World Scientific, Singapore).
- [BS 84] H. D. Bale and P. W. Smith: Small-angle x-ray scattering investigation of submicroscopic porosity with fractal properties. *Phys. Rev. Lett.* **53**, 596–599.
- [BTW 87] P. Bak, C. Tang, and K. Wiesenfeld: Self-organized criticality: An explanation of 1/f noise. *Phys. Rev. Lett.* **59**, 381–384.
- [BTW 88] P. Bak, C. Tang, and K. Wiesenfeld: Self-organized criticality. *Phys. Rev. A* **38**, 364–374.
- [Bur 87] R. W. Burchfield (ed.): *Oxford English Dictionary* (Oxford University Press, Oxford).

- [BW 90] K. L. Babcock and R. M. Westervelt: Avalanche and self-organization in cellular magnetic-domain patterns. *Phys. Rev. Lett.* **64**, 2168–2171.
- [Cam 86] X. Campi: Multifragmentation: Nuclei break up like percolation. *J. Phys. A* **19**, L917–921. See also *Nuclear Phys.* **A459**, 692.
- [Car 85] J. L. Cardy: Conformal invariance and the Yang-Lee edge singularity in two dimensions. *Phys. Rev. Lett.* **54**, 1354–1356.
- [CE 80] P. C. Collet and J.-P. Eckmann: *Iterated Maps of the Interval as Dynamical Systems* (Birkhäuser Boston, Cambridge, Mass.).
- [CJ 87] D. R. Chiavalo and J. Jalife: Nonlinear dynamics of cardiac excitation and impulse propagation. *Nature* **330**, 749–752.
- [CJ most 85] P. Cvitanović, M. H. Jensen, L. P. Kadanoff, and I. Procaccia: Renormalization, unstable manifolds, and the fractal structure of mode locking. *Phys. Rev. Lett.* **55**, 343–346.
- [CLK 88] H. Chen, D. X. Li, and K. H. Kuo: New type of two-dimensional quasicrystal with twelvefold rotational symmetry. *Phys. Rev. Lett.* **60**, 1645–1648.
- [CM 90] R. G. Corzine and J. A. Mosko: *Four-Arm Spiral Antennas* (Artech House, Norwood, Mass.).
- [CMP 87] D. D. Coon, S. N. Maa, and A. G. U. Perera: Farey fraction frequency modulation in the neuron-like output of silicon *p-i-n* diodes at 4.2 K. *Phys. Rev. Lett.* **58**, 1139–1142.
- [COM 66] J. H. Comroe: The lung. *Scientific American* **214**, 56–68 (February 1966).
- [Cri 81] F. Crick: *Life Itself* (Simon & Schuster, New York).
- [CS 88] D. S. Clark and O. Shisha: Invulnerable queens on an infinite chessboard. *3rd Int. Conf. Combinatorial Math.*, Annals of the New York Academy of Sciences.
- [D'An 90] P. D'Antonio: A new 1- or 2-dimensional fractal sound diffusor. *J. Acoust. Soc. Am., Suppl. 1*, **87**, S10.
- [DDI 83] B. Derrida, L. De Seze, and C. Itzykson: Fractal structure of zeroes in hierarchical models. *J. Statist. Phys.* **33**, 559–569.
- [deB 81] N. G. de Bruijn: Sequences of zeros and ones generated by special production rules. *Kon. Ned. Akad. Wetensch. Proc. Ser. A* **84** (*Indagationes* M. Gardner: The fantastic combinations of John Conway's new solitaire of Penrose's nonperiodic tilings of the plane. *Kon. Ned. Akad. Wetensch.* **84**, 39–66.
- [deW 51] H. J. de Wijs: Statistics of ore distribution. *Geologie en Mijnbouw* (Amsterdam) **13**, 365–375. See also **15**, 12–24 (1953).
- [DGJPS 85] A. W. M. Dress, M. Gerhardt, N. I. Jaeger, P. J. Plath, and H. Schuster: Some proposals concerning the mathematical modelling of oscillating heterogeneous catalytic reactions on metal surfaces. In L. Rensing and N. I. Jaeger (eds.): *Temporal Order* (Springer, Berlin), pp. 67–74.

- [DGP 78] B. Derrida, A. Gervois, and Y. Pomeau: Iteration of endomorphisms on the real axis and representation of numbers. *Ann. Inst. Henri Poincaré XXIX*, 305–356.
- [DH 82] A. Douady and J. H. Hubbard: Iterations des polynomes quadratique complexes. *Compt. Rend. Acad. Sci. Paris* **294**, 123–126.
- [DH 85] A. Douady and J. H. Hubbard: On the dynamics of polynomial-like mappings. *Ann. Sci. École Normale Sup. 4e Série*, **18**, 287–343.
- [Dia 77] P. Diaconis: The distribution of leading digit and uniform distributions mod 1. *Ann. Prob.* **5**, 72–81.
- [DK 85] M. Duneau and A. Katz: Quasiperiodic patterns. *Phys. Rev. Lett.* **54**, 2688–2691.
- [DK 88] C. Davies and D. Knuth: Number representations and dragon curves. *J. Recreational Math.* **3**, 66–81 and 133–149.
- [DMP 82] F. M. Dekking, M. Mendès France, and A. van der Poorten: Folds! *Math. Intelligencer* **4**, 130–138, 173–181, and 190–195.
- [Dou 86] A. Doudy: Julia sets and the Mandelbrot set. In H.-O. Peitgen and P. H. Richter: *The Beauty of Fractals* (Springer, Berlin). pp. 161–173.
- [Du 84] B.-S. Du: A chaotic function whose nonwandering set is the Cantor ternary set. *Proc. Math. Soc. Am.* **92**, 277–278.
- [EG 88] R. B. Eggleton and R. K. Guy: Catalan strikes again! *Mathematics Magazine* **61**, 211–219.
- [Ein 05] A. Einstein: Über die von der molekularkinetischen Theorie der Wärme geforderte Bewegung von in ruhenden Flüssigkeiten suspendierten Teilchen. *Annalen der Physik* **17**, 549–560.
- [Els 85] V. Elsner: Indexing problems in quasi-crystal diffraction. *Phys. Rev. B* **32**, 4892–4898.
- [Erd 54] A. Erdélyi: *Tables of Integral Transforms* (McGraw-Hill, New York).
- [Esc 71] M. C. Escher: *The World of M. C. Escher* (H. N. Abrams, New York).
- [EU 86] R. Eykholt and D. K. Umberger: Characterization of fat fractals in nonlinear dynamical systems. *Phys. Rev. Lett.* **57**, 2333–2336.
- [Fal 87] K. J. Falconer: Digital sun dials, paradoxical sets, and Vitushkin's conjecture. *Math. Intelligencer* **9**, 24–27.
- [Far 82] J. D. Farmer: Dimension, fractal measure and chaotic dynamics. In H. Haken (ed.): *Evolution of Order and Chaos* (Springer, Berlin/New York).
- [Far 85] J. D. Farmer: Sensitive dependence on parameters in nonlinear dynamics. *Phys. Rev. Lett.* **55**, 351–354.
- [Fed 88] J. Feder: *Fractals* (Plenum, New York).
- [Fei 79] M. J. Feigenbaum: The universal metric properties of nonlinear transformations. *J. Statis. Phys.* **21**, 669–706.

- [Fei 83] M. J. Feigenbaum: Universal behavior in nonlinear systems. *Physica* **7D**, 16–39.
- [Fel 68] W. Feller: *An Introduction to Probability Theory and Its Applications* (Wiley, New York).
- [FHG 85] A. P. Fein, M. S. Heutmaker, and J. P. Gollub: Physical scaling at the transition from quasiperiodicity to chaos in a hydrodynamic system. *Phys. Scr.* **T9** 79–84.
- [Fib 1202] Leonardo Fibonacci: *Liber Abaci* (Pisa).
- [Fis 90] D. E. Fisher: *Fire and Ice: The Greenhouse Effect, Ozone Depletion, and Nuclear Winter* (Harper & Row, New York).
- [FL 84] F. Family and D. P. Landau (eds.): *Kinetics of Aggregation and Gelation* (North Holland, Amsterdam).
- [Fri 1240] Friedrich II.: *De Arte Venandi cum Avibus*. (The Latin original of *On the Art of Hunting with Birds*, with the emperor's own drawings, was stolen during the siege of Parma in 1248 and subsequently lost. A copy made by his son Manfred was republished by Schneider, Leipzig, 1789.)
- [Gar 70] M. Gardner: The fantastic combinations of John Conway's new solitaire game of life. *Scientific American* **223**, 120–123 (Mathematical Games, April 1970).
- [Gar 77] M. Gardner: Extraordinary nonperiodic tiling that enriches the theory of tiles. *Scientific American* **236**, 110–121 (Mathematical Games, January 1977).
- [Gar 78] M. Gardner: White and brown music, fractal curves and one-over-f noise. *Scientific American* **238**, 16–32 (Mathematical Games, April 1978).
- [Gar 83] M. Gardner: *Wheels, Life and Other Mathematical Amusements* (W. H. Freeman, New York).
- [Gar 89] M. Gardner: *Penrose Tiles to Trapdoor Ciphers* (W. H. Freeman, New York).
- [Gil 58] E. N. Gilbert: Gray codes and paths on the n-cube. *Bell Syst. Tech. J.* **37**, 815–826.
- [Gil 84] W. J. Gilbert: A cube-filling Hilbert curve. *Math. Intelligencer* **6**, 78.
- [Gle 87] J. Gleick: *Chaos: Making a New Science* (Viking, New York).
- [GLL 78] R. L. Graham, S. Lin, and C.-S. Lin: Spectra of numbers. *Mathematics Magazine* **51**, 174–176.
- [GP 83] P. Grassberger and I. Procaccia: Characterization of strange attractors. *Phys. Rev. Lett.* **50**, 346–349.
- [Gra 81] P. Grassberger: On the Hausdorff dimension of fractal attractors. *J. Statist. Phys.* **26**, 173–179.

- [Gra 83] P. Grassberger: Generalized dimensions of strange attractors. *Phys. Lett.* **97A**, 227–230.
- [Gra 85] P. Grassberger: On the spreading of two-dimensional percolation. *J. Phys.* **A18**, L215–219.
- [Gri 89] G. Grimmett: *Percolation* (Springer, New York).
- [Gro 82] S. Grossmann: Diversity and universality. Spectral structure of discrete time evolution. In H. Haken (ed.): *Evolution of Order and Chaos* (Springer, Berlin).
- [GS 87] B. Grünbaum and G. C. Shephard: *Tilings and Patterns* (W. H. Freeman, New York).
- [GT 77] S. Grossmann and S. Thomae: Invariant distributions and stationary correlations of one-dimensional discrete processes. *Zeitschrift für Naturforschung* **32a**, 1353–1363.
- [GW 87] E. G. Gwinn and R. M. Westervelt: Scaling structure of attractors at the transition from quasiperiodicity to chaos in electronic transport in *Ge. Phys. Rev. Lett.* **59**, 157–160.
- [GZR 87] T. Geisel, A. Zacherl, and G. Radons: Generic 1/f noise in chaotic Hamiltonian systems. *Phys. Rev. Lett.* **59**, 2503–2506.
- [Hak 78] H. Haken: *Synergetics* (Springer, Berlin/New York).
- [Hal 28] J. B. S. Haldane: *On Being the Right Size* (Oxford University Press, London).
- [Hal 74] P. R. Halmos: *Naive Set Theory* (Springer, New York).
- [Har 77] S. Harris: *What's So Funny about Science* (Kaufmann, Los Altos, Calif.).
- [Haw 88] S. Hawking: *A Brief History of Time* (Bantam, New York).
- [HBM 39] F. V. Hunt, L. L. Beranek, and D. Y. Maa: *Analysis of sound decay in rectangular rooms*. *J. Acoust. Soc. Am.* **11**, 80–94.
- [HBS 65] H. E. Hurst, R. P. Black, and Y. M. Simaika: *Long Term Storage: An Experimental Study* (Constable, London).
- [Hen 76] M. Hénon: A two-dimensional map with a strange attractor. *Commun. Math. Phys.* **50**, 69–77.
- [Hen 88] M. Hénon: Chaotic scattering modelled by an inclined billiard. *Physica* **D23**, 132–156.
- [HJF 87] E. Hinrichsen, J. Feder, and T. Jøssang: DLA growth from a line. Report Series, Cooperative Phenomena Project, Department of Physics, University of Oslo **87-11**, 1–21.
- [HJKPS 86] T. C. Halsey, M. H. Jensen, L. P. Kadanoff, I. Procaccia, and B. I. Shraiman: Fractal measures and their singularities: The characterization of strange sets. *Phys. Rev. A33*, 1141–1151.

- [HLSTLW 86] G. Hasinger, A. Langmeier, M. Sztajno, J. Trümper, W. H. G. Lewien, and N. E. White: Quasi-periodic oscillations in the X-ray flux of Cyg X-2. *Nature* **319**, 469–471.
- [Hof 80] D. R. Hofstadter: *Gödel, Escher, Bach: An Eternal Golden Braid* (Vintage, 1980).
- [HP 83a] H. G. E. Hentschel and I. Procaccia: The infinite number of generalized dimensions of fractals and strange attractors. *Physica* **8D**, 435–444.
- [HP 83b] H. G. E. Hentschel and I. Procaccia: Fractal nature of turbulence as manifested in turbulent diffusion. *Phys. Rev. A* **27**, 1266–1269.
- [HP 84] H. G. E. Hentschel and I. Procaccia: Relative diffusion in turbulent media: The fractal dimension of clouds. *Phys. Rev. A* **29**, 1461–1470.
- [HS 79] M. Harwit and N. J. A. Sloane: *Hadamard Transform Optics* (Academic Press, New York).
- [Hu 85] B. Hu: Problem of universality in phase transitions on hierarchical lattices. *Phys. Rev. Lett.* **55**, 2316–2319.
- [Huy 1673] C. Huygens: *Horologium Oscillatorium* (Muguet, Paris).
- [HW 84] G. H. Hardy and E. M. Wright: *An Introduction to the Theory of Numbers* (Clarendon, Oxford).
- [INF 85] T. Ichimasa, H.-U. Nissen, and Y. Fukano: New ordered state between crystalline and amorphous in Ni-Cr particles. *Phys. Rev. Lett.* **55**, 511–513.
- [INF 88] T. Ichimasa, H.-U. Nissen, and Y. Fukano: Electron microscopy of crystallloid structure in Ni-Cr small particles. *Phil. Mag. A* **58**, 835–863.
- [Jak 81] M. V. Jakobson: Absolutely continuous invariant measures for one-parameter families of one-dimensional maps. *Commun. Math. Phys.* **81**, 39–88.
- [Jan 89] A. Janner: Symmetries in higher-dimensional crystallography. *Phase Transitions* **16/17**, 87–101.
- [JBB 83] M. H. Jensen, P. Bak, and T. Bohr: Complete devil's staircase, fractal dimension, and universality of mode-locking structure in the circle map. *Phys. Rev. Lett.* **50**, 1637–1641.
- [JBB 84] M. H. Jensen, P. Bak, and T. Bohr: Transition to chaos by interaction of resonances in dissipative systems. *Phys. Rev. A* **30**, 1960–1969.
- [JE 51] E. Jahnke and F. Emde: *Tables of Higher Functions* (Teubner, Leipzig; also published by Dover, New York).
- [JER 90] C. Jekeli, D. H. Eckhardt, and A. J. Romaides: Tower gravity experiment: No evidence for non-Newtonian gravity. *Phys. Rev. Lett.* **64**, 1204–1206.

- [JKLPS 85] M. H. Jensen, L. P. Kadanoff, A. Libchaber, I. Procaccia, and J. Stavans: Global universality at the onset of chaos. *Phys. Rev. Lett.* **55**, 2798–2801.
- [JM 85] R. V. Jensen and C. R. Myer: Images of the critical points of nonlinear maps. *Phys. Rev. A* **32**, 1222–1224.
- [Jon 88] D. Jones: Abstract concrete. *Nature* **332**, 310.
- [Kac 85] M. Kac: *Enigmas of Chance* (Harper & Row, New York).
- [KB 88] B. Klein and I. Bivens: Proof without words. *Mathematics Magazine* **61**, 219.
- [KBJ 83] M. Kolb, R. Botet, and R. Jullien: Scaling of kinetically growing clusters. *Phys. Rev. Lett.* **51**, 1123–1126.
- [KD 86] A. Katz and M. Duneau: Quasiperiodic patterns and icosahedral symmetry. *J. Phys.* **47**, 181–196.
- [Kel 56] J. L. Kelly: A new interpretation of information rate. *Bell Syst. Tech. J.* **35**, 917–926.
- [Kes 87] H. Kesten: *Percolation Theory and Ergodic Theory of Infinite Particle Systems* (Springer, New York).
- [Kim 81] S. Kim: *Inversions* (Byte Books, McGraw-Hill, Peterborough, N. H.).
- [Koh 1847] R. Kohlrausch: Über das Dellman'sche Elektrometer. *Annalen der Physik und Chemie* (Poggendorf) **III-12**, 353–405.
- [Koh 1854] R. Kohlrausch: Theorie des elektrischen Rückstandes in der Leidener Flasche. *Annalen der Physik und Chemie* (Poggendorf) **IV-91**, 56–82 and 179–214.
- [KS 87] J. Koplowitz and A. P. Sundar Raj: A robust filtering algorithm for subpixel reconstruction of chain coded line drawings. *IEEE Trans. Pattern Analysis and Machine Analysis* **9**, 451–457.
- [KW 89] V. Klee and S. Wagon: *New and Old Unsolved Problems in Plane Geometry and Number Theory* (Mathematical Association of America, Washington, D. C.).
- [Las 89] J. Laskar: A numerical experiment on the chaotic behavior of the solar system. *Nature* **338**, 237–238.
- [Law 88] J. H. Lawton: More time means more variation. *Nature* **334**, 563.
- [LC 81] W. Lauterborn and E. Cramer: Subharmonic route to chaos observed in acoustics. *Phys. Rev. Lett.* **47**, 1445–1448.
- [Lei 1714] G. W. Leibniz: *Principia Philosophiae, More Geometrico Demonstrata*. Written in 1714 and generally known as *Monadologia* (*Monadology*), this great opus of Leibniz was first printed in 1720–1721. Several learned academies are still working on a complete edition of his works.
- [Leo 62] L. B. Leopold: Rivers. *Am. Scientist* **50**, 511–537.

- [LF 88] M. S. Lapidus and J. Fleckinger-Pellé: Tambour fractal: vers une résolution de la conjecture de Weyl-Berry pour less valeurs propres du laplacien. *Compt. Rend. Acad. Sci. Paris Math.* **306**, Sér. I, 171–175.
- [LH 86] W. Lauterborn and J. Holzfuss: Evidence for a low-dimensional strange attractor in acoustic turbulence. *Phys. Lett.* **A115**, 369–372.
- [Lin 68] A. Lindemeyer: Mathematical models of cellular interactions in development. *J. Theor. Biol.* **18**, 280–315.
- [Liu 85] S. H. Liu: Fractal model for the ac-response of a rough interface. *Phys. Rev. Lett.* **55**, 529–532.
- [LL 76] L. D. Landau and E. M. Lifschitz: *Mechanics* (Pergamon Press, Oxford), sec. 10.
- [LM 80] A. Libchaber and J. Maurer: Une expérience de Rayleigh-Bénard de géométrie réduite; Multiplication, Accrochage et démultiplication de fréquences. *J. Phys. (Paris) Coll.* **41**, C3–51.
- [LM 85] S. Lovejoy and B. B. Mandelbrot: Fractal properties of rain, and a fractal model. *Tellus* **37A**, 209–232.
- [Lor 80] E. N. Lorenz: Noisy periodicity and reverse bifurcation. In R. H. G. Helleman: *Nonlinear Dynamics (Annals of the New York Academy of Sciences)* **357**, 282–291).
- [Lov 82] S. Lovejoy: Area-perimeter relation for rain and cloud areas. *Science* **216**, 185–187.
- [LP 88] W. Lauterborn and U. Parlitz: Methods of chaos physics and their application to acoustics. *J. Acoust. Soc. Am.* **84**, 1975–1993.
- [LS 84] L. Levin and P. J. Steinhardt: Quasicrystals: A new class of ordered structures. *Phys. Rev. Lett.* **53**, 2477–2480.
- [LY 75] T.-Y. Li and J. A. Yorke: Period three implies chaos. *Am. Math. Monthly* **82**, 985–992.
- [Mac 82] A. Mackey: Crystallography and the Penrose pattern. *Physica* **114A**, 609–613.
- [Man 61] B. B. Mandelbrot: On the theory of word frequencies and on related Markovian models of discourse. In R. Jacobson (ed.): *Structures of Language and Its Mathematical Aspects* (American Mathematical Society, New York).
- [Man 63a] B. B. Mandelbrot: The stable Paretian income distribution when the apparent exponent is near zero. *Int. Econ. Rev.* **4**, 111–115.
- [Man 63b] B. B. Mandelbrot: The variation of certain speculative stock prices. *J. Bus. (Chicago)* **36**, 394–419.
- [Man 63c] B. B. Mandelbrot: New methods in statistical economics. *J. Polit. Econ.* **71**, 421–440.

- [Man 74] B. B. Mandelbrot: Intermittent turbulence in self-similar cascades: Divergence of high moments and dimension of the carrier. *J. Fluid Mech.* **62**, 331–358.
- [Man 80] B. B. Mandelbrot: Fractal aspects of the interation  $z \rightarrow \lambda z(1 - z)$  for complex  $\lambda$  and  $z$ . In R. H. G. Helleman (ed.): *Nonlinear Dynamics (Annals of the New York Academy of Sciences)* **357**, 249–259.
- [Man 83] B. B. Mandelbrot: *The Fractal Geometry of Nature*, updated and augmented (W. H. Freeman, New York).
- [Man 91] B. B. Mandelbrot: *Fractals and Multifractals*, Selecta Vol. 1 (Springer, New York).
- [May 88] R. M. May: How many species are there on earth? *Science* **214**, 1441–1449.
- [MBVB 89] P. Manneville, N. Boccara, G. Y. Vichniac, and R. Bidaux (eds.): *Cellular Automata and Modeling of Complex Physical Systems* (Springer, Berlin).
- [McG 71] *McGraw-Hill Encyclopedia of Science and Technology* (New York).
- [MCSW 86] P. Meakin, A. Coniglio, H. E. Stanley, and T. A. Witten: Scaling properties for the surfaces of fractal and nonfractal objects: An infinite hierarchy of critical exponents. *Phys. Rev. A* **34**, 3325–3340.
- [Mea 83] P. Meakin: Formation of fractal clusters and networks by irreversible diffusion-limited aggregation. *Phys. Rev. Lett.* **51**, 1119–1122.
- [Mea 87] P. Meakin: Scaling properties for the growth probability measure and harmonic measure of fractals. *Phys. Rev. A* **35**, 2234–2245.
- [Mei 82] H. Meinhardt: *Models of Biological Pattern Formation* (Academic Press, London).
- [Mek 90] A. Z. Mekjian: Model of a fragmentation process and its power-law behavior. *Phys. Rev. Lett.* **64**, 2125–2128.
- [Men 79] K. Menger: *Selected Papers in Logic and Foundations, Didactics and Economics* (Reidel, Boston).
- [MH 87] J. E. Martin and A. J. Hurd: Scattering from fractals. *J. Appl. Crystallog.* **20**, 61–78.
- [MK 87] H. Meinhardt and M. Klinger: A model for pattern formation on the shells of molluscs. *J. Theor. Biol.* **126**, 63–89.
- [MM 86] S. Martin and W. Martienssen: Circle maps and mode locking in the driven electrical conductivity of barium sodium niobate crystals. *Phys. Rev. Lett.* **56**, 1522–1525.
- [Moo 84] F. C. Moon: Fractal boundary for chaos in a two-state mechanical oscillator. *Phys. Rev. Lett.* **53**, 962–964.
- [Mor 21] M. Morse: Recurrent geodesics on a surface of negative curvature. *Trans. Am. Math. Soc.* **22**, 84–100.

- [MPP 84] B. B. Mandelbrot, D. Passoja, and A. Paullay: Fractal character of fracture surfaces of metal. *Nature* **308**, 721–722.
- [MPRR 88] M. V. Mathews, J. R. Pierce, A. Reeves, and L. Roberts: Theoretical and experimental explorations of the Bohlen-Pierce scale. *J. Acoust. Soc. Am.* **84**, 1214–1222.
- [MS 87] C. Meneveau and K. R. Sreenivasan: Simple multifractal cascade model for fully developed turbulence. *Phys. Rev. Lett.* **59**, 1424–1427.
- [MSCW 85] P. Meakin, H. E. Stanley, A. Coniglio, and T. A. Witten: Surfaces, interfaces and screening of fractal structures. *Phys. Rev. A* **32**, 2364–2369.
- [MSS 73] N. Metropolis, M. L. Stein, and P. R. Stein: On finite limit sets for transformations of the unit interval. *J. Combinatorial Theory (A)* **15**, 25–44.
- [MW 69] B. B. Mandelbrot and J. R. Wallis: Some long-run properties of geo-physical records. *Water Resources Research* **5**, 321–340.
- [NPW 84] L. Niemeyer, L. Pietronero, and H. J. Wiesmann: Fractal dimension of dielectric breakdown. *Phys. Rev. Lett.* **52**, 1033–1040.
- [NPW 86] L. Niemeyer, L. Pietronero, and H. J. Wiesmann: Response to comments on paper on dielectric breakdown [NPW 84]. *Phys. Rev. Lett.* **57**, 649–650.
- [NS 89] M. Nauenberg and H. J. Schellnhuber: Analytic evaluation of the multifractal properties of a Newtonian Julia set. *Phys. Rev. Lett.* **62**, 1807–1810.
- [OT 86] G. Y. Onoda and J. Toner: Fractal dimensions of model particle packings having multiple generations of agglomerations. *Comm. Am. Ceramic Soc.* **69**, C-278 to C-279.
- [Ott 89] J. M. Ottino: The mixing of fluids. *Scientific American* **260**, 40–49. (January 1989).
- [PA 83] P. Pfeifer and D. Avnir: Chemistry in noninteger dimensions between two and three. *J. Chem. Phys.* **79**, 3558–3565. Erratum: **80**, 4573 (1984).
- [Pag 81] W. Page: Proof without words: Geometric sums. *Mathematics Magazine* **54**, 201.
- [Pai 82] A. Pais: *Subtle Is the Lord . . .* (Clarendon Press, Oxford).
- [Par 1896] V. Pareto: *Oeuvres Complètes* (Droz, Geneva).
- [Pau 85] L. Pauling: Apparent icosahedral symmetry is due to directed multiple twinning of cubic crystals. *Nature* **317**, 512–514.
- [Pen 74] R. Penrose: The role of aesthetics in pure and applied mathematical research. *Bull. Inst. Math. & Its Appl.* **10**, 266–271. See also R. Penrose: Pentaplexity: A class of non-periodic tilings of the plane. *Math. Intelligencer* **2**, 32–37 (1979).

- [PI 87] W. Purkert and H. J. Ilgauds: *Georg Cantor* (Birkhäuser, Basel/Boston).
- [Pie 83] J. R. Pierce: *The Science of Musical Sound* (Scientific American Books, W. H. Freeman, New York).
- [Pin 62] R. S. Pinkham: On the distribution of first significant digits. *Ann. Math. Stat.* **32**, 1223–1230.
- [PPR 85] H. -O. Peitgen, M. Prüfer, and P. H. Richter: Phase transitions and Julia sets. In W. Ebeling and M. Peschel (eds.): *Lotka-Volterra Approach to Cooperation and Competition in Dynamical Systems* (Akademie-Verlag, Berlin).
- [PR 84] H. -O. Peitgen and P. Richter: *Harmonie in Chaos und Kosmos: Bilder aus der Theorie der dynamischen Systeme* (Die Sparkasse in Bremen, Bremen).
- [PR 86a] H. -O. Peitgen and P. H. Richter: *The Beauty of Fractals* (Springer, Berlin).
- [PR 86b] H. -O. Peitgen and P. H. Richter: *Fraktale und die Theorie der Phasenübergänge*. *Phys. Blätter* **42**, 9–22.
- [Pru 87] P. Prusinkiewicz: Applications of L-systems to computer imagery. In H. Ehrig, M. Nagl, A. Rosenfeld, and G. Rozenberg (eds.): *Graph Grammars and Their Application to Computer Science, 3rd Int. Workshop* (Springer, Berlin) pp. 534–548 (*Lecture Notes in Computer Science* **291**).
- [PS 86] L. Pietronero and A. P. Siebesma: Self-similarity of fluctuations in random multiplicative processes. *Phys. Rev. Lett.* **57**, 1098–1101.
- [PS 88] H. -O. Peitgen and D. Saupe: *The Science of Fractal Images* (Springer, New York).
- [PTT 87] I. Procaccia, S. Thomae, and C. Tresser: First return maps as a unified renormalization scheme for dynamical systems. *Phys. Rev. A* **35**, 1884–1900.
- [Pur 77] E. M. Purcell: Life at low Reynolds number. *Am. J. Phys.* **45**, 3–11.
- [Pye 85] L. Pyenson: *The Young Einstein* (Hilger, Bristol/Boston).
- [Rai 76] R. A. Raimi: The first digit problem. *Am. Math. Monthly* **83**, 521–538.
- [Ram 14] S. Ramanujan: Modular equations and approximations to  $\pi$ . *Quar. J. Math.* **45**, 350–372.
- [Ren 55] A. Rényi: On a new axiomatic theory of probability. *Acta Mathematica Hungarica* **6**, 285–335.
- [RI 57] H. Rouse and S. Ince: *History of Hydraulics*. (Iowa Inst. of Hydraulics; republished in 1963 by Dover Publ., New York).
- [Ris 71] J. -C. Risset: Paradoxes de hauteur. *Proc. 7th Int. Cong. Acoustics*, Budapest, paper S10, p. 20.

- [Ris 75] J.-C. Risset: Jugement relatifs de hauteur. *Compt. Rend. Acad. Sci. Paris* **B281**, 289–292.
- [RK 82] A. Rosenfeld and C. E. Kim: How a digital computer can tell whether a line is straight. *Am. Math. Monthly* **89**, 230–235.
- [Rös 86] J. Röschke: Eine Analyse der nichtlinearen EEG-Dynamik. (Dissertation, Göttingen).
- [RP 88] A. Redfearn and S. L. Pimm: *Ecological Monogr.* **58**, 39–55.
- [RS 87] P. Richter and H.-J. Scholz: Der goldene Schnitt in der Natur. In B.-O. Küppers (ed.): *Ordnung aus dem Chaos* (Piper, München), pp. 175–214.
- [RTV 86] R. Rammal, G. Toulouse, and M. A. Virasoro: Ultrametricity for physicists. *Rev. Mod. Phys.* **58**, 765–788.
- [SA 85] M. R. Schroeder and B. S. Atal: Stochastic coding of speech signals at very low bit rates: The importance of speech prediction. *Speech Comm.* **4**, 155–162.
- [Sag 89] Y. Sagher: Counting the rationals. *Am. Math. Monthly* **96**, 823.
- [SASW 66] M. R. Schroeder, B. S. Atal, G. M. Sessler, and J. E. West: Acoustical measurements in Philharmonic Hall (New York). *J. Acoust. Soc. Am.* **40**, 434–440.
- [SBGC 84] D. Shechtman, I. Blech, D. Gratias, and J. W. Cahn: Metallic phase with long-range orientational order and no translational symmetry. *Phys. Rev. Lett.* **53**, 1951–1953.
- [Schr 54] M. Schröder: Die statistischen Parameter der Frequenzkurven von grossen Räumen. *Acustica (Beihef 2)* **4**, 594–600. For an English translation, see M. R. Schroeder: Statistical parameters of the frequency response curves of large rooms. *J. Audio Eng. Soc.* **35**, 299–306 (1987).
- [Schr 64] M. R. Schroeder: Improvement of acoustic feedback stability. *J. Acoust. Soc. Am.* **36**, 1718–1724.
- [Schr 67] M. R. Schroeder: Determination of the geometry of the human vocal tract by acoustic measurements. *J. Acoust. Soc. Am.* **41**, 1002–1010.
- [Schr 69] M. R. Schroeder: Images from computers and microfilm plotters. *Comm. Assoc. Comp.-Mach.* **12**, 95–101. See also M. R. Schroeder: Images from computers. *IEEE Spectrum* **6**, 66–78 (March 1969).
- [Schr 70] M. R. Schroeder: Digital simulation of sound transmission in reverberated spaces. *J. Acoust. Soc. Am.* **47**, 424–431.
- [Schr 73] M. R. Schroeder: An integrable model for the basilar membrane. *J. Acoust. Soc. Am.* **53**, 429–433.
- [Schr 86] M. R. Schroeder: Auditory paradox based on fractal waveform. *J. Acoust. Soc. Am.* **79**, 186–189.

- [Schr 87] M. R. Schroeder: Statistical parameters of the frequency response curves of large rooms. *J. Audio Eng. Soc.* **53**, 299–305.
- [Schr 90] M. R. Schroeder: *Number Theory in Science and Communication, with Applications in Cryptography, Physics, Digital Information, Computing, and Self-Similarity*, 2nd enlarged ed. (Springer, Berlin/New York).
- [Schu 84] H. G. Schuster: *Deterministic Chaos* (Physik-Verlag, Weinheim).
- [Ses 80] G. M. Sessler: *Electrets* (Springer, Berlin).
- [SGS 74] M. R. Schroeder, D. Gottlob, and F. K. Siebrasse: Comparative study of European concert halls: Correlation of subjective preference with geometric and acoustic parameters. *J. Acoust. Soc. Am.* **56**, 1195–1201.
- [Sha 51] C. E. Shannon: Prediction and entropy of printed English. *Bell Syst. Tech. J.* **30**, 50–64.
- [Sha 53] C. E. Shannon: Computers and automata. *Proc. IRE* **41**, 1235–1241.
- [Sha 64] A. N. Sharkovski: Coexistence of cycles of a continuous map of a line into itself. *Ukrain. Math. Zeitschrift* **16**, 61–71.
- [She 62] R. N. Shepard: The analysis of proximities: Multidimensional scaling with unknown distance function. *Psychometrika* **27**, 125–140 and 219–246.
- [She 64] R. N. Shepard: Circularity in pitch judgment. *J. Acoust. Soc. Am.* **36**, 2346–2353.
- [She 82] S. J. Shenker: Scaling behavior in a map of a circle onto itself: Empirical results. *Physica* (Utrecht) **5D**, 405–411.
- [SHJ 88] J. L. C. Sanz, E. B. Hinkle, and A. K. Jain: *Radon and Projection Transform-Based Computer Vision* (Springer, Berlin/New York).
- [Sin 78] D. Singer: Stable orbits and bifurcations of maps of the interval *SIAM J. Appl. Math.* **35**, 260–267.
- [SK 87] W. von Saarloos and D. A. Kurtze: Location of zeros in the complex temperature plane: Absence of Lee-Young theorem. *J. Phys. A* **17**, 1301–1311.
- [Sla 60] P. Slater: The analysis of personal preferences. *Br. J. Stat. Psychol.* **8**, 119–135.
- [Slo 73] N. J. A. Sloane: *A Handbook of Integer Sequences* (Academic Press, New York).
- [SM 88] H. E. Stanley and P. Meakin: Multifractal phenomena in physics and chemistry. *Nature* **335**, 405–409.
- [Sma 67] S. Smale: Differentiable dynamical systems. *Bull. Am. Math. Soc.* **73**, 747–817.
- [SMWC 84] D. W. Schaefer, J. E. Martin, P. Wiltzius, and D. S. Cannell: Fractal geometry of colloidal aggregates. *Phys. Rev. Lett.* **52**, 2371–2374.

- [SO 85] H. E. Stanley and N. Ostrowsky (eds.): *On Growth and Form: Fractal and Non-Fractal Patterns in Physics* (NATO ASI, Martinus Nijhoff, Dordrecht).
- [ST 71] N. Suwa and T. Takahashi: *Morphological and morphometrical analysis of circulation in hypertension and ischemic kidney* (Urban & Schwarzenberg, Munich).
- [Sta 85] D. Stauffer: *Introduction to Percolation Theory* (Taylor & Francis, London).
- [Ste 69] S. S. Stevens: On predicting exponent for cross-modality matches. *Percep. Psychophys.* **6**, 251–256.
- [Sut 89] K. Sutner: Linear cellular automata and the Garden-of-Eden. *Math. Intelligencer* **11**, 49–53.
- [SW 86] J. Salem and S. Wolfram: Thermodynamics and hydrodynamics of cellular automata. In S. Wolfram (ed.): *Theory and Application of Cellular Automata* (World Scientific, Singapore/Teaneck, N.J.), pp. 362–366.
- [SWGDRCL 86] J. P. Stokes, D. A. Weitz, J. P. Gollub, A. Dougherty, M. O. Robbins, P. M. Chaikin, and H. M. Lindsay: Interfacial stability of immiscible displacement in a porous medium. *Phys. Rev. Lett.* **57**, 1718–1721.
- [TB 88] C. Tang and P. Bak: Critical exponents and scaling relations for self-organized critical phenomena. *Phys. Rev. Lett.* **60**, 2347–2350.
- [Tho 61] D'A. W. Thompson: *On Growth and Form* (Cambridge University Press, Cambridge).
- [Thu 06] A. Thue: Über die gegenseitige Lage gleicher Teile gewisser Zeichenreihen. *K. Nord. Vid. Skrifter I Math. Nat.* (Oslo) **7**, 1–22.
- [TKFFHKMM 89] J. Thomas, P. Kasameyer, O. Fackler, D. Felske, R. Harris, J. Kammeraad, M. Millett, and M. Mugge: Testing the inverse-square law of gravity on a 465-m tower. *Phys. Rev. Lett.* **63**, 1902–1905.
- [TM 87] T. Toffoli and N. Margolus: *Cellular Automata Machines* (MIT Press, Cambridge, Mass.).
- [Ula 74] S. Ulam: *Sets, Numbers, and Universes* (MIT Press, Cambridge, Mass.).
- [Ulr 72] S. Ulrich: *Schätze deutscher Kunst* (Bertelsmann, Munich).
- [VC 78] R. V. Voss and J. Clark: 1/f noise in music: Music from 1/f noise. *J. Acoust. Soc. Am.* **63**, 258–263.
- [Ver 1845] P.-F. Verhulst: Récherches mathématiques sur la loi d'accroissement de la population. *Nouv. Mém. de l'Acad. Roy. des Sciences et Belles-Lettres de Bruxelles* XVIII.8, 1–38.
- [Vic 84] G. Vichniac: Simulating physics with cellular automata. *Physica* **10D**, 96–115.
- [Vic 86] G. Vichniac: Cellular automata models of disorder and organization. In Bienenstock, F. Fogelman Soulié, and G. Weisbuch (eds.): *Disordered Systems and Biological Organisation* (Springer, Berlin), pp. 1–20.

- [Vil 87] A. Vilenkin: Cosmic strings. *Scientific American* **257**, 52–60 (December 1987).
- [Vos 85] R. F. Voss: Random fractal forgeries. In R. A. Earnshaw (ed.): *Fundamental Algorithms for Computer Graphics* (Springer, Berlin/New York).
- [Vos 88] R. F. Voss: Fractals in nature: From characterization to simulation. In H.-O. Peitgen and D. Saupe: *The Science of Fractal Images* (Springer, New York).
- [Wag 85] S. Wagon: Is  $\pi$  normal? *Math. Intelligencer* **7**, 65–67.
- [WCK 87] N. Wang, H. Chen, and K. H. Kuo: Two-dimensional quasicrystal with eightfold rotational symmetry. *Phys. Rev. Lett.* **59**, 1010–1013.
- [Wei 90] J. Weiner: *The Next One Hundred Years: Shaping the Fate of Our Living Earth* (Bantam, New York).
- [Wey 81] H. Weyl: *Symmetric* (Birkhäuser, Basel).
- [Wil 67] T. A. Wilson: Design of the bronchial tree. *Nature* **213**, 668–669.
- [Wis 87] J. Wisdom: Chaotic dynamics in the solar system. (Urey Prize Lecture). *Icarus* **72**, 241.
- [WO 84] D. A. Weitz and M. Oliveria: Fractal structures formed by kinetic aggregation of aqueous gold colloids. *Phys. Rev. Lett.* **52**, 1433–1436.
- [Wol 84] S. Wolfram: Cellular automata as models of complexity. *Nature* **341**, 419–424.
- [Wol 86] S. Wolfram (ed.): *Theory and Application of Cellular Automata* (World Scientific, Singapore/Teaneck, N.J.).
- [WPM 83] J. Wisdom, S. Peale, and F. Mignard: The chaotic rotation of Hyperion. *Icarus* **58**, 137–152.
- [WS 83] T. A. Witten and L. M. Sander: Diffusion-limited aggregation: A kinetic critical phenomenon. *Phys. Rev. Lett.* **47**, 1400–1403. See also *Phys. Rev. B* **27**, 5686–5697.
- [WWM 87] M. Werman, A. Wu, and R. A. Melter: Recognition and characterization of digitized curves. *Pattern Recognition Lett.* **5**, 207–213.
- [YL 52] C. N. Yang and T. D. Lee: Statistical theory of equations of state and phase transitions. *Phys. Rev.* **87**, 404–418.
- [ZD 85] R. K. P. Zia and W. J. Dallas: A simple derivation of quasi-crystalline spectra. *J. Phys. A: Math. Gen.* **18**, L341–L345.
- [Zim 78] M. H. Zimmerman: Hydraulic architecture of some diffuse-porous trees. *Can. J. Botany* **56**, 2286–2295.
- [Zip 49] G. K. Zipf: *Human Behavior and the Principle of Least Effort* (Addison-Wesley, Cambridge, Mass.).
- [ZLP 76] G. Zweig, R. Lipes, and J. R. Pierce: The cochlear compromise. *J. Acoust. Soc. Am.* **59**, 975–982.

# Author Index

The codes in brackets refer to the publications listed in the References.

|                 |  |                     |                                    |
|-----------------|--|---------------------|------------------------------------|
| Agu, M.         | [Agu 76]   | Barclay, A.         | [Bar 1509]                         |
| Aiken, C. L. V. | [AZL... 89]  | Barnsley, M.        | [Bar 88]                           |
| Albinet, G.     | [ASS 86]   | Bass, T. A.         | [Bas 90]                           |
| Alpher, R. A.   | [AH 48]  | Beranek, L. L.      | [HBM 39],<br>[Ber 62]              |
| Alstrom, P.     | [AL 85]  | Berlekamp, E. R.    | [BCG 82]                           |
| Alvarez, L. W.  | [AAMA 82],<br>[Alv 87]   | Berry, M. V.        | [Ber 79]                           |
| Alvarez, W.     | [AAMA 82]  | Billingsley, P.     | [Bil 83]                           |
| Ander, M. E.    | [AZL... 89]  | Bivens, I.          | [KB 88]                            |
| Anderson, P. W. | [And 58]   | Bizetti-Sona, A. M. | [BBFT 89]                          |
| Arnold, V. I.   | [Arn 89]   | Bizetti, P. G.      | [BBFT 89]                          |
| Asaro, F.       | [AAMA 82]  | Black, R. P.        | [HBS 65]                           |
| Atal, B. S.     | [ASSW 66],<br>[SASW 66],<br>[SA 85]  | Blech, I.           | [SBGC 84]                          |
| Avnir, D.       | [PA 83]  | Bohr, T.            | [JBB 83],<br>[BBJ 84],<br>[JBB 84] |
| Avron, J. E.    | [AS 81]  | Borwein, J. M.      | [BB 87],<br>[BBB 89]               |
| Babcock, K. L.  | [BW 90]  | Borwein, P. B.      | [BB 87],<br>[BBB 89]               |
| Backus, G.      | [AZL... 89]  | Botet, R.           | [KBJ 83]                           |
| Bahcall, J.     | [BPS 87]   | Bruinsma, R.        | [BB 82],<br>[BB 83]                |
| Bailey, D. H.   | [BBB 89]   | Burchfield, R. W.   | [Bur 87]                           |
| Bak, P.         | [BB 79],<br>[BB 82],<br>[BB 83],<br>[JBB 83],<br>[JBB 84],<br>[BBJ 84],<br>[BTW 87],<br>[BTW 88],<br>[TB 88] | Cahn, J. W.         | [SBGC 84]                          |
| Bale, H. D.     | [BS 84]  | Campi, X.           | [Cam 86]                           |
|                 |  | Cannell, D. S.      | [SMWC 84]                          |
|                 |  | Cardy, J. L.        | [Car 85]                           |
|                 |  | Chalkin, P. M.      | [SWGDRCL 86]                       |
|                 |  | Chen, H.            | [WCK 87],<br>[CLK 88]              |

- |                  |                  |                      |               |
|------------------|------------------|----------------------|---------------|
| Chiavalo, D. R.  | [CJ 87]          | Farmer, J. D.        | [Far 82],     |
| Clark, D. S.     | [CS 88]          |                      | [Far 85]      |
| Clark, J.        | [VC 78]          | Fazzini, T           | [BBFT 89]     |
| Collet, P. C.    | [CE 80]          | Feder, J.            | [HJF 87]      |
| Comve, J. H.     | [Com 66]         | Feigenbaum, M. J.    | [Fei 79],     |
| Coniglio, A.     | [MSCW 85],       |                      | [Fei 83]      |
|                  | [MCSW 86]        | Fein, A. P.          | [FHG 85]      |
| Conway, J. H.    | [BGG 82]         | Feller, W.           | [Fel 68]      |
| Coon, D. D.      | [CMP 87]         | Felske, D.           | [TKFFHKMM     |
| Cooper, A. P. R. | [AZL. . . 89]    |                      | 89]           |
| Corzine, R. G.   | [CM 90]          | Ferguson, J. F.      | [AZL. . . 89] |
| Cramer, E.       | [LC 81]          | Fibonacci, L.        | [Fib 1202]    |
| Crick, F.        | [Cri 81]         | Fisher, E.           | [AZL. . . 89] |
| Cvitanović, P.   | [CJKP 85]        | Fisher, D. E.        | [Fis 90]      |
| Chave, A. D.     | [AZL. . . 89]    | Fleckinger-Pellé, J. | [LF 88]       |
| D'Antonio, P.    | [D'An 90]        | Friedrich II         | [Fri 1240]    |
| Dallas, W. J.    | [ZD 85]          | Fukano, Y.           | [INF 85],     |
| Davies, C.       | [DK 88]          |                      | [INF 88]      |
| de Brujin, N. G. | [deb 81]         | Gardner, M.          | [Gar 70],     |
| Dekking, F. M.   | [DMP 82]         |                      | [Gar 77],     |
| Derrida, B.      | [DGP 78],        |                      | [Gar 78],     |
|                  | [DDI 83]         |                      | [Gar 83],     |
| de Seze, L.      | [DDI-83]         |                      | [Gar 89]      |
| de Wijs, H. J.   | [deW 51]         | Geisel, T.           | [GZR 87]      |
| Diagonis, P.     | [Dia 77]         | Gerhardt, M.         | [DGJPS 85]    |
| Douady, A.       | [DH 82],         | Gervois, A.          | [DGP 78]      |
|                  | [DH 85],         | Gilbert, E. N.       | [Gil 58]      |
|                  | [Dou 86]         | Gilbert, W. J.       | [Gil 84]      |
| Dougherty, A.    | [SWGDRCL<br>86]  | Gleick, J.           | [Gle 87]      |
| Dress, A. W. M.  | [DGJPS 85]       | Gollub, J. P.        | [FHG 85],     |
| Du, B.-S.        | [Du 84]          |                      | [SWGDRCL      |
| Duneau, M.       | [DK 85],         |                      | 86]           |
|                  | [KD 86]          | Gorman, M. R.        | [AZL. . . 89] |
| Eckhardt, D. H.  | [JER 90]         | Gottlob, D.          | [SGS 74]      |
| Eckmann, J.-P.   | [CE 80]          | Graham, R. L.        | [GLL 78]      |
| Eggleton, R. B.  | [EG 88]          | Grassberger, P.      | [Gra 81],     |
| Einstein, A.     | [Ein 05]         |                      | [GP 83],      |
| Elsner, V        | [Els 85]         |                      | [Gra 83],     |
| Emde, F.         | [JE 51]          | Gratias, D.          | [Gra 85]      |
| Eldélyi, A.      | [Erd 54]         | Greer, J.            | [AZL. . . 89] |
| Escher, M. C.    | [Esc 71]         | Grimmett, G.         | [Gri 89]      |
| Eykolt, R.       | [EU 86]          | Grossmann, S.        | [GT 77],      |
| Fackler, O.      | [TKFFHKMM<br>89] |                      | [Gro 82]      |
| Falconer, K. J.  | [Fal 87]         | Grünbaum, B.         | [GS 87]       |
| Family, F.       | [FL 84]          | Guy, R. K.           | [BCG 82],     |
|                  |                  |                      | [EG 88]       |

|                     |                                   |                  |
|---------------------|-----------------------------------|------------------|
| Gwinn, E. G.        | [GW 87]                           | [BBJ 84],        |
| Haken, H.           | [Hak 78]                          | [CJKP 85],       |
| Haldane, J. B. S.   | [Hal 28]                          | [JKLPS 85],      |
| Halmos, P. R.       | [Hal 74]                          | [HJKPS 86]       |
| Halsey, T. C.       | [HJKPS 86]                        | Jensen, R. V.    |
| Hammer, P.          | [AZL . . 89]                      | Jossang, T.      |
| Hansen, B. L.       | [AZL . . 89]                      | Jones, D.        |
| Hardy, G. H.        | [HW 84]                           | Jullien, R.      |
| Harris, S.          | [Har 77]                          | Kac, M.          |
| Harris, R.          | [TKFFHKMM<br>89]                  | Kadanoff, L. P.  |
| Harwit, M.          | [HS 79]                           |                  |
| Hasinger, G.        | [HLSTLW 86]                       | Kammeraad, J.    |
| Hawking, S.         | [Haw 88]                          |                  |
| Hénon, M.           | [Hen 76],<br>[Hen 88]             | Kasameyer, P.    |
| Hentschel, H. G. E. | [HP 83a],<br>[HP 83b],<br>[HP 84] | Katz, A.         |
| Herman, R.          | [AH 48]                           | Kelly, J. L.     |
| Heutmaker, M. S.    | [FHG 85]                          | Kelty, J. R.     |
| Hildebrand, J. A.   | [AZL . . 89]                      | Kesten, H.       |
| Hinkle, E. B.       | [SHJ 88]                          | Kim, C. E.       |
| Hinrichsen, E       | [HJF 87]                          | Kim, S           |
| Hofstadter, D. R.   | [Hof 80]                          | Klee, V.         |
| Holzfuss, J.        | [LH 86]                           | Klein, B.        |
| Hu, B.              | [Hu 85]                           | Klinger, M.      |
| Hubbard, J. H.      | [DH 82],<br>[DH 85]               | Knuth, D.        |
| Hunt, F. V.         | [HBM 39]                          | Kohlrausch, R.   |
| Hurd, A. J.         | [MH 87]                           | Kolb, M.         |
| Hurst, H. E.        | [HBS 65]                          | Koplowitz, J.    |
| Huygens, Ch.        | [Huy 1673]                        | Kuo, K. H.       |
| Ichimasa, T.        | [INF 85],<br>[INF 88]             | Kurtze, D. A.    |
| Ilgauds, H. J.      | [PI 87]                           | Landau, D. P.    |
| Ince, S.            | [RI 57]                           | Landau, L. D.    |
| Itzykson, C.        | [DDI 83]                          | Langmeier, A.    |
| Jaeger, N. I.       | [DGJPS 85]                        | Lapidus, M. S.   |
| Jahnke, E.          | [JE 51]                           | Laskar, J.       |
| Jain, A. K.         | [SHJ 88]                          | Lauterborn, W.   |
| Jakobson, M. V.     | [Jak 81]                          |                  |
| Jalife, J.          | [CJ 87]                           | Lautzenhiser, T. |
| Janner, A.          | [Jan 89]                          | Lawton, J. H.    |
| Jekell, C.          | [JER 90]                          | Lee, T. D.       |
| Jensen, M. H.       | [JBB 83],<br>[JBB 84],            | Leibniz, G. W.   |
|                     |                                   | Leopold, L. B.   |

- Levin, L. [LS 84]  
 Levinson, M. T. [AL 85]  
 Lewien, W. H. G. [HLSTLW 86]  
 Li, D. X. [CLK 88]  
 Li, T.-Y. [LY 75]  
 Libchaber, A. [LM 80],  
     [JKLPS 85]  
 Lin, C.-S. [GLL 78]  
 Lin, S. [GLL 78]  
 Lindemayer, A. [Lin 68]  
 Lindsay, H. M. [SWGDRCL 86]  
 Lipes, R. [ZLP 76]  
 Liu, S. H. [Liu 85]  
 Lorenz, E. N. [Lor 80]  
 Lovejoy, S. [Lov 82],  
     [LM 85]  
 Maa, S. N. [CMP 87]  
 Maa, D. Y. [HBM 39]  
 Mackay, A. [Mac 82]  
 Mandelbrot, B. B. [Man 61],  
     [Man 63a],  
     [Man 63b],  
     [Man 63c],  
     [MW 69],  
     [Man 74],  
     [Man 80],  
     [Man 83],  
     [MPP 84],  
     [LM 85],  
     [Man 91]  
 Margolus, N. [TM 87]  
 Martienssen, W. [MM 86]  
 Martin, J. E. [SMWC 84],  
     [MH 87]  
 Martin, S. [MM 86]  
 Mathews, M. V. [MPRR 88]  
 Maurer, J. [LM 80]  
 May, R. M. [May 88]  
 McGraw-Hill [McG 71]  
 McMechan, G. A. [AZL... 89]  
 Meakin, P. [Mea 83],  
     [MSCW 85],  
     [MCSW 86],  
     [Mea 87]  
 Meinhardt, H. [Mei 82],  
     [MK 87]  
 Mekjian, A. Z. [Mek 90]
- Melter, R. A. [WWM 87]  
 Mendès France, M. [DMP 82]  
 Meneveau, C. [MS 87]  
 Menger, K. [Men 79]  
 Metropolis, N. [MSS 73]  
 Michel, H. V. [AAMA 82]  
 Mignard, F. [WPM 83]  
 Millett, M. [TKFFHKMM 89]  
 Moon, F. C. [Moo 84]  
 Morse, M. [Mor 21]  
 Mosko, J. A. [CM 90]  
 Mugge, M. [TKFFHKKM 89]  
 Myer, C. R. [JM 85]  
 Nauenberg, M. [NS 89]  
 Niemeyer, L. [NPW 84],  
     [NPW 86]  
 Nieto, M. M. [AZL... 89]  
 Nissen, H.-U. [INF 85],  
     [INF 88]  
 Oliveria, M. [WO 84]  
 Onoda, G. Y. [OT 86]  
 Ostrowsky, N. [SO 85]  
 Ottino, J. M. [Ott 89]  
 Page, W. [Pag 81]  
 Pais, A. [Pai 82]  
 Pareto, V. [Par 1896]  
 Parker, R. L. [AZL... 89]  
 Parlitz, U. [LP 88]  
 Passajo, D. [MPP 84]  
 Pauling, L. [Pau 85]  
 Paullay, A. [MPP 84]  
 Peale, S. [WPM 83]  
 Peitgen, H.-O. [PR 84],  
     [PPR 85],  
     [PR 86a],  
     [PR 86b],  
     [PS 88]  
 Penrose, R. [Pen 74]  
 Perera, A. G. U. [CMP 87]  
 Pfeiffer, P. [PA 83]  
 Pierce, J. R. [ZLP 76],  
     [Pie 83],  
     [MPRR 88]  
 Pietronero, L. [NPW 84],  
     [NPW 86],  
     [PS 86]

- Pimm, S. L. [RP 88]  
 Pinkham, R. S. [Pin 62]  
 Piran, T. [BPS 87]  
 Plath, P. J. [DGJPS 85]  
 Pomeau, Y. [DGP 78]  
 Procaccia, I. [GP 83],  
     [HP 83a],  
     [HP 83b],  
     [HP 84],  
     [JJKLPS 85],  
     [HJKPS 86],  
     [PTT 87]  
 Prüfer, M. [PPR 85]  
 Prusinkiewicz, P. [Pru 87]  
 Purcell, E. M. [Pur 77]  
 Purkert, W. [PI 87]  
 Pyenson, L. [Pye 85]  
 Radons, G. [GZR 87]  
 Raimi, R. A. [Rai 76]  
 Ramanujan, S. [Ram 14]  
 Rammal, R. [RTV 86]  
 Rényi, A. [Ren 55]  
 Redfearn, A. [RP 88]  
 Reeves, A. [MPRR 88]  
 Richter, P. H. [PR 84],  
     [PPR 85],  
     [PR 86a],  
     [PR 86b],  
     [RS 87]  
 Risset, J.-C. [Ris 71],  
     [Ris 75]  
 Röschke, J. [Rös 86]  
 Robbins, M. O. [SWGDRCL  
86]  
 Roberts, L. [MPRR 88]  
 Romaides, A. J. [JER 90]  
 Rosenfeld, A. [RK 82]  
 Rouse, H. [RI 57]  
 Sagher, Y. [Sag 89]  
 Salem, J. [SW 86]  
 Sander, L. M. [WS 83]  
 Sanz, J. L. C. [SHJ 88]  
 Sasagawa, G. [AZL... 89]  
 Saupe, D. [PS 88]  
 Schaefer, D. W. [SMWC 84]  
 Schellnhuber, H. J. [NS 89]  
 Scholz, H.-J. [RS 87]  
 Schröder, M. [Schr 54] .
- Schroeder, M. R. [Schr 64],  
     [ASSW 66],  
     [SASW 66],  
     [Schr 67],  
     [Schr 69],  
     [Schr 70],  
     [Schr 73],  
     [SGS 74],  
     [SA 85],  
     [Schr 86],  
     [Schr 87],  
     [Schr 90]  
 Schuster, H. [DGJPS 85]  
 Schuster, H. G. [Schu 84]  
 Searby, G. [ASS 86]  
 Sessler, G. M. [ASSW 66],  
     [SASW 66],  
     [Ses 80]  
 Shannon, C. E. [Sha 51],  
     [Sha 53]  
 Sharkovskii, A. N. [Sha 64]  
 Shechtman, D. [SBGC 84]  
 Shenker, S. J. [She 82]  
 Shepard, R. N. [She 62],  
     [She 64]  
 Shephard, G. C. [GS 87]  
 Shisha, O. [CS 88]  
 Shraiman, B. I. [HJKPS 86]  
 Sidles, C. [AZL... 89]  
 Siebesma, A. P. [PS 86]  
 Siebrasse, F. K. [SGS 74]  
 Simaika, Y. M. [HBS 65]  
 Simon, B. [AS 81]  
 Singer, D. [Sin 78]  
 Slater, P. [Sla 60]  
 Sloane, N. J. A. [Slo 73],  
     [HS 79]  
 Smale, S. [Sma 67]  
 Smith, P. W. [BS 84]  
 Sreenivasan, K. R. [MS 87]  
 Stanley, H. E. [SO 85],  
     [MSCW 85],  
     [MCSW 86],  
     [SM 88],  
     [Sta 88]  
 Stauffer, D. [Sta 85],  
     [ASS 86]  
 Stavans, J. [JKLPS 85]

- Stein, M. L. [MSS 73]  
 Stein, P. R. [MSS 73]  
 Steinhardt, P. J. [LS 84]  
 Stevens, S. S. [Ste 69]  
 Stevenson, J. M. [AZL . . 89]  
 Stokes, J. P. [SWGDRCL 86]  
 Sundar Raj, A. P. [KS 87]  
 Sutner, K. [Sut 89]  
 Suwa, N. [ST 71]  
 Sztajno, M. [HLSTLW 86]  
 Taccetti, N. [BBFT 89]  
 Takahashi, T. [ST 73]  
 Tang, C. [BTW 87], [BTW 88], [TB 88]  
 Thomae, S. [GT 77], [PTT 87]  
 Thomas, J. [TKFFHKMM 89]  
 Thompson, D'A. W. [Tho 61]  
 Thue, A. [Thu 06]  
 Toffoli, T. [TM 87]  
 Toner, J. [OT 86]  
 Toulouse, G. [RTV 86]  
 Tressor, C. [PTT 87]  
 Trümper, J. [HSLSTLW 86]  
 Ulam, S. [Ula 74]  
 Ulrich, S. [Ulr 72]  
 Umberger, D. K. [EU 86]  
 Verhulst, P.-F. [Ver 1845]  
 Vichniac, G. [Vic 84], [Vic 86]  
 Vilenkin, A. [Vil 87]  
 Virasoro, M. A. [RTV 86]  
 von Boehm, J. [BB 79]  
 von der Poorten, A. [DMP 82]  
 von Saarloos, W. [SK 87]  
 Voss, R. F. [VC 78], [Vos 85], [Vos 88]  
 Wagon, S. [Wag 85], [KW 89]  
 Wallis, J. R. [MW 69]  
 Wang, N. [WCK 87]  
 Weinberg, S. [BPS 87]  
 Weiner, J. [Wei 90]  
 Weitz, D. A. [WO 84], [SWGDRCL 86]  
 Werman, M. [WWM 87]  
 West, J. E. [ASSW 66], [SASW 66]  
 Westervelt, R. M. [GW 87], [BW 90]  
 Weyl, H. [Wey 81]  
 White, N. E. [HLSTLW 86]  
 Wiesenfeld, K. [BTW 87], [BTW 88]  
 Wiesmann, H. J. [NPW 84], [NPW 86]  
 Wilson, T. A. [Wil 67]  
 Wiltzius, P. [SMWC 84]  
 Wirtz, J. [AZL . . 89]  
 Wisdom, J. [WPM 83], [Wis 87]  
 Witten, T. A. [WS 83], [MSCW 85], [MCSW 86]  
 Wolfram, S. [Wol 84], [Wol 86], [SW 86]  
 Wright, E. M. [HW 84]  
 Wu, A. [WWM 87]  
 Yang, C. N. [YL 52]  
 Yorke, J. A. [LY 75]  
 Zacherl, A. [GZR 87]  
 Zia, R. K. P. [ZD 85]  
 Zimmerman, M. H. [Zim 78]  
 Zipf, G. K. [Zip 49]  
 Zumberge, M. A. [AZL . . 89]  
 Zweig, G. [ZLP 76]

# Subject Index

- absolute temperature, 124, 144  
absorption, 69  
abstract concrete, 225  
accumulation point, 281  
accumulation point of period-doubling, 298  
acoustic cortex, 224  
acoustic feedback, 73  
acoustic nerve, 71, 122  
acoustic panel, 74  
acoustic preference, 75  
acoustical quality, 73, 74, 77  
Addams, C., 82  
affine transformation, 29  
algebraic behavior, 366  
algebraic irrational number, 242  
algebraic numbers, 163  
all-1s problem, 382  
phanumeric display, 302  
Alpher, R. A., 115  
Alvarez, L. W., 33, 105  
amorphous solid, 302  
analog computer, 151  
Anderson, P. W., 319, 366  
Anderson localization, 36, 88  
anechoic environment, 77  
angular momentum, 66  
antiferromagnetic interaction, 320, 324, 362, 363  
antiharmonic of an orbit, 284  
aperiodic tiling, 313  
aperiodic window, 183  
aperiodicity, 240, 266, 304, 309  
apparent length, 71  
arcsine law, 146, 293  
area-filling curve, 10  
arithmetic-geometric mean, 257  
Arnol'd, V. I., 175, 332  
Arnold's cat map, 253, 256  
Arnold tongues, 174, 175, 332, 334  
Arrhenius, S. A., 124  
articulator, 45  
articulatory ambiguity, 45  
asymptotic self-similarity, 99  
AT&T Bell Laboratories, 57, 150  
atomic size, 113, 114  
atomic lattice, 362  
atomic spectra, 114  
atomic unit of length, 113  
attractor, 40, 169, 244, 271  
audio frequency range, 71, 97  
auditory center, 71  
auditory neutron, 87  
auditory paradox, 95  
auditory research, 34  
autocatalytic interaction, 384  
Avnir, D., 236  
Bach, J. S., 101, 107  
backbone resistors, 31  
Bak, P., 320, 333, 389  
baker's transformation, 251  
Bale, H. D., 236  
bare winding number, 175, 331, 334  
Barnsley, M., 28, 261  
basilar membrane, 85, 87, 122  
basins of attraction, 27, 28, 39, 181, 206, 243  
Beatty pair, 53  
Beatty sequence, 53, 55, 307, 325  
Beranek, L. L., 74  
Bernoulli, D., 148  
Bernoulli, Jakob, 148  
Bernoulli, Johann, 148

- Bernoulli, N., 148  
 Berry, M. V., 27, 41  
 Bessel, F. W., 172  
 Bethe lattice, 87, 353,  
   363  
 bifurcation, 117, 269,  
   271  
 big bang, 107  
 binary number system,  
   163, 169, 383  
 binary-shift map, 292  
 biological pattern  
   formation, 382  
 biological shape, 259  
 Birkhoff, G. D., 69, 109  
 black hole, 155  
 black noise, 112, 122,  
   129  
 blackbody radiation, 40,  
   115, 188  
 block renaming, 265,  
   306, 310, 329  
 Bohr, N., 319  
 Bohr, T., 333  
 Bohr radius, 113  
 Boltzmann, L., 8, 140,  
   143  
 Boltzmann's constant,  
   124  
 Bolzano, B., 13, 187  
 bond percolation, 30,  
   365  
 Bose, S. N., 334  
 Bose condensation, 334  
 Bose-Einstein  
   distribution, 189, 334  
 boson, 334  
 Botet, R., 232  
 Bouligand, G., 41  
 boundary, 40  
 boundary point, 39  
 bounded motion, 67  
 box counting, 213, 221  
 branching ratio, 119,  
   190  
 broken symmetry, 379  
 bronchial tree, 119  
 brown music, 109  
 brown noise, 109, 111,  
   122, 128  
 Brown, R., 128, 140  
 Brownian motion, 86,  
   128, 133, 140, 142,  
   144  
 Bruinsma, R., 320  
 burning forest model,  
   346  
 bush in a breeze, 261  
 Butler, D., 345  
 Cantor, G., 15, 161,  
   187, 242  
 Cantor sets, 2, 10, 16,  
   97, 153, 155, 162,  
   179, 165, 167, 181,  
   207, 217, 227, 275,  
   321, 391  
 Cartesian product, 177  
 Cassini's divisions, 316  
 Catalan number, 147  
 catalytic converter, 386  
 catalytic oxidation, 386  
 catalytic reaction, 233  
 Cauchy, A. L., 158  
 Cauchy distribution, 158  
 Cauchy variable, 159  
 Cayley, A., 39  
 Cayley tree, 87, 227,  
   353, 363  
 celestial mechanics, 67  
 cellular automa, 371,  
   379  
 cellular computer, 372  
 cellular growth and  
   decay, 375  
 cellular telephone, 73  
 central limit theorem,  
   157, 160  
 chain code, 57  
 chain rule, 271  
 chance, 148, 149, 152,  
   207, 208  
 channel capacity, 128,  
   150, 151  
 chaos, 25, 52, 126, 289,  
   319, 343  
 chaos band, 279, 287  
 chaos game, 27  
 chaotic mapping, 240  
 chaotic mixing, 251  
 chaotic motion, 185  
 chaotic orbit, 252  
 chaotic system, 167, 205  
 chaotic tail, 52  
 chaotic tent map, 292  
 characteristic function,  
   158  
 characteristic impedance,  
   226  
 characteristic length, 34,  
   107, 347  
 characteristic scale, 389  
 characteristic time, 356  
 Chen, H., 326  
 Cheshire cat, 375  
 Chinese boxes, 81  
 chord, 97  
 Chudnovsky, D., 258  
 Chudnovsky, G., 258  
 circle map, 174, 331,  
   334  
 circularly polarized  
   waves, 90  
 Clark, D. S., 7  
 classical mechanics, 150  
 classical vacuum, 114  
 closed set, 162  
 clouds, 231  
 cluster aggregation, 232  
 cluster size, 31  
 clustering, 152  
 coastline, 137  
 coherence length, 114  
 coherence time, 114  
 cohesion, 132  
 colloidal aggregation,  
   235  
 color photography, 66  
 commensurate  
   frequencies, 324  
 commensurate orbital  
   periods, 316  
 commodity exchange,  
   126

- communication theory, 127  
 complete chaos, 291  
 completion time, 157  
 complex base, 47  
 complex number system, 48  
 complex plane, 40  
 computer graphics, 57, 249  
 computer tomography, 44, 133, 135  
 computing space, 371  
 concert hall acoustics, 40, 69, 72, 74, 125  
 condenser microphone, 73  
 conditional expectation, 157  
 confluence of rivers, 117  
 conformal mapping, 298, 299, 369  
 connected sets, 298  
 consensus preference, 77  
 Constance (Norman queen), 84  
 continued fraction, 51, 52, 57, 91, 100, 102, 116, 226, 315, 325, 328, 337, 392  
 continuous function, 140  
 contractive transformation, 29  
 control group, 147  
 convolution integral, 132, 133, 134  
 Conway, J. H., 55, 57, 335, 373  
 Conway's sequence, 59  
 coordination number, 352  
 coprime, 100, 323  
 corner the lady, 53  
 correlation dimension, 205, 221  
 correlation length, 31, 43, 352, 355, 361, 367  
 cosmic background radiation, 115  
 cosmic shower, 106  
 cosmic string, 139  
 cosmology, 41  
 countable set, 163, 334  
 coupled oscillators, 324, 338  
 coupling parameter, 175  
 Cramer, E., 277  
 Cranmer, T., 114  
 Crick, F., 296  
 critical circle map, 340, 343  
 critical density, 352  
 critical exponent, 347, 350, 352, 361, 367, 390  
 critical frequency-band, 71  
 critical opalescence, 357  
 critical phenomenon, 115, 367  
 critical point, 115, 350  
 critical state, 389  
 critical temperature, 361  
 cross entropy, 127  
 cross-talk compensation, 77  
 crude oil extraction, 219, 220  
 crystal growth, 196  
 crystal lattice, 43  
 cubic irrational number, 394  
 cumulative distribution, 171  
 Curie point, 36, 346  
 cutting line sequence, 56  
 Cvitanović, P., 334  
 dangling bond, 31  
 dark matter, 155  
 Darwin, C., 147  
 daughter orbit, 285  
 da Vinci, L., 117  
 decimal data, 116  
 Dedekind, R., 164  
 deflation, 265, 306, 310  
 dendrite, 200  
 determinism, 167  
 deterministic chaos, 20, 27, 166, 167, 224, 293, 320, 340  
 deterministic diffusion, 249  
 devil's staircase, 2, 167, 209, 321  
 de Haas, W. J., 302  
 De Morgan's rule, 180  
 de Wijs, H. J., 188  
 Diaconis, P., 116  
 diagonal method, 163  
 dice, 126  
 difference equation, 145  
 diffraction, 44, 304, 315  
 diffraction from fractals, 44, 233  
 diffusion, 198, 352, 381  
 diffusion constant, 143  
 diffusion equation, 143  
 diffusion-limited aggregation, 196, 198, 201, 232  
 digital chip, 151  
 digital filter, 266  
 digital sundial, 181  
 digital system, 98  
 digital-to-analog converter, 95  
 digitization, 57  
 dimensionless number, 70  
 direct product, 181, 239  
 discrete logarithm, 79  
 disordered system, 302, 366  
 dissimilarity, 61, 75, 77  
 distribution of galaxies, 152, 155, 356  
 DLA, *see* diffusion-limited aggregation

- Douady, A., 296, 298, 299  
 double star, 25  
 Dönitz, K., 33  
 drag force, 70  
 dragon curve, 47  
 Dress, A. W. M., 386  
 dressed winding number, 175, 331, 334  
 drift, 381  
 Du, B.-S., 166  
 duration of the game, 210  
 dynamic system, 166
- Earth, 338  
 economics, 34  
 EEG, *see*  
     electroencephalogram  
 effective velocity, 173  
 Eggleton, R. B., 147  
 Eiffel, G., 19  
 eightfold symmetry, 318  
 Einstein, A. 1, 3, 5, 139, 140, 143, 144, 155, 189, 302, 334  
 Einstein, J., 3  
 electrical breakdown, 197  
 electric circuit, 225  
 electrical conduction, 227  
 electrical potential, 198  
 electroencephalogram, 223  
 electrolytic deposition, 233  
 electromagnetic cavity, 69, 189  
 electromagnetic field, 69, 189  
 electromagnetism, 106  
 electron mass, 106, 113  
 electrostatics, 299  
 elliptic integral, 258
- embedding dimension, 224  
 embedding space, 350  
 energy barrier, 123  
 energy dissipation, 63  
 energy fluctuation, 114  
 energy loss mechanisms, 69  
 entropy, 35, 203, 206, 222  
 entropy function, 128, 191  
 equation of motion, 66  
 equipartition of energy, 144  
 equipotential surface, 198  
 equivalent number, 343, 392  
 error probability, 128, 151  
 error-free computing, 88  
 error-free transmission, 151  
 Escher, M. C., 17, 361  
 Euclidean scaling, 14, 137, 237  
 Euler's function, 336  
 Euler's infinite product, 98  
 even period length, 287  
 exactly solvable model, 366  
 expected duration, 146, 210  
 expected gain, 146, 148  
 experimental aesthetics, 70  
 external angle, 298  
 external field, 390
- fair coin tossing game, 146, 148  
 Falconer, K. J., 182  
 Farey tree, 2, 336, 339  
 Farmer, J. D., 185  
 fast algorithm, 385
- fast Fourier transform, 239  
 fat fractal, 183  
 Fatou, P., 39, 298  
 Fatou set, 39  
 Fechner, G. T., 70  
 Feder, J., 213  
 Feigenbaum, M., 274  
 Feigenbaum constant, 2, 280  
 Feynman, R., 112  
 FFT, *see* fast Fourier transform  
 Fibonacci, L. 85, 304  
 Fibonacci nim, 53  
 Fibonacci number system, 49, 55, 91, 171, 256, 306, 308, 328, 337, 393  
 fifth force, 33, 106  
 filled-in Julia set, 297  
 finite field, 79  
 finite precision, 52, 294  
 finite-size scaling, 354  
 finite-state algorithm, 258  
 finite-state automata, 291  
 first digit distribution, 116  
 Fisher, M., 357  
 fivefold symmetry, 301, 318, 325, 328  
 fixed point 240, 268  
 Fleckinger-Pellè, J., 41  
 forbidden symmetry, 301, 315  
 four-dimensional space, 41  
 Fourier spectrum, 122  
 Fourier transform, 133, 158, 266  
 fractal boundary, 244  
 fractal coast, 213  
 fractal colloid, 235  
 fractal diffraction gratings, 236

- fractal diffraction, 44  
 fractal dimension, 16,  
   153, 160, 192, 193,  
   202, 320, 354, 363  
 fractal growth, 198  
 fractal inner surface, 236  
 fractal interface, 225,  
   228  
 fractal landscape, 137  
 fractal lattice, 350  
 fractal paradox, 15  
 fractal perimeter, 48  
 fractal phenomenon, 389  
 fractal subset, 193  
 fractal support, 201  
 fractal tile, 14  
 fractional differentiation,  
   132  
 fractional exponent, 103,  
   115  
 fractional integration,  
   132  
 fracton, 43  
 fracture, 230  
 Fraunhofer diffraction,  
   44  
 Frederick II, 84  
 free of scale, 31  
 frequency plane, 133  
 frequency pulling, 171  
 frequency ratio, 98, 171,  
   175, 334  
 frequency response, 72,  
   73, 74  
 frequency vector, 133  
 friction, 69, 151  
 Fuller, R. B., 20  
 fundamental physical  
   constants, 113  
  
 Galileo, 63, 64, 67, 105,  
   163  
 Galton, F., 147  
 Galton board, 147  
 gambler's ruin paradigm,  
   145  
  
 gambling, 128, 129,  
   148, 149, 150, 151,  
   152, 168, 207, 208  
 game of Life, 373  
 Garden of Eden pattern,  
   382  
 Gauss, C. F., 70, 117,  
   124, 171, 215  
 Gauss map, 51  
 Gaussian distribution,  
   73, 133, 157  
 Gaussian noise, 129  
 Gaussian plane, 39  
 GCD, *see* greatest  
   common divider  
 Gedanken experiment,  
   112  
 Geisel, T., 125  
 general relativity, 41  
 generalized dimension,  
   203  
 generalized entropy,  
   203  
 generating function,  
   145, 266  
 genetic drift, 382  
 Genghis Khan, 33  
 geometric distribution,  
   188  
 George III, 215  
 Gibbs, J. W., 206  
 Gierer, A., 382  
 global warming, 131  
 golden angle, 339  
 golden mean, 50, 51,  
   52, 54, 55, 91, 95,  
   226, 304, 316, 319,  
   324, 325, 329, 337,  
   339, 343, 394  
 golden-mean slope, 56  
 Gödel, K., 177  
 graph theory, 363  
 Grassberger, P., 233,  
   276, 352  
 gravitational attraction,  
   33  
 gravitational lens, 155  
  
 gravity, 65, 67, 106  
 Gray, code, 12, 282  
 greatest common  
   divider, 237  
 greedy algorithm, 210  
 greenhouse effect, 131  
 Gregory-Leibniz series,  
   257  
 Grossmann, S., 275  
 growth parameter, 268,  
   274  
 growth rate, 128, 201  
 Guy, R. K., 147  
 gyromagnetic ratio of  
   the electron, 302  
  
 Hadamard, J., 295  
 Hadamard transform,  
   239  
 Haldane, J. B. S., 9, 63  
 half integration, 132  
 Halmos, P. R., 82  
 Halsey, T. C., 205  
 Hamiltonian systems,  
   125, 256  
 harmonic of an orbit,  
   284  
 Hausdorff, F., 2, 10  
 Hausdorff dimension, 2,  
   9, 15, 137, 141, 153,  
   177, 179, 181, 201,  
   207, 213, 216, 229,  
   230, 276, 334, 388,  
   391  
 Hawking, S., 98  
 hearing research, 44,  
   122  
 Heisenberg, W., 107  
 Heisenberg's uncertainty  
   principle, 63, 73, 112  
 Hensel code, 88  
 Hentschel, H. G. E., 232  
 Henze, H., 315  
 Herman, R., 115  
 Hermite, C., 7, 242

- Hénon, M., 169, 170  
 Hénon attractor, 255  
 Hénon's map, 253  
 hierarchical construction, 225  
 hierarchical lattice, 362  
 hierarchical neighborhood, 364  
 hierarchical structure, 88  
 Hilbert, D., 40  
 Hilbert curve, 2, 10  
 Hilbert envelope, 108  
 Hilbert space, 113  
 Hilbert space-filling curve, 282  
 Hilbert transform, 108  
 Hirzebruch, F., 150  
 Hofstadter, D. R., 237  
 Hogarth, W., 215  
 holes on all scales, 43  
 hologram laser speckle, 73  
 holography, 114, 147  
 homogeneous power laws, 33, 103, 108, 122  
 homograph, 37  
 Hubbard, J. H., 296, 298  
 Hubble, E., 345  
 human hearing, 44, 85, 97  
 human perception, 34, 38  
 human speech production, 44  
 Hurst, H. E., 129, 131  
 Hurst exponent, 130, 137  
 Hutton, E. F., 121  
 Huygens, C., 171  
 Huygens principle, 171  
 hydrodynamic instability, 200  
 hydrodynamics, 68, 70, 372  
 hyperbolic distribution, 124  
 hyperbolic fixed point, 256  
 hyperbolic law, 35, 108, 113, 125  
 hyperbolic map, 51  
 hypercubic lattice, 313  
 hyperfine structure, 114  
 image coding, 57  
 image scanning, 10  
 imaging, 133, 134  
 immiscible liquid, 200  
 inclusion-exclusion principle, 179  
 incommensurate frequencies, 309  
 independent increments, 144  
 index sequence, 307, 310  
 infinitely long chess game, 267  
 inflation, 265  
 information dimension, 195, 205, 207, 221  
 information theory, 35, 127, 151, 222  
 inner ear, 34, 70, 71, 122  
 innovation process, 121, 126  
 input impedance, 45, 226  
 interatomic force, 34  
 intercontinental distance, 159  
 intermediate scales, 143  
 intermittency, 289, 290  
 interquartile range, 158, 160  
 invariant distribution, 160, 242, 292  
 invariant set, 165  
 invariant under addition, 157  
 invasion percolation, 354  
 inverse filtering, 77  
 inverse Fourier transform, 133, 159  
 inverse mapping, 27, 40, 243  
 inverse orbit, 244  
 inverse problem, 44  
 inverse Radon transform, 135  
 inverse square law, 33  
 irrational frequency dependence, 226  
 irrational number, 52, 100, 237, 241, 242, 328  
 Ising, E., 361  
 Ising spin, 321, 322, 330, 324, 361, 380  
 iterated function system, 29, 261  
 iterated mapping, 165, 305, 315  
 iterated-logarithmic law, 258  
 iteration, 39, 237, 257  
 Jensen, M. H., 333  
 Jones, D., 225  
 Julia, G., 39, 298  
 Julia set, 2, 39, 244, 297  
 Jullien, R., 232  
 Jupiter, 171  
 just noticeable difference, 72  
 Kac, M., 109, 161  
 Kadanoff, L. P., 334, 357  
 Kelly, J. L., 151  
 Kepler, J., 279  
 Kepler's third law, 67  
 kinetic energy, 67  
 Klein, F., 8, 141, 143  
 kneading sequence, 277  
 Koch curve, 7, 63  
 Koch flake, 2  
 Kolb, M., 232

- Kolmogorov entropy, 205  
 Kronecker, L., 237  
 Kuo, K. H., 326
- l'Hospital, G. F. A. de, 145  
 ladder network, 226  
 Lagrangian function, 66  
 Lapidus, M. S., 41  
 Laplace equation, 198  
 Laplace triangle, 20  
 largest common divisor, 323  
 laser light diffraction pattern, 114, 190, 316  
 lateral sound wave, 79  
 lattice gas, 373  
 Lauterborn, W., 277  
 law of large numbers, 140  
 Lebesgue measure, 180, 291  
 Lee, T. D., 363  
 left shift, 57  
 Legendre transform, 206  
 Leibniz, G. W., 132, 383  
 length of observation, 131  
 length scaling, 368  
 Leonardo da Pisa, 54  
 Lettvin, J., 124  
 Levin, L., 313  
 Lévy, P., 155  
 Levy flight, 155  
 Li, T.-Y., 279, 289  
 Libchaber, R., 277  
 Lichtenberg, G. C., 211, 215  
 Lichtenberg figure, 197, 215  
 Lie, S., 68  
 life-time, 390  
 Life game, 373  
 Lifson, S., 3  
 lightning, 198
- lignite, 236  
 Lindemann, F., 237, 242  
 Lindenmayer, A., 261  
 linear oscillator, 66  
 linear prediction, 127  
 linear resonator, 158  
 Liouville, J., 86, 242  
 Liouville number, 241  
 Lipchitz, J., 74  
 Lipschitz-Hölder exponent, 192, 193  
 lipreading, 44  
 liquid crystal, 302  
 local interaction, 372  
 locked frequency, 172  
 locked frequency interval, 175, 336  
 locked-in frequency ratio, 334  
 locked-in intervals, 169  
 log-periodic antenna, 85, 90  
 logarithmic mapping, 85  
 logarithmic spiral, 47, 67, 68, 89, 90  
 logistic parabola, 207, 268, 279  
 long-range dependence, 129  
 long-range order, 55, 302, 304, 306, 309  
 long-range structure, 266  
 look-see proof, 93  
 Lorentz, H. A., 40  
 Lorentz invariance, 4  
 loudness, 34, 71  
 loudness doubling, 71  
 Lovejoy, S., 232  
 low-loss transmission, 159  
 Lucas number, 171, 318, 328  
 lumped element, 225  
 lung development, 119  
 Lyapunov exponent, 243
- magnetic domain, 379  
 magnetic susceptibility, 353  
 magnetism, 115  
 majority voting, 380  
 Mallows, C., 59  
 Mandelbrot, B. B., 2, 8, 107, 117, 119, 129, 139, 162, 179, 196, 232, 296  
 Mandelbrot set, 279, 296, 298  
 Manin, Y., 301  
 market analysis, 127  
 Markov, A. A., 145  
 Markov process, 150, 357  
 Markov source, 358  
 Markov-Wiener process, 145  
 Marx, K., 145  
 mass dimension, 216  
 mass distribution, 44  
 mass exponent, 32, 33  
 matter density, 115  
 Maurer, J., 277  
 Maxwell's equation, 369  
 Meakin, P., 196, 198, 232  
 mean, 148  
 mean free path, 143  
 median, 148, 158  
 median, 335  
 Meinhardt, H., 382  
 melting, 115  
 memoryless source, 358  
 Menger, K., 179  
 Menger sponge, 179  
 Mercury, 332, 338  
 meson, 106  
 metallic glass, 302  
 Metropolis, N., 371  
 microwave cavity, 69  
 microwave transmission, 231  
 middle-third-erasing set, 16

- minimally stable state, 390  
 Minkowski, H., 41  
 Minkowski-Bouligand dimension, 42  
 Minkowski content, 41  
 Minkowski dimension, 216  
 Minkowski sausage, 42, 213  
 mixing process, 251  
 mode density, 43  
 mode locking, 171, 172, 175, 333, 343  
 model basin, 70  
 Moebius function, 24  
 Moebius strip, 24  
 molecular collision, 143  
 molecular structure, 235  
 molecular theory of heat, 140  
 monkey language, 35, 37  
 monophonic sound, 79  
 Monte Carlo method, 371  
 Monte Carlo simulation, 30  
 Morse, M., 263, 267  
 Morse-Thue constant, 241, 279, 299  
 Morse-Thue sequence, 2, 264, 278, 283  
 most irrational number, 338  
 most significant digit, 116  
 Mössbauer quanta, 112, 258  
 Mössbauer spectroscopy, 114  
 MT, *see* Morse-Thue sequence  
 multidimensional scaling, 75  
 multifractal, 187, 192, 193, 200, 204, 206, 245, 333  
 multifractal Julia set, 245  
 multifractal spectrum, 193, 206, 207, 334, 343  
 multipath propagation, 73  
 multiple images, 155  
 multiplicative random process, 190, 193  
 muon, 106  
 musical instruments, 44, 74, 101  
 musical scale, 102  
 musical sound, 97, 101  
 natural length scale, 33  
 Nauenberg, M., 245  
 near noble number, 392  
 nearest-neighbor coupling, 361  
 negative curvature, 267  
 neural network, 302, 366  
 neuron, 302  
 neutrino, 106, 155  
 neutron scattering, 236  
 neutron spectroscopy, 114  
 neutron, 232  
 Newton, I., 67, 239  
 Newton's iteration, 38, 239, 243  
 Newton's universal law of gravitation, 67, 103, 106  
 Newton's tangent method, 38  
 Newtonian attraction, 67  
 noble mean, 316, 339, 343, 392  
 1/f noise, 34, 289  
 noise abatement, 79  
 noise in the frequency domain, 73  
 noise intensity, 34  
 non-euclidean paradox, 3  
 nondifferentiability, 140  
 nondifferentiable function, 140, 143  
 nonlinear coupling, 324, 334  
 nonlinear dynamic system, 181, 205, 253, 267  
 nonlinear dynamics, 357  
 nonlinear mechanics, 172  
 nonlinear oscillator, 67  
 nonlinear physics, 338  
 nonlinear problem, 243  
 nonlinear system, 185  
 nonlinearity, 175  
 nonnormal irrational number, 241  
 nonperiodic orbit, 183  
 nonstandard statistics, 160  
 nonzero Lebesgue measure, 183  
 normal law of probability, 113  
 normal mode, 43  
 normal number, 241  
 nuclear force, 106, 389  
 nuclear fragmentation, 356  
 number, 161  
 number of molecules, 144  
 number system, 47  
 number theory, 100  
 number-theoretic fluke, 101, 102  
 numerical divergence, 244  
 numerical precision, 244  
 octave, 97, 99, 101, 122  
 odd period length, 285  
 odd-parity cover, 382  
 odds, 148, 150, 207, 208  
 Oliveria, M., 232

- one-hump (unimodal)  
map, 285
- one-to-one mapping,  
164
- optical fiber, 159
- orbit, 40, 166, 240, 269
- orbit interpolation, 285
- orbital period, 67, 171
- order parameter, 347
- outguessing machine,  
149
- Pagels, H., 357
- painting turtle state, 259
- paired comparison, 76
- Pallas, 171
- paper folding, 45
- paradox, 97, 155, 157
- paradoxical self-similar  
waveform, 96
- paradoxical sound, 95
- parallel mirror, 82
- parallel processing, 167,  
363, 372
- paramagnetic, 346
- parameter sensitivity,  
185
- parametric amplifier, 171
- parenting of orbits, 282
- Pareto, V., 34
- parity, 279, 376
- partial differential  
equation, 69
- particle velocity, 372
- partition function, 206
- Pascal's triangle, 386
- Passoja, D., 230
- Pauli, W., 230, 350
- Pauling, L., 302
- Paullay, A., 230
- Peano, G., 13, 187
- Peitgen, H.-O., 244,  
299, 363
- Penrose tiling, 265, 313
- Penzias, A., 115
- perceived weight, 71
- perceptual paradox, 95
- perceptual space, 77
- percolating cluster, 31,  
33
- percolation threshold,  
30, 345
- percolation, 30, 39, 345,  
355
- perfect fifth, 99
- perfect set, 162
- perimeter, 41, 354
- period doubling, 208,  
271, 273, 275
- period-doubling  
bifurcation, 279
- period-3, 279, 291
- period-tripling operator,  
284
- periodic binary number,  
240
- periodic crystal, 302
- periodic point, 24, 257
- periodic window, 279,  
281, 291
- periodicity, 98, 319
- Perrin, J. B., 8, 140, 144
- Pfeifer, P., 236
- phase locking, 171
- phase space, 253, 267,  
320
- phase space trajectory,  
324
- phase transition, 353,  
357
- phonon, 43
- photon, 43, 106, 189
- photon statistics, 334
- phylogenetic tree, 87
- physically realizable  
inverse, 77
- pi value, 257
- pi-meson, 106
- picture recognition, 57
- piecewise linear  
function, 249
- Pierce, J. R., 101, 102,  
114
- pink music, 110
- pink noise, 34, 109, 111,  
122, 125
- pion, 106
- pipe model, 117
- pitch, 95, 122
- Planck length, 33, 107
- Planck's constant, 112
- Planck's law, 189
- planetary system, 27
- Pluto, 25
- Poincaré, H., 25, 187
- Poincaré mapping, 243
- Poincaré section, 324
- point process, 152
- point set, 39
- Poisson distribution, 190
- Poisson process, 71
- population dynamics,  
167
- population variation,  
131
- potential energy, 66, 67
- potential theory, 198
- power law, 31, 33, 103,  
184, 227, 350, 356,  
389
- power spectrum, 121,  
122, 123, 144
- power-law distribution,  
103
- power-law noise, 126
- power-law relation, 71
- power-law scaling, 390
- practical fractal, 211
- prediction residuals, 127
- preference space, 75
- preimage, 39, 244
- preperiodic binary  
fractions, 240
- prime factor, 363
- prime number, 101
- prime-number  
decomposition, 164
- primitive polynomial,  
79, 236
- primitive root, 236
- primitive scaling factor,  
93
- probability amplitude,  
151

- probability distribution, 188, 203  
 probability theory, 157, 171  
 Procaccia, I., 232, 334, 342  
 projection method, 312  
 projection, 181, 183  
 proof by self-similarity, 93, 94  
 proper fraction, 48  
 Prusinkiewicz, P., 261  
 pseudorandom number, 258  
 psychoacoustics, 71, 123  
 psychological scaling, 70, 74  
 psychophysics, 71  
 psychovisual mode-locking, 34  
 Purcell, E. M., 70  
 Pythagoras's theorem, 3  
 Pythagorean comma, 101
- quadratic irrational number, 319  
 quadratic map, 207, 268, 291  
 quadratic potential, 66  
 quadratic residue, 79, 236  
 quantum gravity, 106  
 quantum mechanical vacuum, 114  
 quantum mechanics, 122, 133  
 quasar, 155  
 quasicrystal, 57, 302, 304, 310, 312, 315, 319, 325  
 quasiperiodic lattice, 57, 310, 312  
 quasiperiodic spin, 329  
 quasiperiodicity, 319  
 quasi-stellar object, 155  
 quintic algorithm, 258
- rabbit constant, 55  
 rabbit lattice, 311  
 rabbit mapping, 56  
 rabbit sequence, 55, 306, 308, 309, 311, 315, 329  
 Rabi, I., 106  
 radar clutter, 44  
 radar intensity, 33  
 radiation density, 115  
 radioactive decay, 389  
 Radon transform, 135  
 Ramanujan, S., 239, 257  
 random fractal, 30, 196  
 random interference, 73  
 random noise, 320  
 random number, 125  
 random resistor network, 367  
 random sequence, 150, 359  
 random walk, 145, 146, 350  
 rank-ordering, 147  
 ratio scale, 71  
 rational approximation, 100  
 rational frequency ratio, 172, 324  
 rational function, 40, 244  
 rational function of frequency, 226  
 rational numbers, 163  
 Rayleigh-Bénard experiment, 277  
 reaction rate, 387  
 real number, 163  
 real-time computation, 150  
 reality of atoms, 144  
 reciprocal scaling, 113  
 reciprocity failure, 65  
 recursive computation, 99  
 redundancy, 35, 127  
 reflection phase grating, 79, 236
- relativity, 113  
 relaxation process, 123  
 remodeling, 69  
 renaming, 265  
 renormalization, 357, 367  
 renormalization theory, 265, 306, 342, 361  
 renormalized lattice, 368  
 repellor, 40, 244, 271  
 rescaled range, 129  
 rescaling, 33  
 resonance, 40  
 resonant mode, 69  
 response fluctuation, 73  
 response maximum, 73  
 rest mass, 106  
 reverberation time, 73, 74, 125  
 reverse bifurcation, 279, 281  
 Reynolds number, 70, 277  
 Rényi, A., 203  
 Richter, P. H., 299, 363  
 Riemann, B., 336  
 room resonance, 73  
 Rosenfeld, A., 57  
 rotating cylinder lens, 134  
 rotational symmetry, 302  
 rough surface, 227  
 roulette, 128, 150  
 ruin, 152  
 ruin-free time zones, 153  
 run length, 57  
 Russell, B., 301  
 Russian dolls, 81, 383
- saddle point, 256  
 safe square, 54  
 Sander, L. M., 198  
 satanic staircase, 174  
 Saturn, 316, 338  
 Saupe, D., 134, 244

- sawtooth map, 249  
 scale factor, 122  
 scale model, 69  
 scale-invariant, 390  
 scaling difficulty, 69  
 scaling exponent, 184,  
   201, 347  
 scaling factor, 93, 153  
 scaling failure, 65  
 scaling invariance, 122,  
   304, 330  
 scaling law, 63, 216,  
   329, 330, 347  
 scaling test, 71  
 scaling, 356, 360  
 scattering angle, 235  
 scattering fractal, 44  
 scattering surface, 79  
 Schaefer, D. W., 232  
 Schellnhuber, H. J., 245  
 Schmidt, P. W., 236  
 Schmitt, F. O., 38  
 Schwartzian derivative,  
   286  
 Schwarzschild, K., 65  
 Schwarzschild exponent,  
   66  
 Schwarzschild radius, 65  
 self-affine distribution,  
   188, 190  
 self-affine fractal, 191  
 self-affine function, 209  
 self-affine, 112, 122,  
   141, 174  
 self-affinity, 153  
 self-generating sequence,  
   264  
 self-organization, 357  
 self-organized criticality,  
   389  
 self-similar agglomerate,  
   218  
 self-similar cascade, 279  
 self-similar data, 116  
 self-similar distribution,  
   157  
 self-similar lattice, 362  
 self-similar scaling, 341
- self-similar sequence,  
   386  
 self-similar set, 163, 201  
 self-similar tiling, 13, 14  
 self-similar tree, 37, 119  
 self-similar TV antenna,  
   86  
 self-similarity in  
   architecture, 84  
 self-similarity, 31, 39,  
   47, 59, 122, 153, 190,  
   211, 237, 255, 260,  
   272, 276, 278, 307,  
   310, 330, 333, 346,  
   356, 357, 363, 367,  
   383, 385, 389  
 semiconductor, 34, 123  
 semitone, 95, 96, 101  
 Shannon, C. E., 35, 127,  
   149, 360  
 Shannon's information  
   capacity, 128  
 Shannon's information  
   theory, 151  
 Shannon's outguessing  
   machine, 150  
 Sharkovskii's ordering,  
   2, 281, 285  
 Shechtman, D., 302  
 Shenker, S. J., 333, 343  
 Shepard, R. N., 95  
 shepherding moon, 338  
 Shisha, O., 7  
 short range law, 306  
 short-time spectral  
   analysis, 73  
 Sierpinski, W., 17  
 Sierpinski gasket, 2, 17,  
   388  
 Sierpinski point, 24, 25  
 sigma sequence, 283,  
   288  
 silver mean, 49, 51, 92,  
   316, 327  
 silver-mean slope, 56  
 similarity, 61, 79  
 similarity dimension,  
   216, 391
- similarity factor, 93,  
   167  
 similarity principle, 67  
 similarity solution, 69  
 sinc function, 98  
 Sir Pinski's game, 20  
 site percolation, 30  
 size scale, 380  
 slaved oscillator, 338  
 Smale's horseshoe map,  
   253  
 Smoluchowski, M., 140  
 solar system, 316  
 sound absorption, 69  
 sound decay, 125  
 sound diffraction, 77  
 sound diffusion, 125  
 sound intensity, 34  
 sound reproduction, 79  
 sound-scattering surface,  
   79  
 sound transmission, 72  
 space normalization,  
   368  
 space time, 41  
 spanning cluster, 368  
 spatial chaos, 319  
 spatial correlation, 249  
 spatial frequency, 235  
 special relativity, 4  
 specific heat, 40, 353  
 spectral dimension, 43  
 spectral exponent, 130,  
   137  
 speech signal, 127  
 speed, 34  
 spin, 320, 361  
 spin domain, 379  
 spin glass, 302, 322,  
   366  
 spin interaction, 362  
 spin pattern, 324, 329  
 square lattice, 30, 55,  
   312, 348, 365  
 St. Petersburg paradox,  
   148  
 stability, 316  
 staircase, 169

- staircase distributions, 171  
 staircase function, 57  
 Stanley, H. E., 198  
 state diagram, 358  
 stationary distribution, 242  
 stationary source, 359  
 statistical analysis, 71  
 statistical artifact, 131  
 statistical fluctuation, 72  
 statistical mechanics, 206, 222  
 statistical misdemeanor, 147  
 statistical self-similarity, 152  
 statistically self-similar process, 112, 141  
 statistically similar, 141  
 Stauffer, D., 345, 354, 367  
 Steinhardt, P. J., 313  
 stereophonic sound, 79  
 Stevens, S. S., 70  
 stock market, 127, 128  
 strange attractor, 27, 28, 201, 206, 207, 253  
 Strauss, E., 3  
 strong nuclear interaction, 106  
 Strube, H. W., 12, 315, 391  
 subjective brightness, 71, 95  
 subjective loudness, 34  
 subjective rating, 74  
 subjective variable, 71  
 subset of multifractal, 193  
 sundial, 181  
 sunlight-blocking dust, 105  
 supercomputer, 167, 258, 363  
 superconductivity, 43, 334  
 supercritical liquid, 361  
 superfast algorithm, 258  
 superionic conductor, 172  
 superlattice, 368  
 supersite, 367  
 superstable fixed point, 269  
 superstable orbit, 269, 273, 277, 285, 294, 341  
 support interval, 202  
 support of a multifractal, 192  
 support of a fractal set, 245  
 support of the attractor, 201  
 supporting fractal, 201  
 surface dimension, 136  
 surface fractal, 234  
 surface reaction, 143  
 surface tension, 200  
 symbolic dynamics, 166, 267, 277, 284, 285, 324, 342  
 symbolic sequence, 279  
 synchronization problem, 306  
 synchronization of two oscillators, 171  
 Szell, G., 74  
 Tang, C., 389  
 tangent bifurcation, 289, 290  
 tempered scale, 101  
 tent map, 165, 288, 292  
 ternary number system, 162, 163, 169  
 test of relativity, 114  
 thermal noise, 121  
 thermal velocity, 144  
 thermodynamics, 206  
 Thomae, S., 275, 342  
 Thompson, D'Arcy, 63  
 three-body encounter, 25  
 three-body problem, 338  
 thrice-iterated quadratic map, 289, 291  
 Thue, A., 264  
 tidal force, 338  
 time plane, 133  
 time series, 223  
 time vector, 133  
 time-limited data, 131  
 tomographic imaging, 134  
 topological dimension, 153  
 totally disconnected set, 162  
 tower of Hanoi problem, 238  
 traditional scale, 102  
 transcendental number, 242  
 transfer matrix, 77  
 transfinite number, 17  
 transition probability, 150  
 transition to chaos, 342  
 transitivity, 71  
 translational symmetry, 302  
 trapped iterate, 290  
 tree design, 117  
 Tresser, C., 342  
 triadic Cantor set, 31  
 triangular lattice, 353, 365, 367  
 tritave, 102  
 true on all scales, 33, 63, 107, 112, 162  
 turbulence, 167, 195, 320  
 turtle algorithm, 259  
 turtle interpretation, 260  
 twelvefold symmetry, 318  
 twin dragon, 47, 50

- two-dimensional Fourier transform, 133
- two-dimensional quasicrystal, 313
- two-nation boundary, 38
- Ulam, S., 371
- ultrametric space, 88
- uncertainty, 71, 113
- uncertainty principle, 112
- uncertainty relation, 114
- uncountable set, 16, 161, 242
- undecidability in number theory, 177
- unimodal map, 279, 283
- unimodular fractions, 335
- universal function, 350
- universal mechanism, 115
- universal order, 285
- universality, 332, 350, 352, 361, 390
- universe, 98, 115, 139, 152, 155
- unpredictability, 167, 245, 294
- unstable equilibrium, 256
- vacuum, 114
- vacuum fluctuation, 114
- Valéry, P., 61
- van der Pol, B., 109
- vascular system, 119
- velocity profile, 159
- Verhulst, P.-F., 269
- Verhulst equation, 269
- vibrating fractal, 44
- virial theorem, 67, 113
- viscous boundary layer, 70
- viscous fingering, 199, 219
- visual perception, 340
- vocal tract, 44
- von Koch, H., 7
- von Neumann, J., 371
- Voss, R. F., 109, 126, 134
- Wall Street, 126
- Wang, N., 326
- wave diffraction, 235
- weak nuclear interaction, 106
- weather forecasting, 167
- Weber, E. H., 70
- Weber's law, 70
- Weber, W., 70, 124
- Weber-Fechner law, 70
- Weierstrass, K., 7, 96, 143
- Weierstrass function, 96, 97, 140
- Weitz, D. A., 232
- well-tempered instrument, 101
- well-tempered scale, 85
- Wente, E. C., 72
- Wentzel-Kramers-Brillouin approximation, 86
- Weyl, H., 17, 40
- white music, 110
- white noise, 109, 121
- Whitehead, A. N., 301
- Wiener, N., 140, 145
- Wiener process, 140
- Wiesenfeld, K., 389
- Wilson, K., 357
- Wilson, R., 115
- winding number, 324, 329, 341, 343
- Witten, T. A., 198
- Wolfram, S., 371
- word frequency, 35
- work rank, 35, 37
- Wythoff's nim, 53
- x ray, 134, 232
- x-ray scattering, 235, 236
- x-ray shadow, 44
- Yang, C. N., 363
- Yorke, J. A., 279, 289
- Yukawa, H., 106
- Zech logarithm, 236
- zero free region, 153
- zero measure, 16
- zeta function, 336
- Zipf, G. K., 35
- Zipf's law, 35
- Zuse, K., 371